REMOVAL OF DYE FROM WASTEWATER OF TEXTILE INDUSTRY USING BANANA STEM-DERIVED BIOCHAR

WEN CHANG QI

FACULTY OF SCIENCE
UNIVERSITY OF MALAYA
KUALA LUMPUR

2017

REMOVAL OF DYE FROM WASTEWATER OF TEXTILE INDUSTRY USING BANANA STEM-DERIVED BIOCHAR

WEN CHANG QI

DISSERTATION SUBMITTED IN PARTIAL FULFILMENT OF THE REQUIREMENTS FOR THE DEGREE OF MASTER OF TECHNOLOGY (ENVIRONMENTAL MANAGEMENT)

INSTITUTE OF BIOLOGICAL SCIENCES
FACULTY OF SCIENCE
UNIVERSITY OF MALAYA
KUALA LUMPUR

2017

UNIVERSITY OF MALAYA
ORIGINAL LITERARY WORK DECLARATION

Name of Candidate: **WEN CHANG QI**

Matric No: **SGH140014**

Name of Degree: **MASTER OF TECHNOLOGY(ENVIRONMENTAL MANAGEMENT)**

Title of Thesis: **REMOVAL OF DYE FROM WASTEWATER OF TEXTILE INDUSTRY USING BANANA STEM-DERIVED BIOCHAR**
Field of Study: **ENVIRONMENTAL MANAGEMENT**

I do solemnly and sincerely declare that:

(1) I am the sole author/writer of this Work;
(2) This Work is original;
(3) Any use of any work in which copyright exists was done by way of fair dealing and for permitted purposes and any excerpt or extract from, or reference to or reproduction of any copyright work has been disclosed expressly and sufficiently and the title of the Work and its authorship have been acknowledged in this Work;
(4) I do not have any actual knowledge nor do I ought reasonably to know that the making of this work constitutes an infringement of any copyright work;
(5) I hereby assign all and every rights in the copyright to this Work to the University of Malaya ("UM"), who henceforth shall be owner of the copyright in this Work and that any reproduction or use in any form or by any means whatsoever is prohibited without the written consent of UM having been first had and obtained;
(6) I am fully aware that if in the course of making this Work I have infringed any copyright whether intentionally or otherwise, I may be subject to legal action or any other action as may be determined by UM.

Candidate's Signature Date:

Subscribed and solemnly declared before,

Witness's Signature Date:

Name:

Designation:

REMOVAL OF DYE FROM WASTEWATER OF TEXTILE INDUSTRY USING BANANA STEM-DERIVED BIOCHAR

ABSTRACT

Banana stem is a natural, low-cost agricultural by-product in Malaysia which has been studied for its potential application as an adsorbent in its raw and biochar form to remove methylene blue (MB) and congo red (CR) dyes from aqueous solution. The banana stem was carbonized at various temperatures (300-700°C) using the muffle furnace with limited oxygen conditions. The experiments were conducted by using the batch adsorption technique under different conditions of adsorbents dosage, initial dye concentration, contact time, agitation speed, solution pH, and temperature on the removal of MB. The characteristics of adsorbents were determined by using BET, FTIR, SEM and proximate analysis. The adsorption isotherms of Langmuir and Freundlich were employed to examine the equilibrium adsorption data. The adsorption kinetics of pseudo-first-order and pseudo-second-order were employed to explore the mechanism of adsorption. Thermodynamic parameters such as the changes in ΔG, ΔH and ΔS were also determined. Desorption studies were carried out in order to further study the stability of MB adsorbed on the adsorbent. The results showed that biochar produced at 700°C (BC700) is the best in removing MB as it can achieve maximum removal percentage of more than 98% due to it has high surface area, high porosity, and high fixed carbon content. The adsorption of MB can be best described by Langmuir isotherm and the pseudo-second order kinetic model and the adsorption process was found to be exothermic for biochars (BC300 and BC700) and endothermic for raw banana stem. The desorption study indicated that the dye was firmly adsorbed onto the biochar. Thus, all results indicated that biochars prepared from banana stem adsorbed MB efficiently and could be employed as a low cost alternative in wastewater treatment for the removal of cationic dyes.

Keywords: adsorbent, adsorption, methylene blue, congo red, biomass.

PENYINGKIRAN PEWARNA DARI SISA EFLUEN DARI INDUSTRI TEKSTIL MENGGUNAKAN BIOCHAR DARIPADA BATANG PISANG

ABSTRAK

Batang pisang, satu sisa pertanian kos rendah di Malaysia telah dikaji untuk mengenalpasti potensinya sebagai bahan penjerap dalam bentuk mentah dan bentuk biochar, bagi menyingkirkan pewarna metilena biru (MB) dan congo merah (CR) dari larutan akueus. Batang pisang telah dibakar pada pelbagai suhu (300-700°C) dengan menggunakan relau muffle dalam keadaan oksigen yang terhad. Kajian ini telah dijalankan mengguna-pakai teknik penjerapan kumpulan di bawah keadaan yang berbeza seperti dos adsorben, kepekatan pewarna, masa sentuhan, kelajuan pergolakan, pH larutan, dan suhu, bagi menyingkirkan MB. Ciri-ciri adsorben ditentukan dengan menggunakan BET, FTIR, SEM dan analisis proksimat. Isoterma penjerapan Langmuir dan Freundlich telah digunakan untuk memeriksa data keseimbangan penjerapan. Kinetik penjerapan pseudo-tertib pertama dan pseudo-kedua telah digunakan untuk mengaji mekanisme penjerapan. Parameter termodinamik seperti perubahan dalam ΔG, ΔH dan ΔS juga ditentukan. Kajian desorption telah dijalankan untuk mengkaji kestabilan MB terjerap pada penjerap. Hasil kajian menunjukkan bahawa biochar yang dihasilkan pada suhu 700°C (BC700) adalah paling efektif dalam menyingkirkan MB kerana ia boleh mencapai penyingkiran maksimum yang lebih daripada 98% disebabkan luas permukaan yang tinggi, keliangan yang tinggi, dan kandungan karbon kekal yang tinggi. Penjerapan MB dapat diterangkan dengan baik oleh Langmuir isoterma dan perintah pseudo-kedua model kinetik dan proses penjerapan didapati eksotermik untuk biochar (BC300 dan BC700) dan endotermik untuk batang pisang mentah. Kajian penjerapan menunjukkan bahawa pewarna dapat diserap ke atas biochar dengan baik. Oleh itu, semua hasil kajian menunjukkan bahawa biochar yang disediakan dari batang pisang dapat menjerap MB dengan cekap dan boleh digunakan sebagai alternatif kos rendah dalam rawatan air sisa bagi penyingkiran pewarna kationik.

Katakunci: penjerapan, penyerapan, metilina biru, congo merah, biojisim.

ACKNOWLEDGMENTS

I would like to express my deepest appreciation and gratitude to my supervisors Dr. Fauziah Shahul Hamid and Dr. Sumathi d/o Sethupathi for their invaluable guidance, constructive criticism and continuous encouragement throughout every stage of this project work. I appreciate their patient and understanding which enabled me to develop an understanding of this research thoroughly.

I would like to offer my special thanks to the Institute of Research Management and Monitoring (IPPP), University of Malaya (UM) for providing the research fund (PO028-2016A). The Institute of Biological Sciences and Faculty of Science had also given a lot of supports and for that I am thankful. My extended thanks to all lab assistants and seniors of Central Analytical Laboratory and Environmental Microbiology Laboratory for their unconditional cooperation to accomplished this research by offering technical support and knowledge sharing.

Last but not least, my deepest gratitude to my beloved family who spends their time years after years to grow me up, have given me endless love and encourage me with moral and spiritual supports throughout my studies. Thank you very much.

TABLE OF CONTENTS

LIST OF FIGURES

LIST OF PLATES

LIST OF TABLES

LIST OF SYMBOLS AND ABBREVIATIONS

AOX : Adsorbate Organic Halides

q_e : Adsorption Capacity

NH_4Cl : Ammonium Chloride

Å : Angstrom

AC : Ash Content

atm : Atmospheric Pressure

BC : Biochar

BOD : Biological Oxygen Demand

BET : Brunauer-Emmett-Teller

$CaCl_2$: Calcium Chloride

cm : Centimetre

cm^3 : Centimetre Square

cm^2/g : Centimetre Square Per Gram

COD : Chemical Oxygen Demand

CR : Congo Red

^{o}C : Degree Celsius

K_2HPO_4 : Dipotassium Phosphate

$Na_2HPO_4 \bullet 7H_2O$: Disodium Phosphate Heptahydrate

DO : Dissolved Oxygen

ΔH : Enthalpy Change

ΔS : Entropy Change

EPA : Environment Protection Agency

$FeCl_3 \bullet 7H_2O$: Ferric Chloride Heptahydrate

FC : Fixed Carbon

FAU	Formazin Attenuation Unit
FTIR	Fourier Transform Infrared Spectroscopy
K_F	Freundilich Constant
n	Freundlich Exponent Related To Adsorption Intensity
$J\ K^{-1}\ mol^{-1}$	Gas Constant
ΔG	Gibbs Free Energy Change
g	Gram
g/L	Gram Per Litre
g/mol	Gram Per Mole
HCl	Hydrogen Chloride
H_2O_2	Hydrogen Peroxide
K	Kelvin
KJ/mol	Kilojoule Per Mole
R^2	Linear Correlation
L	Litre
$MgSO_4 \cdot 7H_2O$	Magnesium Sulfate Heptahydrate
MIDA	Malaysia Industrial Development Authority
Q_m	Maximum Amount of Adsorption
mV	Megavolt
MB	Methylene Blue
m^2/g	Metre Aquare Per Gram
m^3/mol	Metre Square Per Mole
µm	Micrometre
mg/g	Milligram Per Gram
mg/L	Milligram Per Litre
mL	Millilitre

MITI	Ministry of International Industry
min	Minute
mol/L	Mole Per Litre
KH_2PO_4	Monopotassium Phosphate
nm	Nanometre
%	Percentage
rpm	Rate Per Minute
SEM	Scanning Electron Microscopy
NaOH	Sodium Hydroxide
TGA	Thermo-gravimetric Analysis
IMP3	Third Industrial Master Plan
TDS	Total Dissolved Solids
TSS	Total Suspended Solids
UV-Vis	Visible and Ultraviolet Spectroscopy
VM	Volatile Matter
V	Volume
cm^{-1}	Wavenumber

CHAPTER 1: INTRODUCTION

1.1 Background of Study

1.1.1 Dye Effluents

With the rapid development of the textile industries and population growth, a large amount of dye effluent is produced every year due to improper processing. This associated wastewater pollution has aroused widespread concern (Kaur *et al*., 2008). The textile industry is a very complex industry and the dye wastewater treatment is one of the important issues faced by textile manufacturers. Dyes are usually synthetic and have complex aromatic molecular structure, hence, dye molecules are stable and difficult to be biodegraded (Gupta, 2009). If the treatment is not effective, it will cause serious water pollution. Since the textile industry uses a variety of dyes in their processes and not all dyes can be transferred onto the fabric (Yasmin, 2004). Hence, residuals will lead to the production of coloured wastewater. A large amount of dye wastewater is produced in the different steps during dyeing and finishing processes (Babu *et al*., 2007). The dye effluent is characterized by strong colour, high pH, temperature, chemical oxygen demand and biodegradable materials, therefore, it belongs to organic wastewater (Syafalni *et al*., 2012). The coloured wastewater has become one of the chief causes of environment pollution as millions tons of highly coloured wastewater are emitted into the environment and these industries include plastics, textiles, paper, printing, cosmetics, dye manufacturing and leather industries (Chatterjee *et al*., 2009). Report shows that nearly 10,000 different known commercial dyes and pigments with total worldwide annual production over 7 x 105 tons are estimated to be lost in industrial effluents during the dyeing processes for about 5-10% of dyestuffs (Garg *et al*., 2004; Sen *et al*., 2011). The dye effluents are highly visible and toxic, even with very minimum amount (Alkan *et al*., 2004).

1.1.2 Environmental Impacts of Dye Effluents

The release of dyestuffs from textile industries contains many hazardous substances, which can cause serious environment problems, not only toxic to microorganisms but also have a variety of negative effects on human health. The coloured wastewater is objectionable aesthetically pollutant, it has adverse effect on the environment and marine life by its blocking the light to penetrate into the water (Soni *et al*., 2012; Giwa *et al*., 2013; Sheng *et al*., 2009). Thus, it is not conducive for water self-purification and also easily lead to visual pollution. They can persist in the environment as they are highly stable against light, water, soap, chemicals, temperature, detergents and other parameters such as bleach and perspiration (Couto, 2009). In Malaysia, effluent from textile industry contains many pollutants which impose a lot of negative impacts on the environment and human health. In addition, the workers in the textile industry are exposed to high risk of not only malfunctioning of reproductive system, brain, liver, kidney and central nervous system but also vulnerable to bladder cancer due to toxic effects of some dyes being used in the textile industry (Kadirvelu *et al*., 2003; Singh & Chadha, 2016). Hence, it is important that these wastewaters are treated before released into the environment and the discharge of dye effluent must be strictly controlled. The need to remove colour from dye effluent has become very important to the environment and researchers are investigating and trying to develop more options to prevent the environment from further deterioration.

Methylene blue is one of the most commonly used cationic dyes, which is mainly used for silk, cotton, wood and other materials dyeing process. However, methylene blue can cause eyes burns to both human and animal, which likely to cause permanent damage to their eyes (Tan *et al*., 2008). In addition, methylene blue in human can also cause heart rate increasing, cyanosis, jaundice, vomiting, shock, Heinz body formation and tissue necrosis (Vadivelan & Kumar, 2005). Congo red is a known anionic dye that can cause an allergic reaction and can be metabolized into a known human carcinogen, namely benzidine (Zhang *et al*., 2011). Therefore, there is an escalating concern to focus on the removal of such dyes from water bodies.

1.1.3 Dye Removal Techniques

At present, various conventional methods have been widely used for the treatment of dye wastewater which includes chemical, biological and physical processes. However, most of these conventional methods have some limitations. For example, a large amount of sludge is produced at the end of the process, which creates problems in sludge disposal and high treatment costs (Ghoreishi & Haghighi, 2003).

(A) Chemical Treatments

Coagulants and flocculants are the main agents used in the chemical treatment of dye wastewater (Shi *et al*., 2007). Flocculants are formed by the addition of several substances such as calcium, ferric ions and aluminium to the effluent (Zhou *et al*., 2008). Generally, chemical treatment is economically feasible and efficient, but the main drawback is the high cost of chemicals and the price of chemicals in the global market are greatly fluctuating due to the escalating demand and low production of chemical rate. In addition, despite its efficiency, the overall disadvantage of chemical treatment is the ending stage that generates huge amount of sludge, which creates problems in sludge disposal (Lee *et al*., 2006).

(B) Biological Treatments

There are many methods of biodegradation currently used to remove colour and organic matter from wastewater. Generally, it is easy to apply the adsorption of living or dead microbial biomass, bioremediation systems, fungal decolourization and microbial degradation. Biological treatment methods can be divided into aerobic and anaerobic treatments according to the oxygen requirements (Bhattacharyya & Sharma, 2004). However, many dyes are difficult to be biodegraded by conventional biological processes as the structure of most commercial dye compounds are generally complex with its chemical properties and the molecular size of dyes (Kim *et al*., 2004). The main disadvantage is that it requires considerable land area and is limited by the sensitivity of chemical toxicity and diurnal variation (Crini, 2006). Robinson *et al*. (2001) noted that the current conventional biological techniques may not result in eliminating colour successfully (Robinson *et al*., 2001). Besides, dyes such as azo are not easy to be degraded due to their synthetic organic origin, xenobiotic properties, and complex chemical structure. The conventional biological methods in removing basic dyes are effective, but not for complex dyes (Banat *et al*., 2007).

(C) Physical Treatments

Among the treatment in the physical process are reverse osmosis, electrolysis, membrane filtration and adsorption techniques. The membrane filtration draws several limitations, such as its limited lifecycle for its membrane. For the analysis of economic viability, the cost of periodic replacement must be added to ensure the sustainability of the process. Among all the physical treatments, adsorption has been proven as a most effective and reliable separation technique for removing dyes from wastewater and such effective technology has been frequently applied due to its relatively less investment, simple design, easy operation and insensitivity to toxic substances characteristics (Sen *et al*., 2011; Yao *et al*., 2009). A major concern of adsorption technique is the choice of the adsorbents used. The adsorbent that is commonly used is activated carbon. It is efficient for dye wastewater remediation, but the cost of preparing activated carbon is relatively higher than that of biochar. In order to develop economical and effective adsorbents, various unconventional low-cost adsorbents have been widely focused, such as agricultural wastes, siliceous materials, clay materials and industrial waste products (Crini, 2006; Rauf *et al*., 2009). Adsorbent produced from agricultural waste not only will reduce the treatment cost of textile effluent, but also reduce the amount of waste from entering landfill.

1.1.4 Biochar

Recently, many studies have focused on the use of agricultural wastes to produce biochar, which has been used as inexpensive adsorbents to remove dyes from dye wastewater. Bamboo (González *et al*., 2014), fruit shell (Tongpoothorn *et al*., 2011), wool wastes (Gao *et al*., 2013), peanut hull (Zhong *et al*., 2012), sugarcane leaves (Qingye *et al*., 2012) and rice husk (Mianwu *et al*., 2011; Qingye *et al*., 2012) are considered to be the economic sources for the preparation of biochars. Biochar, the solid by-product of slow pyrolysis is produced by undergoing this combustion (biomass) under limited oxygen conditions and at a relatively low temperature (< 700°C) (Sohi *et al*., 2010; Joseph & Lehmann, 2009). Biochar has abundant pore structure, large specific surface area, surface functional groups, high charge density and high surface negative charge characteristics (Liang *et al*., 2006; Laird *et al*., 2009). These properties of biochar make it be used as an adsorbent to adsorb contaminants (Zhang *et al*., 2013; Meng *et al*., 2014). As a result, pyrolysis essentially not only reduces pollutants but also produces environmentally friendly products. In this study, the banana stem waste was converted into biochar through pyrolysis technology to determine its adsorption capacity on textile wastewater.

1.2 Problem Statement

In Malaysia, the textile industry is a very well-known and it is one of the fastest growing industries that provides a significant contribution to Malaysia's economic growth. It stands an important role in Malaysia because it meets people’s basic needs and has maintained sustainable economic growth over the years. However, this industry produces dye effluent that contains many pollutants, including dyes and other chemicals that can cause a lot of serious impacts to the environment and human health. Currently, there are many ways to remove dyes from textile effluent includes chemical treatment, biological treatment, and physical treatment. However, chemical methods are rather expensive, limit versatility and require a significant amount of energy. Besides, biological treatment is less flexible in design and the operation requires considerable land area while physical treatment through adsorption process can be considered as a more suitable way and now it is frequently applied in the dye wastewater treatment due to less investment requirement, easy operation, simple design and insensitive to toxic substances characteristics (Yao *et al*., 2009; Sen *et al*., 2011). In the adsorption process, the application of activated carbon in dye wastewater remediation was discovered to have high efficiency due to its high specific surface area and adsorption capacity, but the application is limited by its expensive cost and the more complex production processes.

Many extensive discoveries were done by using non-conventional low-cost adsorbents to develop efficient and cheaper adsorbents, such as agricultural wastes, siliceous material, clay materials, zeolites and industrial waste products (Crini, 2006; Rauf *et al*., 2009). Thus, in this study, adsorption of dye effluent by biochar was selected as the treatment since it is considered to be less expensive and more efficient technique as compared to other technologies. The most important reason for choosing biochar is that it is easier to produce with no harmful substances during and after the treatment. In addition, the waste of banana stem is a potential waste that can be converted into a useful product to contribute in protecting our environment. On the other hand, the banana stem is one of the major agricultural waste in Malaysia in which if it can be utilized properly, it can be a value-added product from waste. Hence, it is essential to develop a comprehensive reuse plan for agricultural wastes. The aim of this study is to convert banana stem from agricultural waste into useful product namely, biochar, and to investigate its potential to remove dyes. This product can reduce pollution potential and be used as an adsorbent to remove dye from the textile wastewater. The results of this study can be used as an energy-saving protocol for highly efficient adsorbent.

1.3 Objectives of Study

There are three main objectives of this study, which include:

(1) To produce and characterize biochar from banana stem.

(2) To determine the preparation conditions of biochars from banana stem.

(3) To investigate the adsorption capacity and process of banana stem and biochars for synthetic and actual dye wastewater.

1.4 Significance of Study

The result of this research is useful due to the following reasons:

(1) Preparation of low cost and highly efficient adsorbents from agricultural waste can help textile industrial to treat dye wastewater efficiently.

(2) Reduction of the amount of banana stem waste and provide a new approach for banana stem wastes reuse.

(3) Reuse of agricultural waste to provide a new approach for the treatment of dye-contaminated wastewater and creates potential economic benefits to the society.

CHAPTER 2: LITERATURE REVIEW

2.1 Textile Industry in Malaysia

The textile industry is one of the fastest developing ventures and provides significant contribution to Malaysia's economic growth. Because a large amount of water and chemicals were consumed in the wet processing phase of the textile industry, the wastewater from the textile industry contains a considerably high amount of colourants and other chemicals. The main pollutants released into the environment by the textile industries are mainly derived from some of their wet processing operations such as dyeing, bleaching, scouring and mercerizing (Radha *et al*., 2009). In these various activities, the dyeing process usually requires the use of large amounts of water and dyes for dyeing, washing and fixing procedures (Rajkumar *et al.*, 2007). Therefore, the main characteristics of textile wastewater are high COD concentration, widely fluctuating in pH, strong colour, large amounts of suspended solids, high temperature, and low biodegradability (Chen *et al.*, 2003).

The Malaysian Industrial Development Authority (MIDA) clarified that the textile industry has turned into the tenth largest contributor to Malaysian manufacturing export earnings contributing approximately 1.7% of total exports of manufactured goods to Malaysia in 2015. Besides, exports of textile products reached RM13.2 billion in 2015 on which includes apparels, yarn and woven fabrics (MIDA, 2015). Malaysian apparel manufacturers have vast experience and continue to maintain an excellent reputation for the production of world-renowned brands reflecting superior quality such as Nike, Adidas, Armani, DKNY, Ann Taylor and Tommy Hilfiger (MIDA, 2015). United States, European Union, Canada, and Turkey are the main exporters for Malaysian textile and apparels, while China, Japan and Taiwan are the main import market. The import of raw materials is mainly used for the production of fabrics and made-up garments of textile yarns, and knitted. The main reason for the import of these materials is due to the lack of quantity and quality of these materials in local supplies (Seong, 2007).

In the early 1970s, when the country begins the export-oriented industrialization, the growth rate of Malaysia's textiles and apparel industries was increasing (MIDA, 2015). In addition, as the global competition intensifies, Malaysian textile manufacturers diversify their value chains to produce more value-added textiles and seeking business cooperation with foreign companies through the implementation of automated and computerized manufacturing processes to obtain new technologies and to implement more research activities to study new processes, newer and more novel applications and value-added products, the industry currently employed more than 68,000 workers (MIDA, 2015). Malaysia’s textile industry consists of these four sub-sectors, namely, primary textiles (involving polymerization, spinning, knitting, weaving and wet processing activities), made-up textiles, made-up garments, and textile accessories. Currently, there are more than 645 licensed companies producing various textile products from fibers, yarns, and fabrics to made-up garments and dyeing, printing, and finishing of yarn and fabrics (Seong, 2007). The textile industry has always been an important industry for the Malaysian economy. Many ongoing investments and new investors indicate that Malaysia still has the sufficient ability to maintain the competitiveness of their domestic and global markets because of the high quality of textiles, and the ability to deliver in a timely manner for the Malaysian textile manufacturers to win an excellent reputation (MIDA, 2015). Most of the projects approved in the textiles and textile products industry are for the export of a large portion of the output. After the implementation of these projects, Malaysia will be able to generate a lot of export earnings amounting to about RM671 million per year (MIDA, 2015). The new growth areas of the textiles industry are encouraged by the Third Industrial Master Plan (IMP3) (MITI, 2006). The industry growth areas include functional fabrics, ethnic fabrics and key support facilities, home and industrial textiles, high-end garments and fabric, services such as design houses and fashion centers, and for specialized dyeing and finishing equipment to name but a few (MIDA, 2015).

2.2 Wastewater from Textile Industry

2.2.1 Textile Wastewater Characteristics

It is estimated that about 280,000 tons of textile dyes from the textile industry are discharged as industrial wastewater into the environment each year worldwide, mainly due to the low efficiency of the dyeing operations (Jin *et al.*, 2007). The amount of wastewater varies according to the type of plant operation process. In addition, a variety of toxic chemicals were used by the wet processes, which mainly consist of dyeing, scouring, mercerizing, bleaching, and finishing (Meriç *et al.*, 2005). The varying procedure for each textile resulted in the generation of different composition of wastewater, that the treatments are greatly differ as well. The wastewater from the textile plant can be classified into (Grande, 2015):

- Wastewater discharged from different processes is characterized by low flow rate and high loads of pollutants, such as dyeing, bleaching, desizing, printing and other processes.
- Wash-off water has the characteristics of high flow rate and medium pollutant load.
- The temperature of the cooling water can be viewed as the unique pollution parameters.

Figure 2.1 shows the percentage of water used in the wool production chain from weaving, finishing, spinning and dyeing (Grande, 2015).

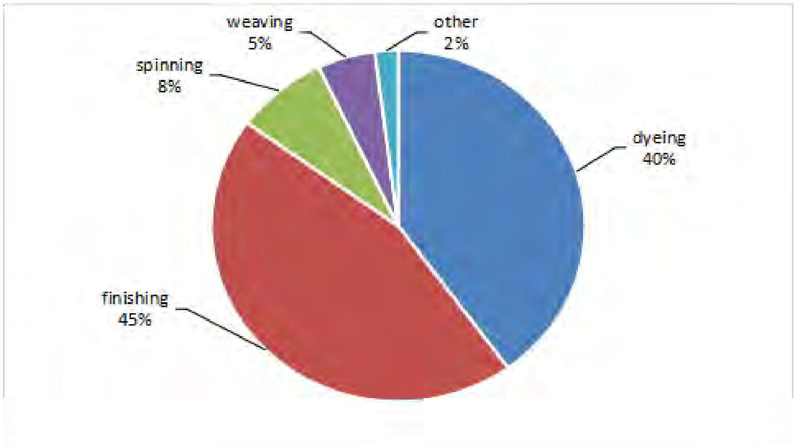

Figure 2.1: Percentage of water usage for a wool milling process (Grande, 2015)

The characteristics of the textile wastewater vary greatly according to the types of inorganic and organic compounds used in each procedure. Typically, the wastewater contains obvious colour (mainly from the dyes that are not fixed on the fibre during the dyeing process), high COD concentrations (due to the presence of organic molecules such as dyes, dyeing auxiliaries and surfactants) and some dye structures that typically contain heavy metals (Chen *et al*., 2003). In addition, there are a number of chemicals used to adjust the pH of solution, which is also included in the textile wastewater, such as salts, acids, bases, and buffers. The processes involved in textile dyeing and printing are pre-treatment, dyeing/printing, finishing and few other technologies. In the pretreatment process, desizing, scouring, and washing are among the steps required. During the pretreatment, it produces pollutants that are resulting from pulp, alkali, cotton gum, hemicellulose, and cellulose process. The dyes and additive used in printing also contribute to the pollutions (Ashfaq & Khatoon, 2014). The main purpose of dyeing is to dissolve the dye in water and to transfer it to the fabric under certain conditions to produce coloured fabrics. Printing is categorized as part of dyeing and is usually defined as ‘localized dyeing’. Besides, all the process in finishing contributes to water pollution. Bleaching is an important process in the textile dyeing industry, which can comprise of hydrogen peroxide bleaching, sodium hypochlorite and sodium chlorite bleaching (Ashfaq & Khatoon, 2014). The potential specific contaminants derived from the dyeing and printing of textiles is presented in Table 2.1 (Allègre *et al*., 2006).

Table 2.1: Specific pollutants from textile and dyeing processes (Allègre *et al*., 2006)

Process	**Compounds**
Printing	Urea, metals, colour, solvents.
Finishing	Resins, softeners, stearate, acetate, spent solvents, waxes, chlorinated compounds.
Mercerizing	High pH, NaOH
Dyeing	Colour, metals, salts, surfactants, sulphide, formaldehyde, organic processing assistants, acidity/alkalinity.
Desizing	Sizes, ammonia, starch, waxes, enzymes.
Scouring	Disinfectants and insecticides residues, NaOH, sizes, soaps, waxes, enzymes, pectin, oils, fats, surfactants, spent solvents, antistatic agents.
Bleaching	H_2O_2, high pH, organic stabilizer or sodium silicate, AOX.

Composite textile wastewater is characterized by a high COD concentration, broad pH fluctuations, strong colour, high temperature, a large number of suspended solids and low biodegradability within the environment of the water due to the extreme fluctuations in many pollutants (Chen *et al*., 2003). The composition of the wastewater primarily depends on the degree of the use of different dyes, chemicals, and organic compounds in the dyeing and wet processes (Santos *et al*., 2007). The main pollutants in textile wastewater are toxicants, coloured and chlorinated compounds, recalcitrant organic, surfactant, and salts (Mansour *et al*., 2012). A composite wastewater from an integrated textile mill is composed of the following contaminants that include dyes, pigments, starches, soap, dextrin, detergents, fatty acids, sulphides, gelatine, waxes, pectin, glucose, carbonates, chlorides, and resins (Mansour *et al*., 2012). Typical features of textile industry effluent are shown in Table 2.2 (Kdasi *et al*., 2004).

Table 2.2: The typical features of textile effluent (Kdasi *et al*., 2004)

Parameters	**Values**
pH	7.0 - 9.0
Temperature (°C)	35 – 45
Chemical Oxygen Demand (mg/L)	150 - 12,000
Biochemical Oxygen Demand (mg/L)	80 - 6,000
Total Dissolved Solids (mg/L)	2,900 -3,100
Total Suspended Solids (mg/L)	15 - 8,000
Total Kjeldahl Nitrogen (mg/L)	70 – 80
Colour (Pt-Co)	50 – 2500
Chloride (mg/L)	1000 – 1600
Sodium (mg/L)	6,000

2.2.2 Toxicological and Environmental Considerations

Discharge of industrial wastewater under uncontrolled and inappropriate conditions caused serious environmental problems. If the wastewater from the textile mill is discharged directly into the local environment without any pre-treatment, it will seriously affect the lands and natural water bodies in the encompassing zone due to its high contents of colour and organic matter. Dye is a colouring material capable of applying colour onto substrate in a solution, thereby imparting a colour appearance to the textile products. Even if only a small amount of dye is discharged into the water resources, the colour will still have certain impacts on the aquatic life and food web (Ashfaq & Khatoon, 2014). The coloured effluent does not only bring about toxicity but has an adverse aesthetic effect on receiving water bodies as well. This is so because the coloured effluents contain visible contaminants. The visible contaminants contained in these coloured effluents can cause significant harm to human beings. So the removal of colour from the coloured effluent becomes an important aspect to ensure a healthy environment (Verma *et al*., 2012).

Common organic pollutants in the textile wastewater include sediments, oil, high values of BOD_5 and COD, grease and particulate matter. When these organic pollutants are released into the receiving water bodies, this can lead to the depletion of dissolved oxygen. This situation will have a lot of negative impacts on the aquatic ecosystem. Besides, textile wastewater also contains chromium with a cumulative effect and is more likely to enter the food chain (Ashfaq & Khatoon, 2014). The result of the use of large quantities of dyes and chemicals in the processing of the textile mills means that the colour of the effluent is dark, which not only increases the turbidity of the water body but also makes it aesthetically displeasing. On the other hand, the colour interferes sunlight penetration through the water bodies, which in turn will weaken the process of photosynthesis, leading to changes in the habitat of aquatic life (Ashfaq & Khatoon, 2014). Even at low concentration, dyes can impact on the aquatic life and food web. Furthermore, eutrophication was occurred due to the coloured allergens may experience chemical and biological assimilations, depletion of dissolved oxygen, inhibition of the system's re-oxygenation capacity and chelate metal ions, and acceleration of genotoxicity and micro-toxicity (Verma *et al*., 2012). Additionally, dyes can be amassed on the places where wastewater is being discharged then it would affect the stability of the aquatic system. These contaminants can also be leached from the soil and can affect the groundwater system (Namasivayam & Sumithra, 2005). Sporadic and excessive exposure of dye effluents to the human body not only greatly reduces the immune defense ability, but can also cause reproductive system, kidney dysfunction, central nervous system and liver brain (Kadirvelu *et al*., 2003). EPA (2004) also demonstrated that organic pollutant BOD or COD discharged into the receiving water bodies will likely lead to the depletion of dissolved oxygen in the water to form an anaerobic condition. Foul-smelling compounds such as hydrogen sulphides can be produced under anaerobic condition, leading to the destruction of the biological activity of the receiving water bodies (EPA, 2004). Table 2.3 summarizes the major direct/indirect influences of dyed wastewater to the environment (Verma *et al*., 2012).

Table 2.3: The effects of dyed wastewater to the environment (Verma *et al*., 2012)

Direct effects	**Indirect effects**
Aesthetically displeasing	Eutrophication
Interferes with the ability of the sunlight penetration: damage of aquatic life	Coloured allergens accelerate genotoxicity and microtoxicity
Inhibit the system's re-oxygenation capacity	Reduce the immune defense ability of human beings
Groundwater pollution	Killing aquatic life

2.3 Dye

Dyes are considered to be one of the most significant pollutants and are known as 'visible pollutants'. Historians are accustomed to use fur, textiles and other natural substances (mainly vegetables, but also animal sources) to produce dyes. According to Saxena and Raja (2014), dyes are not only come from natural sources, but also produce by synthetic dyes. In the contemporary competitive marketplace, almost every textile industry uses dyes to colour their goods. It is reported that nearly 10,000 different known commercial dyes and pigments have a total global annual output of more than 7 x 10^5 tons and it is estimated that 5-10% of the dyestuff in the industrial effluents are lost during the dyeing processes (Garg *et al.*, 2004). The development of the dye industries has been inseparable from the textile industry. In Malaysia, there is an extensive use of dyes in the textile industry in general and batik industry in particular.

2.3.1 Composition of Dyes

Dyes contain a lot of specific groups that give colour, which are of the chromophore and auxochromes groups (Lam, 2005). The main function of the chromophore groups is to produce the colour and the auxiliary pigments that not only complement the chromophore but also give the molecule the ability to dissolve in water. Besides, because of their ability to absorb a portion of the visible light, it gives a stronger affinity for the fibres (Gupta, 2009). In general, the chromophore groups are predominantly the following groups:

- –C=O (carbonyl)
- –C=C– (ethenyl)
- –CH=S (thiocarbonyl)
- –C=N– (imino)
- –N=O (nitroso)
- –N=N– (azo)

The number of these previous groups can be used to determine the intensity of the colour. A compound containing a chromophore group of benzene is called a chromogen. Auxochromes (-NH_3, -COOH, -SO_3H and -OH) other than the chromophore also make the molecule soluble in water and improve the affinity for fibres (Zahrim *et al.*, 2011).

Furthermore, depending on the chromophores of the dyes, the dyes can be divided into 20 to 30 different groups. As shown in Figure 2.2, the most important dyes are the azo, anthraquinone, phthalocyanine and triaryl methane dyes. Azo dyes accounted for about 70% on a weight basis of the world's total annual production (Santos *et al*., 2003).

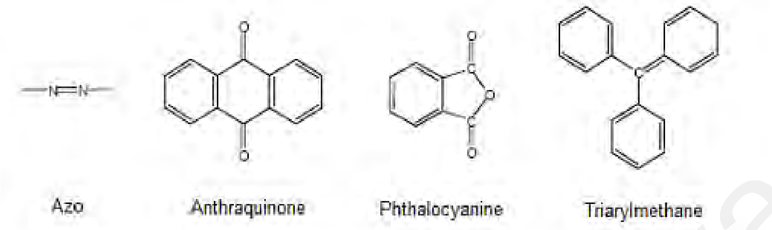

Figure 2.2: Most important chromophores (Santos *et al*., 2003)

2.3.2 Classification of Dyes

Normally, dyes can be classified by two different principles, namely chemical structure and application areas of dyeing methods (Hunger, 2007). The former method is carried out by dye chemists using azo dyes, phthalocyanine dyes, and anthraquinone dyes. The latter method is mainly implemented by the dye technologists that used phthalocyanine reactive dyes for cotton and azo disperse dyes in polyesters (Hunger, 2007). In addition to the above, dyes also can be classified according to their particle charges when dissolved in an aqueous application medium, such as cationic, anionic, and non-ionic (Robinson *et al*., 2001). Fu and Viraraghavan (2002) stated that basic dyes are usually cationic dyes in nature whereas reactive, acid and direct dyes are intrinsically anionic dyes. Nonionic dyes are dispersed dyes because they do not ionize in an aqueous medium. Moreover, the main chromophores in nonionic and anionic dyes are anthraquinone types or azo groups (Fu & Viraraghavan, 2002).

(A) Chemical Structure

There are two advantages to the classification of dyes through chemical structure. Firstly, it is easy to identify the dye as a group with characteristic properties such as that azo dyes are strong, possess good overall performance and are cost effective while anthraquinones dyes are weak and expensive. Secondly, there are a few (about a dozen) chemical groups for structural changes. The classification of the common categories of dyes as indicated by the chemical structure and is shown in Table 2.4 (Ali, 2010).

Table 2.4: The dyes classification according to the chemical structure (Ali, 2010)

Class	Chromospheres	Example
Azo dyes		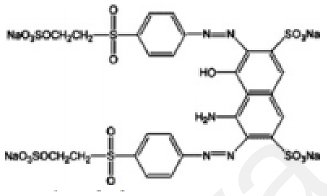 Reactive Black 5
Anthraquinone dyes	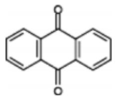	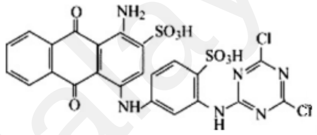 Reactive Blue 4
Indigoid dyes	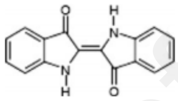	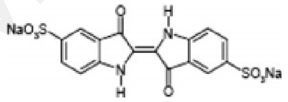 Acid Blue 71
Nitroso dyes	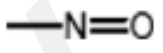	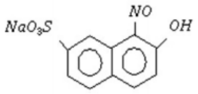 Acid green 1
Nitro dyes	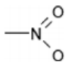	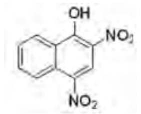 Acid Yellow 24
Triarylmethane dyes	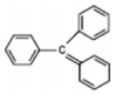	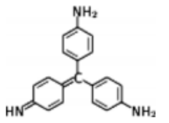 Basic Red 9

(B) Usage or Application

Colour Index is one of the most well-known systems of classification that is being used internationally. Most dyes are used for dyeing the cotton, polyester, and polyester-cotton blends due to the fact that cotton and polyester are the most important textile fibres. Other textile fibres are nylon, cellulose acetate, and polyacrylonitrile. The application categories of dyes are summarized in Table 2.5 (Chun, 2010).

Table 2.5: The application categories and their chemical types of dyes (Chun, 2010)

Class	Substrate	Method of Application	Chemical types
Acid	Wool, inks, silk, paper, nylon, and leather.	Usually from neutral to acidic bath	Azo (including premetallized), anthraquinone, triphenylmethane, xanthene, azine, nitro and nitroso
Basic	Modified nylon, polyacrylonitrile, inks, paper, and polyester	Applied from acidic dye baths	cyanine, hemocyanin, diaza Hemi cyanine, diphenylmethane, triaryl methane, xanthene, azine, azo, oxazine, acridine and anthraquinone
Reactive	Wool, silk, cotton, and nylon	Reactive site on dye reacts with functional group on fibre to bind the dye covalently under influence of heat and pH (alkaline)	Anthraquinone, oxazine, formazan, basic, phthalocyanine and azo
Direct	Rayon, paper, nylon, leather, and cotton	Applied from neutral or slightly alkaline baths containing the additional electrolyte	Azo, stilbene, oxazine, and phthalocyanine
Disperse	Acrylic, acetate, plastic, polyamide, and polyester	Fine aqueous dispersions often applied by high temperature/pressure or lower temperature carrier methods; dye may be padded on cloth and baked on or thermal fixed	Azo, nitro, styryl, anthraquinone, and benzo difuran one
Solvent	Varnishes, inks, stains, lacquers, gasoline, fats, plastics, waxes, and oils	Dissolution in the substrate	Azo, phthalocyanine, anthraquinone, and triphenylmethane
Sulfur	Rayon and cotton	Aromatic substrate vatted with sodium sulfide and reoxidized to insoluble sulfur-containing products on fiber	Indeterminate structures
Vat	Rayon, wool and cotton	Water-insoluble dyes solubilized by reducing with sodium hydrogensulfite then exhausted on fiber and reoxidized	Indigoids and anthraquinone (including polycyclic quinones)

2.4 Treatment Technologies of Textile Wastewater

As many dyes have a negative impact on human beings, it is necessary to study some appropriate technologies to remove the colour from effluents or processes to ensure a healthy environment. The textile wastewater treatment is quite difficult due to the multi-component wastewater and because it contains many contaminants that can vary daily and even hourly, make it very difficult to handle (Arumai, 2008). Some of the plants do not go through some pretreatment technologies to treat their wastewater and directly discharge their wastewater into the environment. This situation not only leads to environmental pollution but also results in the production of their products being not economical. In Malaysia, the discharge standard is shown in the Third Schedule Environmental Quality Act, 1974 - Environmental Quality (Sewage and Industrial Effluents) Regulations, 1979. At present, there are many methods to treat the dyed effluent. According to the size of plant, the type of waste, and the degree of pollution, the treatment method varies from plant to plant. Generally, the technologies used for the decolourization of textile wastewater can be divided into biological, physical and chemical methods, as shown in Table 2.6 (Foo & Hameed., 2010).

Table 2.6: Existing and Emerging dyes removal processes (Foo & Hameed., 2010)

Physical/Chemical Methods	**Method Description**	**Advantages**	**Disadvantages**
Fenton reagents	Oxidation reaction using mainly H_2O_2-Fe(II)	Effective decolourization of both soluble and insoluble dyes	Sludge generation
Ozonation	Oxidation reaction using ozone gas	Application in gaseous state: no alteration of volume	Short half-life (20 min)
Photochemical	Oxidation reaction using mainly H_2O-UV	No sludge production	Formation of by-products
NaCl	Oxidation reaction using Cl_+ to attack the amino group	Initial and acceleration of azo bond cleavage	Release of aromatic amines
Electrochemical destruction	Oxidation reaction using Electricity	Breakdown compounds are non-hazardous	High cost of electricity
Activated carbon	Dye removal by adsorption	Good removal of a wide variety of dyes	Regeneration difficulties
Membrane filtration	Physical separation	Removal of all dye types	Concentrated sludge production
Ion exchange	Ion exchange resin	Regeneration: no adsorbent loss	Not effective for all dyes
Electro kinetic coagulation	Addition of ferrous sulfate and ferric chloride	Economically feasible	High sludge production

2.4.1 Biological Methods

In comparison to physical and chemical processes, the application of biological treatment is relatively cheap (Kim *et al*., 2004). Biological treatment methods are diversified such as trickling filters, anaerobic process, activated sludge process.

Biological treatment methods can be classified into aerobic and anaerobic treatments according to the oxygen requirements (Bhattacharyya & Sharma, 2004). Aerobic biological treatment is often applied in conventional biological treatment based on its high efficiency. However, the main disadvantage is that it uses considerable land area amount and is affected by the diurnal difference and toxic in chemical (Crini *et al*., 2007). In the process of activated sludge after the initial precipitation, wastewater is allowed to be flowed into a tank and the microorganisms are suspended in the wastewater as aggregates in the activated sludge. Compresses air suspend the sludge and wastewater by providing ample oxygen for biological activities. The aerated waste is withdrawn and settled. A feedback mechanism draws a segment of the sludge to return to the influent (Kornaros & Lyberatos, 2006). Commonly used biodegradation methods for industrial wastewater treatment include microbial decolourization, adsorption by (living or dead) microbial biomass, fungal decolourization and bioremediation systems. Numerous microorganisms such as yeasts, fungi, algae, and bacteria are equipped for accumulating and degrading distinctive dyes but their applications are often limited to some techniques (Bekchanov *et al*., 2012). The important factors of safe handling of severely hazardous organic wastes are the reasonable cost and the use of environmentally acceptable methods. There is no doubt that biological processes may meet the requirements, which states that it can still be used as a basic treatment method to deal with most of the organic wastewaters. However, some contradictory results were reported in the current technical review (Robinson *et al*., 2001), which indicates that biological treatment does not always achieve satisfactory results, and is ineffective in colour elimination using current conventional technology. Among the reasons are many commercial dyes may cause sludge expansion, sludge rising, and are toxic to the organism, and because some chemical and related industries' production of many organic substances are inhibitory, toxic or resistant to biological treatment (Ahn *et al*., 2013). It has been demonstrated that biological methods may be effective to reduce chemical oxygen demand and remove suspended solids, but is significantly ineffective in terms of colour removal (Rai *et al*., 2005).

2.4.2 Coagulation/Flocculation

The coagulation and flocculation processes are commonly used alone or in combination with biological treatments to eliminate organic matters and suspended solids, as well as, to effectively remove colour from textile effluent (Meriç *et al.*, 2005). Aluminum, sulphate, ferrous sulphate and ferric chloride are the coagulants that are often used in conventional wastewater treatment processes. The coagulants/flocculants are the main agents for chemical treatment of dyed wastewater (Shi *et al*., 2007). It leads to the formation of flocs after these substances such as aluminium, ferric ions, or calcium are added into the wastewater (Zhou *et al*., 2008). Commonly used coagulants are alum or ferric chloride. Although electrokinetic coagulation can remove small colloidal particles, it is not suitable to remove a wide range of dyes. The coagulation-flocculation treatment can be effectively used to remove disperse, sulfur and reactive dyes. However, they form fewer flocs with other types of dyes. The main drawbacks are that the process requires a lot of chemicals and a large amount of sludge will be produced. Excessive use of chemicals can cause a secondary pollution problem, produce a large amount of sludge during the process and become the pollutant itself. Thus, increases the treatment cost further (Ahn *et al*., 2013).

2.4.3 Ion-exchange Resins

Dyes are categorized as cationic and anionic. Therefore, these dyes can be combined with the ion-exchange resins to form complexes that can be separated by filtration, called flocs (Verma *et al*., 2012). Although this technology has shown good results in the absorption of dyes, its regeneration is still quite difficult (Grande, 2015). The main drawbacks are the low hydrodynamic properties and large amounts of sludge will be generated. Compared with activated carbon, the resin is intolerable to high pressure which requires a large volume of liquid, at a high liquid flow rate through the bed. The end product of sludge needed to be incinerated or dump, which will end up as air pollution and disposal in landfill which are costly (Gupta, 2009). Grande (2015) reported that the ion exchange system enables decolourization of the diluted mixture of coloured wastewater samples. Nevertheless, the regeneration of this technology is not possible due to the fact that the colourant was irreversibly adsorbed onto the resin, hence, this technology also seems to have little effect on the treatment of wastewater. The success of testing the application of ion exchange-macroreticular polymer system might have been realized, but because the estimation of the initial cost, the need for off-site resin regeneration and secondary waste disposal cause technology is limited to coloured wastewater treatment (Morali, 2010). Robinson *et al*. (2001) also stated that ion exchange is not suitable to treat dye-containing effluents because of high cost and its ineffectiveness for disperse dyes.

2.4.4 Separation Techniques

Separations techniques including nanofiltration, ultrafiltration, and reverse osmosis are often used in chemical recovery and water reuse applications. For example, reverse osmosis can be very effective in separating salts from water (Babu *et al*., 2007). Ultrafiltration and nanofiltration techniques are effective in removing dyes, but they also have some restrictions, such as the high cost of investment, rapid membrane fouling and concentrated baths production which requires to be further processed, these constraints affect the widespread use of membrane technology (Zhang *et al*., 2011).

(A) Membrane Filtration

Membrane filtration is the method to filter and separate certain substances in the wastewater using the membrane's micropores and the selective permeability of the membrane. Membrane-based separation processes have gradually become an effective way to remove pollutants from textile wastewaters (Ahmad *et al*., 2002). But, the use of membrane filtration technique is still limited because the membrane filtration has a very limited lifetime before membrane fouling occurs and the initial investment cost is high due to the periodic replacement of membrane being extremely high (Joshi *et al*., 2004).

(B) Ultrafiltration

The pore size of the ultrafiltration is only about 1 nm to 0.05 µm, which makes it possible to eliminate macromolecules and particles, but the removal of dyes has never been completed (Zhang *et al*., 2011). In the textile industry (rinsing and washing) 40% of the treated water by ultrafiltration technique can be repeated during a process known as "minor" of which salinity is not considered as a problem (Babu *et al*.,2007). The only usage of ultrafiltration is for reverse osmosis pretreatment or combining with bioreactor. The high molecular weight and insoluble dyes such as indigo and disperse, auxiliary chemicals, and water can be recycled by ultrafiltration in an effective manner. On the other hand, removal of low molecular weight and soluble dyes such as reactive, acid and basic cannot be done by this method (Babu *et al*.,2007). Fersi *et al*. (2005) asserted that applying reverse osmosis and nanofiltration are the best substitutions for removing the colours in the wastewater.

(C) Reverse Osmosis

For most types of ionic compounds, the reverse osmosis membrane has a retention rate of 90% or more and produces high-quality permeate (Kumar *et al*., 2013). The decolourization of wastewater by chemical auxiliaries can be implemented by reverse osmosis in a single step. All hydrolyzed reactive dyes and chemical auxiliaries in the wastewater can be effectively removed by reverse osmosis. It is significant to note that the higher dissolved salt concentration, the more energy is required for the separation process, and the more important the osmotic pressure becomes (Babu *et al*., 2007).

(D) Nanofiltration

Nanofiltration can also be used to treat coloured wastewater. The combination of adsorption and nanofiltration is an effective treatment. The adsorption process is carried out prior to nanofiltration since this sequence reduces polarization concentration during the filtration process, thereby increasing the output of the process. Nanofiltration membrane maintains large monovalent ions, low molecular weight organic compounds, dyeing auxiliaries and hydrolyzed reactive dyes. Many researchers have found that nanofiltration treatment as an alternative is quite satisfactory (Wang *et al*., 2011).

(E) Microfiltration

Microfiltration is a type of physical filtration process which is often used in combination with various other separation methods such as ultrafiltration and reverse osmosis. The pore size of microfiltration, which is about 0.1 to 1 μm, is appropriate to treat the dyed bath and a subsequent rinsing bath (Wang *et al*., 2011). However, microfiltration cannot filter the chemicals used in the dye bath and these chemicals will persist in the bath. Microfiltration can be applied as the pretreatment for reverse osmosis or nanofiltration (Babu *et al*., 2007).

2.4.5 Adsorption

The adsorption process has been considered as an economical and effective method to remove dyes, pigments and other colourants (Joshi *et al.*, 2004). The adsorption technology is superior to other wastewater treatment technologies and is currently the most popular research topic. The advantages of adsorption process include low initial costs, easy operation, simple design and not sensitive to toxic substances (Garg *et al.*, 2004). The term adsorption refers to the accumulation of adsorbate (usually a liquid phase or gas phase) on the surface of an adsorbent (solid). The term of this reverse process is desorption. The adsorbent surface area, solution pH, temperature, initial dye concentration, contact time and particle size are the main factors affecting the dye adsorption. According to Grande (2015), high affinity for target adsorbates is the main criteria for selecting adsorbents, in order to improve economic efficiency, he emphasized that the adsorbents should have high regeneration capacity (Grande, 2015). The basic process of adsorption theory is illustrated in Figure 2.3 (Worch, 2012).

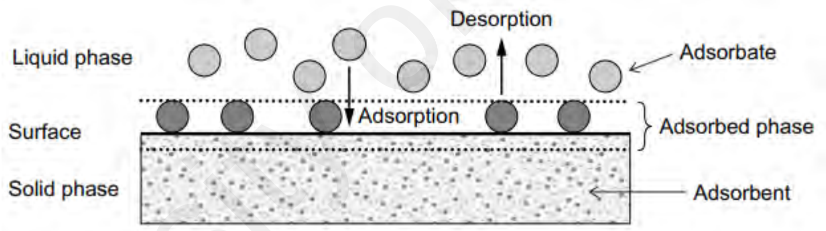

Figure 2.3: The basic process of adsorption (Worch, 2012)

The two types of adsorption are chemical adsorption and physical adsorption. According to Wang *et al*. (2011), due to the exchange of electrons, when there is a formation of strong chemical bonds on the surface of the adsorbate and adsorbent, the reaction is called chemical adsorption which is an irreversible reaction (Wang *et al*., 2011). It is described to have (Jaafar, 2006):

(a) Adsorption occurs in monolayer.

(b) High activation energy.

(c) High temperature.

(d) High enthalpy: $\Delta H \sim 400$ KJ/mol.

(e) Interaction type: strong covalent bond between adsorbate and surface.

In contrast, for physical adsorption, in most cases, the reactions are reversible due to the low energy interactions, it is described by van der Waals forces, dipole-dipole interaction, hydrogen bonds, and the polarities between adsorbates and adsorbents (Grande, 2015). Physical adsorption is defined as physical adsorption of the adsorbate attached to the surface by weakly intermolecular interactions. Physisorption is an effective approach to quickly lower the dissolved dyes concentration in an wastewater (Jaafar, 2006). As indicated by Jaafar (2006), it is described to have:

(a) Adsorption occurs in multilayer.

(b) Low activation energy.

(c) Low temperature, always under the critical temperature of the adsorbate.

(d) Low enthalpy: ∆H < 20 KJ/mol.

(e) Interaction type: intermolecular forces, dipole-dipole interactions, dispersion forces, induction forces (Van der Waals forces).

Table 2.7 demonstrations the differences between chemisorption and physisorption (Jaafar, 2006).

Table 2.7: The differences between chemical and physical adsorption (Jaafar, 2006)

Chemisorption	Physisorption
Selective surface attachment.	Nonselective surface attachment.
Non-reversible.	Reversible can be desorption.
With chemical bonding.	Without chemical bonding.
Monomolecular layer on the surface.	Molecular condensation in the capillaries.

2.4.5.1 Adsorption Isotherms

The fundamental requirements for the adsorption process design are adsorption isotherms. It is delineated by fixed constants having values describing the balance among the quality and adsorbents, adsorption affinity, and properties of the surface and the adsorption capacity of the adsorbent (Lee *et al.*, 2006; Oladoja *et al.*, 2009). Fitting the equilibrium adsorption data into different isothermal models for analysis is a key step in finding appropriate models (Lee *et al.*, 2006). The two well-known isotherms used to carry out the adsorption isotherms are Langmuir and Freundlich. The Langmuir isotherms are used to describe and correspond to the homogeneous monolayer adsorption process where the occupancy occurs at the homogeneous surface with no further adsorption taking place once the active sites are covered with dye molecules (Fytianos *et al*., 2000). However, the Freundlich model assumes that adsorption occurs on a heterogeneous surface containing unequally available sites with different energies of adsorption (Weber & Chakkravorti, 1974).

2.4.5.2 Adsorption Kinetics

In order to explore the adsorption mechanism, adsorption kinetics is necessary because it can predict the removal rate of contaminants from aqueous solutions and provides valuable data to understand the mechanism of adsorption reactions (Li *et al*., 2010). The mechanism and the reaction rate are two important assess factors for an adsorption process operation unit. A large number of attempts have been made in the development of general expressions to define the adsorption kinetics on solid surfaces for the liquid-solid adsorption systems (Shan, 2004). The rate of adsorption is a critical evaluation element for better selection of the material utilized as an adsorbent, and a rapid adsorption rate and a large adsorption capacity are the basic characteristics of an excellent adsorbent (Bharathi & Ramesh, 2013). The residence time required to complete the adsorption reaction is determined by the rate of solute uptake (Bharathi & Ramesh, 2013). Kinetics of adsorption process is mainly used to describe the adsorption rate. The whole adsorption process can be controlled either by one or a combination of more than one step, such as surface diffusion, film or external diffusion, pore diffusion and adsorption on the pore surface (Srivastava *et al*., 2006). In the adsorption kinetics, the pseudo-first-order and the pseudo-second-order models are considered to identify the adsorption isotherm and are typically used to examine and fit the experimental data for adsorbing methylene blue by adsorbents (Tan *et al*., 2008).

2.4.5.3 Factors Affecting Adsorption

(i) Effect of initial dye concentration

The initial dye concentration of a wastewater is one of the vital factors affecting the adsorption of adsorbents. Benaissa (2008) mentioned that decrease in the amount of dye removal is contributed by the increase in the concentration of initial dye. This is because the amount of dye adsorbed for a given mass of adsorbent material is fixed. The higher the dye concentration, the lesser the volume that can be removed. The adsorbent surface for the active sites will be entirely unoccupied, as the concentration of the initial dye is low. The dye adsorption that requires the active sites will be insufficient when the concentration of the initial dyes increases (Kannan & Sundaram, 2001).

(ii) Effect of adsorbent dosage

Dye adsorption is affected by the dosage of the adsorbent which can be achieved by adding different dosages of the adsorbent with a fixed initial dye concentration to prepare an adsorbent-adsorbate solution. Usually, the increasing dye percentage is proportional to the increase of adsorbent dosage (Bharathi & Ramesh, 2013).

(iii) Effect of contact time

The contact time effect on the dye adsorption can be investigated by preparing an adsorbent-adsorbate solution with a fixed adsorbent dose and initial dye concentration at different time intervals. According to Bharathi and Ramesh (2013), the relation of removal rate of dye and contact time is proportional. Usually, the removal rate of dye increases as the contact time increases to a certain extent, and a further increase in the contact time does not increase the uptake (Bharathi & Ramesh, 2013).

(iv) Effect of pH

For the adsorption process, pH is used as a vital parameter. It is used to measure the acidity (pH < 7) or basicity (pH > 7) of an aqueous solution. Önal *et al*. (2006) stated that the magnitude of electrostatic charges imparted by the ionized dye molecules is controlled by the medium pH. Therefore, the change in the pH of an aqueous medium also causes a change in the adsorption rate (Önal *et al*., 2006).

(v) Effect of agitation speed

The agitation speed is also an essential factor for the adsorption process, which will affect the solute distribution in the external boundary film and the bulk solution (Crini *et al*., 2007). In general, the adsorption percentage of dyes increases as the agitation speed increases. The four steps are involved in the mechanism of adsorbate removal (Bharathi & Ramesh, 2013):

(1) Intraparticle diffusion into the interior of the adsorbent.
(2) Adsorption at a site.
(3) Diffusion through the boundary layer toward the adsorbent surface.
(4) The adsorbate molecules migrate from the bulk solution to the adsorbent surface.

(vi) Effect of temperature

Research on the dependence of temperature on the adsorption reactions enables researchers to understand the entropy and enthalpy changes during the process of adsorption (Alkan & Doğan, 2003). An indicator of adsorption nature is temperature, to confirm whether an adsorption process is an exothermic or endothermic (Salleh *et al*., 2011). If there is an increase of adsorption capacity as the temperature increases, the adsorption is an endothermic process. In contrast, when the adsorption capacity decreases as the temperature increases, the adsorption is an exothermic process (Senthilkumaar *et al*., 2006).

(vii) Surface area of adsorbent

Large sizes indicate a greater adsorption capacity as the number of surface area increases (Jaafar, 2006).

(viii) Solubility of solute (adsorbate) in liquid (wastewater)

Less soluble substances are easier and faster to eliminate from aqueous solution (i.e. adsorbate) than high-solubility substances. Nonpolar substances are easier to eliminate from aqueous solution than polar substances since the latter has a better affinity for water (Jaafar, 2006).

(ix) Numbers of carbon atoms

A huge amount of carbon atoms are usually associated with a lower polarity for substances in the same homologous sequence since the higher potential for being adsorbed will be favoured (e.g., the degree of adsorption increases in the sequence formic-aceticpropionic-butyric acid) (Jaafar, 2006).

(x) Size of molecule relative to the size of the pores

The larger the molecules the difficult it becomes to penetrate the small pores. Thus, this will decrease the ability of adsorption independently of other causes (Jaafar, 2006). Smaller particle sizes reduce internal diffusion and mass transfer limitation to the penetration of the adsorbate inside the adsorbent (e.g., equilibrium is more easily achieved and nearly full adsorption capacity can be attained) (Shah *et al*., 2016).

2.4.5.4 Mechanism of Adsorption

The basics of sorption/ion-exchanged kinetics have been established by the Reichenberg (1953) and Boyd *et al*. (1947) who with the help of mathematical treatment abled to distinguish the exchange mechanisms amongst film diffusion, particle and mass-action-controlled (Singh *et al*., 2003). Generally, the external transport is the rate-restracting phase in those systems that include small particle sizes, dilute adsorbate concentration, poor mixing, and high affinity of the adsorbate for adsorbent. In contrast, the intraparticle step is to limit the entire transfer in the opposite systems that have large particle size, high adsorbate concentration, good mixing, and low affinity of the adsorbate for adsorbent (Singh *et al*., 2003). Three consecutive steps are recommended for determining the adsorption of a solid chemical substance on a porous adsorbent (Gupta *et al*., 2004):

(1) The adsorbate ions are moved to the external surface of the adsorbent (film diffusion).

(2) The adsorbate particles are moved into the pores of adsorbent in addition to the small amount of adsorption on the external surface of the adsorbent (particle diffusion).

(3) The adsorbate ions are adsorbed on the interior surface of the adsorbent.

In a condition where external transport < internal transport, particle diffusion will take place. Meanwhile, if external transport > internal transport, film diffusion process will control the adsorption. On the other hand, if external transport = internal transport, the movement of adsorbate ions to the boundary at a significant rate may be impossible, because of the possibility of liquid film forming around the solid adsorption particles (Gupta *et al*., 2004). Mechanism of the dye adsorption based on four-stage mechanism is depicted in Figure 2.4 (Sivakumar & Palanisamy, 2010).

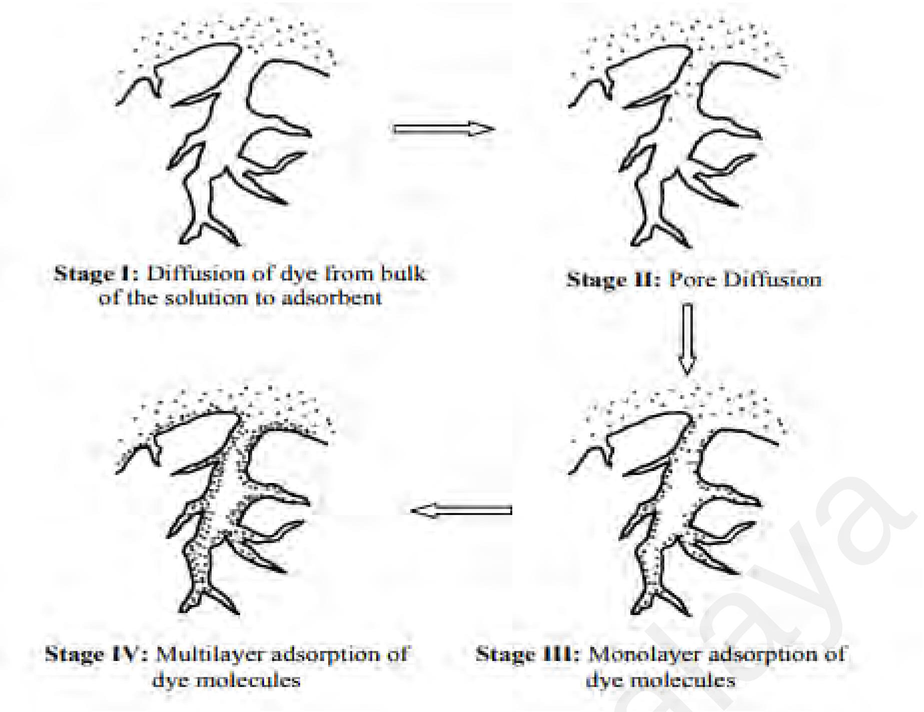

Figure 2.4: Mechanism of the dye adsorption based on four-stage mechanism (Sivakumar & Palanisamy, 2010)

2.4.5.5 Desorption

Desorption studies are beneficial for elucidating the adsorption nature and recycling the dyes and the spent adsorbent. If neutralized water can be used to desorb the adsorbed dye, the dye attached to the adsorbent is through the weak bonds. If acidic or alkaline water can be used to desorb the adsorbed dye, the adsorption is carried out by ion-exchange (Arivoli *et al*., 2009). Mahmoodi *et al*. (2011) investigated the desorption of acid black 26, acid green 25 and acid blue 7 from Pinecone, the result showed that the maximum desorption of acid black 26 and acid blue 7 were more than 90.00%, and acid green 25 was only 26.97%. The crystal violet dye was desorbed from ginger waste by Kumar and Ahmad (2011), it was found that acetic acid was able to desorb about 35-50% of the dye, while NaOH and H_2O did not show any desorption.

2.4.6 Activated Carbon

The adsorption using activated carbon has quickly become a prominent way to remove dyes and a variety of purification and separation processes. The performance of the treatment primarily depends on the characteristics of the effluent and the type of activated carbon used (Joshi *et al*., 2004). Commercial activated carbon is an important adsorbent with high adsorption properties, which can be used to remediate the coloured wastewater and the contaminated groundwater (Joshi *et al*., 2004). Previous studies on the use of commercial activated carbon and coal in the removal of dyes are presented in Table.2.8 (Crini, 2006; Rafatullah *et al*., 2010).

Table 2.8: Removal of dyes by commercial activated carbon and coal (Crini, 2006; Rafatullah *et al*., 2010)

Adsorbents	**Dye**	**q_m (mg/g)**	**Sources**
Commercial activated carbon	Methylene blue	980.3	(Kannan & Sundaram, 2001)
Commercial activated carbon	Basic red 46	106	(Martin *et al*., 2003)
Commercial activated carbon	Reactive orange 107	714	(Aksu & Tezer, 2005)
Commercial activated carbon	Basic red 22	720	(Allen *et al*., 2003)
Activated carbon produced from New Zealand coal	Methylene blue	588	(Qada *et al*., 2008)
Activated carbon-Bagasse	Acid blue 80	391	(Valix *et al*., 2004)
Durian shell activated carbon	Methylene blue	289.26	(Chandra *et al*., 2007)
Activated carbon	Methylene blue	400	(Kumar & Sivanesan., 2006)
Peat	Methylene blue	324	(Fernandes *et al*., 2007)
Coal	Methylene blue	323.68	(Mckay *et al*., 1999)
Picacarb	Methylene blue	246	(Raposo *et al*., 2009)
Charcoal	Methylene blue	62.7	(Banat *et al*., 2007)

The most effective adsorbents to absorb dyes in wastewater are the commercial activated carbon, their porous structure enables their chemical properties and surface areas can be easily changed and improved by chemical treatment. But, activated carbon is very expensive, especially for some small textile enterprises, it is also non-selective and ineffective against vat and disperse dyes (Babel & Kurniawan, 2003). The regeneration of saturated carbon is likewise costly and lead to loss of adsorbents. For most pollution control applications, it is also unreasonable to use relatively expensive starting materials to produce carbon (Rauf *et al*., 2009). Therefore, many researchers have developed a number of effective and unconventional low-cost adsorbents, for instance, using agricultural wastes, siliceous material, clay materials, zeolites and industrial waste products (Crini, 2006; Rauf *et al*., 2009). Besides, "sustainable" biochar has the characteristics of less investment, high regeneration ability, and simple design. Hence, the research of biochar adsorption is attracting more and more attention.

2.4.7 Low-Cost Adsorbents Derived from Agricultural Wastes

In recent years, in order to improve the economics of treatment process, low-cost adsorbents have been widely used to remove dyes from wastewater. The term “low-cost adsorbents” refers to the adsorbents prepared with very little pretreatment to effectively remove the pollutants from the wastewater, rich in nature, and basically are from the agricultural, industry or by-products of common solid waste (Gupta, 2009). Some researchers have shown that adsorbents prepared from agricultural residues are likely to remove dyes from textile effluents in most cases (Kanawade *et al*., 2010). Agricultural waste is almost or without monetary esteem and regularly cause a disposal issue. These materials are abundant in nature and may have potential as adsorbents to adsorb the contaminants in the wastewater due to their physicochemical properties and low cost (Bharathi & Ramesh, 2013). Table 2.9 illustrates some examples of agricultural wastes as adsorbents to absorb dyes from wastewater (Bharathi & Ramesh, 2013).

Table 2.9: Examples of different agricultural wastes as adsorbents to absorb dyes from wastewater (Bharathi & Ramesh, 2013)

Adsorbent	**Dye**	**Maximum Adsorption Capacity (mg/g)**	**References**
Neem leaf	Methylene blue	19.16	(Bhattacharyya & Sharma, 2005)
Citrullus lanatus rind	Crystal violet	11.9	(Suyamboo & Perumal, 2012)
Guava (psidium guajava) leaf powder	Methylene blue	185.2	(Ponnusami *et al*., 2008)
Date pit	Basic blue 9	17.3	(Banat *et al*., 2003)
Rice husk	Methylene blue	40.58	(Vadivelan & Kumar, 2005)
Orange peel	Aid violet	19.88	(Sivaraj *et al.,* 2001)
Straw	Basic blue 9	19.82	(Kannan & Sundaram, 2001)
Coir pith	Congo red	2.6	(Namasivayam & Kavitha, 2002)
Broad bean peel	Methylene blue	192.7	(Hameed & El-Khaiary, 2008b)
Oil palm trunk fibre	Malachite green	149.35	(Hameed & EI-Khaiary, 2008a)
Almond shell	Direct red 80	90.09	(Ardejani *et al*., 2008)
Peanut hul	Reactive dye	55.5	(Tanyildizi, 2011)
Durian peel	Acid green 25	63.29	(Hameed & Hakimi, 2008)
Banana peel	Basic blue 9	20.8	(Annadurai *et al*., 2002)

2.4.8 Banana Stem Waste

Bananas are four most important food crops after rice, maize and wheat. In the tropical and subtropical areas, it is mass produced and consumed in more than 100 countries (Shkuri, 2015). In Malaysia, the total planted area of banana (2001) covers about 33,704.2 hectares (Khalil *et al*., 2007). For decades, banana commercial breeds have increased by 24-27%, where Johor, Pahang, and Sarawak became the largest banana producers with an area of 27,453 hectares in 2009 (Shkuri, 2015). Banana bears fruit only once in a lifetime, and from planting to harvest it takes 10-12 months (Abdullah *et al*., 2013). After harvesting the fruit, the tree will be cut, leaving the bottom part of the stem and rhizome untouched in order to grow new sucker. For every tonne of bananas picked, 100 kg of fruit is rejected and about 4 tonnes of wastes are generated (Abdullah *et al*., 2013). This means that four times of wastes will be produced in each production cycle. Banana wastes range from the leaves, pseudo-stem, empty fruit bunch, peel, and rotten fruit. The stem as the main ingredient is often abandoned on the plantation or processed into low-grade animal feed by local farmers. However, these treatments can lead to serious environmental and ecological problems, such as eutrophication (Abdullah *et al*., 2013). Therefore, it is imperative to find environmentally friendly methods for pollution control and efficient utilization of the waste biomass from banana stem.

Banana wastes can be utilized in many ways. The leaves can be used to wrap food, the rotten fruits and the peels can be used to feed animals, and the stems can be processed into crafts, ropes and textiles. All parts of banana wastes can also be composted as fertilizer and a potential source of energy. In Malaysia, farmers only pick banana fruits for food, and fresh leaves for wrapping food. The rest of the banana plant are dumped as wastes and accumulated in banana growing areas (Abdullah *et al*., 2013). Thus, farmers often face the stems disposal problem. Transforming these wastes into energy should be a good consideration for Malaysian banana culture. Banana waste as a feedstock for energy generation has great potential and it will be an environmentally friendly way to solve the country's agricultural disposal problems (Abdullah *et al*., 2013). In addition, banana stem waste is a lignocelluloses waste, which consists of lignin, cellulose and hemicellulose. By exploiting this waste material, high value compound can be produced at a low cost (Shkuri, 2015). A group of researchers studied the pyrolysis behaviour of four biomass materials: banana stem, bamboo, bagasse and castor oil plant. They found that pyrolytic carbon from banana stem exhibits higher liquid adsorption (Manocha *et al*., 2000). Characterization of lingo-cellulosic materials extracted from the banana stem has also been reported, it was suggested that more studies should be done for thermal conversion on banana waste (Abdullah *et al*., 2013).

2.4.9 Biochar

Generally, the structure of biochar maintains more hydrogen, oxygen, and ash from the biomass since it is less carbonized than activated carbon. Biochar has a great potential to purify water and improve soil quality as it can absorb hydrocarbons, other organic substances, and some inorganic metal ions (Hale *et al*., 2012). Thus, biochar can replace activated carbon as a low-cost adsorbent to remove contaminants and pathogens from wastewater and can be loaded with nutrients for subsequent use as soil amendments to provide long-term adsorption capacity (Bernd *et al*., 2013).

2.4.9.1 Background and Definition of Biochar

The use of biochar to improve soil fertility originated from the ancient Amerindian populations in the Amazon region at least 2500 years ago, locally known as Terra Preta de Indio (Joseph & Lehmann, 2009). The study of the effects of biochar on Terra Preta soils (Hortic Anthrosols) functionalization was revealed in the soils of the Amazonia region (Lehmann, 2009). Since this period, many researchers and farmers around the world have carried out many types of research to explore the secrets hidden in biochars because the biochar has great benefits for soil fertility and sustainability. It has been considered as an excellent soil amendment. Since then, biochar has been considered to play an essential role in the development of sustainable energy production and environmental management (Lehmann, 2009; Joseph & Lehmann, 2009). Biochar is a newly constructed scientific term defined as "a type of carbon-rich product obtained by heating biomass in a sealed container with little or no available air, called pyrolysis" (Joseph & Lehmann, 2009). The biomass is mainly from wood, manure, leaves or wastes generated from industrial activities. Biochar is an adsorbent that is produced by thermal decomposition of organic materials at relatively low temperatures (< 700°C) and limited oxygen supply (Nartey & Zhao, 2014). In recent years, many studies have shown that biochar can be widely used in many fields, for example, to enhance soil fertility, retain nutrients, improve water quality, increase crop productivity and sequester carbon (Liang *et al.*, 2006). In addition, biochar is a good tool to slow down the release of carbon into the atmosphere (Srinivasan *et al.*, 2015). These unique properties make it a highly attractive and powerful tool for mitigating climate change, improving soil quality, increasing agricultural outcomes, combating food shortages and generating green energy (Sohi *et al.*, 2010). As a result, biochar has received increasing attention due to the fact that it cannot only be used as a soil amendment but also as an adsorbent for adsorbing contaminants in the wastewater, an important role in agricultural development and environment remediation (Mohan *et al.*, 2014).

2.4.9.2 Sources of Feedstock for Biochar Production

The production of sustainable biochar is mainly from a variety of biomass resources, but the mass production of biochar can be limited by these biomass resources.

For instance, if the biomass derived from agricultural crops or plantations is used extensively for the production of biochar, it may lead to an increase in soil erosion and a decrease in soil fertility (Cowie *et al*., 2012). Brick and Lyutse (2010) divided the feedstock into the main production of biomass as a resource of bioenergy and biochar, and by-products as waste biomass. Compared with other types of biomass, the waste biomass has cost-effective and food security advantages, hence it has been widely used to produce biochar (Brick & Lyutse, 2010). There are many types of biomass used to produce biochar, such as woody plants, sewage sludge, palm oil sludge and algae waste (Wang *et al*., 2015). Woody plants such as straw and maple contain an important substance, namely lignocellulose. After the fibres contained in these plants are dried up, the remaining material will be lignocellulose. The composition of lignocellulose depends on the resources of biomass. It is mainly composed of cellulose, lignin, hemicelluloses and other substances (Yuan *et al*., 2015). Besides, it has become a hot topic of research in recent years due to the conversion capability of lignocellulose and its potential in bioconversion (Mohammed *et al*., 2011). A variety of feedstocks can produce different types and natures of biochar, so when it is applied to different soil and environmental pollution treatment, they will also produce different effects.

2.4.9.3 Biochar Production Technologies

The preparation of biochar includes the following three important elements (Nartey & Zhao, 2014):

(1) Temperature and time control in the production process.

(2) The selection of feedstock types (such as municipal solid wastes, wood chips, rice hulls, food-processing wastes, animal manure, etc.).

(3) The manufacturing technology (large-scale pyrolysis, gasification and hydrothermal carbonization units, small farm-scale units, etc.).

There are three methods for the production of biochar, namely pyrolysis, gasification and hydrothermal carbonization (Qian *et al*., 2015). These three processes belong to the thermochemical processes of biomass. They not only produce biochar but also produce bio-oil and tar, depending on the process conditions (Qian *et al*., 2015).

(A) Pyrolysis

Pyrolysis is the main pathway for the preparation of biochar, which refers to the thermochemical decomposition of biomass at temperatures of 200°C to 900°C in the presence of little or no oxygen (Demirbaş & Arin, 2002). According to the residence time and temperature, pyrolysis can be divided into three types, namely, fast pyrolysis, intermediate pyrolysis and slow pyrolysis (Mohan *et al*., 2006).

(i) Slow/Intermediate Pyrolysis

The slow and intermediate pyrolysis processes refer to the fact that the biomass is heated at a low heating rate and a relatively long residence time to produce the biochar. The residence time can vary from a few minutes to several hours or even up to several days (Brown, 2009). The vapours in the rapid pyrolysis can quickly escape from the biomass, but the vapours in the conventional pyrolysis do not escape rapidly unlike in fast pyrolysis (Brown, 2009).

(ii) Fast Pyrolysis

Fast pyrolysis is essentially different from slow pyrolysis. Fast pyrolysis is commonly used to produce a high yield of bio-oil while slow pyrolysis contributes to the production of high yield of biochar. Fast pyrolysis requires dry feedstock (< 10% by weight moisture), rapid heat transfers, and rapid rise in temperature by heating small biomass particles during a very short residence time (less than 5s) (Lima *et al*., 2010).

(B) Gasification

Gasification is different from the general pyrolysis process. For gasification, the biomass reacts under controlled oxygen condition and at a temperature above 700°C, which converted into gases rich in carbon monoxide and hydrogen. The resulting gas mixture is referred to as synthetic gas or syngas (Mohan *et al*., 2006). The product yields of fast pyrolysis, slow pyrolysis, and gasification are compared in Table 2.10 (Brown, 2009; Mohan *et al*., 2014).

Table 2.10: Comparison of the product distributions of biomass after pyrolysis and gasification (Brown*,* 2009; Mohan *et al*., 2014)

Mode	**Product Distribution (wt%)**		
	Liquid (bio-oil)	Solid (biochar)	Gas (Syngas)
Fast pyrolysis	70%*	10%	20%
Intermediate pyrolysis	50%*	25%	25%
Slow pyrolysis (carbonization)	30%	35%*	35%
Gasification	5%	10%*	85%*

*Desired product

(C) Hydrothermal Carbonization (HTC) – Hydrochar

Biochar and hydrochar are two different scientific terms. It is important to distinguish between biochar and hydrochar. Hydrochar is produced by hydrothermal carbonization (HTC) of biomass under high temperature and pressure in water, producing a char-water-slurry (Libra *et al*., 2011). The physical and chemical properties of biochar and hydrochar are almost different from the initial biomass. The hydrochar is easy to separate. Hydrochar from agricultural residues is also used for soil and water remediation (Jindo *et al*., 2014). Because of the different chemical properties of hydrochar, it is not included in the ‘‘European Biochar Certificate’’ (EBC) standardization (Wiedner *et al*., 2013). In contrast, biochar is prepared by pyrolysis (slow or rapid) or gasification at different temperatures, pressures and carbonation times. Therefore, the production methods are essentially different. Table 2.11 compares the chemical properties of biochar from gasification or pyrolysis with the hydrochar from HTC, it can be seen that they have the following difference (Wiedner *et al*., 2013).

Table 2.11: The chemical properties of biochar from gasification or pyrolysis with the hydrochar from HTC (Wiedner *et al.*, 2013)

Properties	Hydrochar	Biochar
Stability	Unstable	Highly stable
Dominated compound	Alkyl moieties	Aromatics
Nutrient retention capacity	Higher	Lower

(D) Torrefaction and Rectification

The product obtained by “rectification” is considered to be resistant to biological attack. Its main feature is that the wood "rectification" takes place at a temperature of 230°C to 250°C and the wood colour turns reddish brown/chocolate. Similarly, torrefaction refers to the occurrence of wood at low heating rates and in the temperature range of 250°C to 280°C, which produces a very low-strength brown or black product (Mohan *et al.*, 2014; Antal & Grønli, 2003). Torrefaction greatly reduces the weight of biomass, increases the biomass energy density and enhances its hydrophobic nature. On the other hand, its transportation costs are greatly reduced, which provides great benefits for the commercial use of wood in energy production. Normally, torrefaction and rectification cannot be used to produce adsorbent char because only part of biomass decomposition occurs to avoid rot and cause water loss (Mohan *et al.*, 2014). Table 2.12 summarizes the process of biomass conversion with pyrolysis divided into three types namely fast pyrolysis, intermediate pyrolysis, and slow pyrolysis. Various pyrolysis processes produce different products (Brewer, 2012; Ameloot *et al.*, 2013).

Table 2.12: The results of the conversion of biomass in different thermochemical processes (Brewer, 2012; Ameloot *et al.*, 2013)

Thermochemical Process	Temperature Range (℃)	Heating Rate	Pressure	Residence Time	Desired Product
Slow pyrolysis	350-800	Slow (<10℃ /min)	Atmospheric	Hours-seconds	Biochar
Torrefaction	200-300	Slow (<10℃ /min)	Atmospheric	Minutes-hours	Stabilized friable biomass
Fast pyrolysis	400-600	Very fast (1000℃ /s)	Vacuum-atmospheric	Seconds	Bio-oil
Gasification	700-1500	Moderate-very fast	Atmospheric-elevated	Seconds-minutes	Syngas/producer gas
HTC	175-250	Slow	-	Hours	Hydrochar

2.4.9.4 Characterization of Biochars

The chemical and physical properties (e.g. pore size distribution, particle, and composition) of the biochar are largely dependent on the pyrolysis conditions and the properties of the raw materials, which determine the suitability of biochar in a given application (Khanmohammadi *et al*., 2015). Since the adsorption capacity of biochar is different under different production conditions, the physical, chemical and mechanical properties of biochar show different results as the production conditions change, which also makes the design for carbon sequestration, nutrient storage, water holding capacity, and adsorption of specially optimized biochar very difficult (Sun *et al*., 2012). The International Biochar Initiative (IBI) has divided biochar into three classes in view of the carbon content:

(1) Class 1 biochar contains 60% or more of carbon.

(2) Class 2 biochar has a carbon content of between 30% and 60%.

(3) Class 3 biochar has a carbon content of between 10% and 30%.

The particle size of biomass, and the heating rate and residence time of pyrolysis have significant effects on the pore structure, aromaticity and chemical composition of biochar (Sun *et al*., 2012). In the fast pyrolysis, the shorter the vaporization residence time, the less important is for the secondary reactions between vapour and the developing char. Therefore, the chemical composition of the bio-oil phase and the resulting gas is primarily affected by the reaction in the vapor phase and the aerosol phase. In the slow pyrolysis, the vapour is limited and react extensively with the solid phase, more mass eventually turns into char. Increasing the pyrolysis time and temperature not only increases the C% in the char but also reduces the O% and its surface hydrophilicity (Mohan *et al*., 2014).

2.4.9.5 Potential Benefits and Application of Biochar

Many countries in the world are facing food security problems. As soil amendment, the biochar can potentially improve fertility of the soil and enhance the productivity of crop, it is seemed as a promising way for the food security issues. In addition, biochar helps to maintain the soil nutrients and water, hence, it can reduce the cost of irrigation and fertilizers, as well as, improve the barren soil in the long run (Qian *et al*., 2015; Kulyk, 2012). Compared with agricultural fertilizers, biochar is a more persistent soil additive and does not need to be added annually, so biochar is more favorable. In addition, the ability of biochar to sequester carbon is linked to other climate change mitigation mechanisms, such as reforestation and afforestation. Biochar can be used in a number of ways (Mohan *et al*., 2014; Qian *et al*., 2015):

- As upper dressing for shallow rooted plants (grasses, cacao trees).
- As an additive for composting.
- As a one-time use of soil amendment, in the range of 400 g to 2 kg per square meter.
- As a seed compost ingredient at a level of 1 kg per 20 liter compost.
- Spraying of biochar which will minimize the impact of transplanting shock with trees, shrubs and vegetable plugs.

Compared with other processes, the most attractive feature of biochar is a very low investment cost, sustainable characteristics, and its simple preparation process (Qian *et al*., 2015). Even though biochar application is still in its infancy, but it is used widely in many environmental fields and has achieved remarkable results instead of dealing with only one environmental problem. Those fields contain water purification, soil amendment, energy storage, and catalysis. The main advantages and disadvantages of various biochar application are summarized in Table 2.13 (Qian *et al*., 2015).

Table 2.13: The main advantages and disadvantages of various biochar applications (Qian *et al*., 2015)

Application	Purpose	Advantage	Disadvantage	Reference
Adsorbent of contaminant	Adsorption of heavy metals and organic contaminants present in water and soil	Abundant and sustainable resource and oxygenated groups on biochar surface facilitate adsorption, low cost	Persistence of heavy metals, and effectiveness of organic/inorganic contaminants remediation is still uncertain	(Ahmad *et al*., 2014a; Houben *et al*., 2013; Oleszczuk *et al*., 2012)
Activated carbon	Precursor for making activated carbon	Abundant and sustainable resource, low cost	Properties vary with different precursors, may not produce desired granular or spherical activated carbon	(Gil *et al*., 2013; Ioannidou & Zabaniotou, 2007)
Soil amendment	Carbon sequestration, soil Quality improvement	Reduce greenhouse gas emission and nutrient losses, reduce fertilizer consumption, sustainable resource, retain water and nutrient, low cost	Possible PAHs and heavy metal contaminants	(Lehmann *et al*., 2011; Sohi *et al*., 2010; Zhang *et al*., 2012)
Fuel cell	Fuel for fuel cell	Renewable fuel compared with coal	Relatively low power output and voltage, high ash content	(Ahn *et al*., 2013)
Catalyst	Syngas cleaning, biodiesel production, Fischer–Tropsch synthesis	Easy to recycle supported metal, co-catalyst, low cost	Relative low abrasive resistance and low efficiency compared with the commercial catalyst	(Dehkhoda *et al*., 2010; Mani *et al*., 2013; Kastner *et al*., 2012)
Storage material	CO_2 sequestration, H_2 storage	High recyclability, low cost, sustainable and abundant resource	Require surface treatment	(Hao *et al*., 2013; Zhao *et al*., 2005; Zhang *et al*., 2013; Gil *et al*., 2013)

(A) Biochar As a Soil Amendment

There are many applications of biochar in the soil. It not only separates the carbon in the soil but can also neutralize the acid in soil and increase the activity of soil microorganisms to improve the soil quality (Ahmad *et al*., 2014a). In soil remediation, the most important advantage of biochar is that it can neutralize acidic soil because biochar is an alkaline substance (Gul *et al*., 2015). Furthermore, biochar has functional groups such as phenolic, carboxyl, and hydroxyl. These functional groups in biochar have a very important role because they can react with H^+ ions in the soil to reduce the concentration of H^+ ions and increase the pH of the soil. In addition, bicarbonates, carbonates, and silicates in biochar can also be combined with H^+ to control the soil pH (Gul *et al*., 2015). Yuan *et al*. (2011) studied the effect of biochar on soil pH 10 g/kg of nine different types of biochar were applied to soil, that soil pH increased by 0.59 to 1.05 within 60 days. Biochar contains high concentrations of N, P, Ca, and K. These substances can directly provide nutrients for the soil and can be used as nutrients for microorganisms (Yuan *et al*., 2011). Soil porosity also increases when biochar is used in soil remediation. Each pore provides a space for the growth of the microorganisms and increases the amount of air, moisture and the residence time of nutrients, resulting in the increased activity of the microorganisms thereby increased the growth rate of plants in that soil (Ghezzehei *et al*., 2014). The direct combustion of biomass converts carbon from biomass into CO_2 and releases it into the atmosphere, but the pyrolysis or gasification of biomass will convert carbon into biochar and can be stored in the soil because the biochar is almost not decomposed by microorganisms or through mineralization, hence, the preparation of biochar not only reduces carbon emissions but also improves soil quality (Qian *et al*., 2015). Lehmann *et al*. (2006) reported that the conversion of carbon from biomass to biochar enable to separate 50% of the initial carbon content of the soil. Relatively, it is much higher than the 3% produced from combustion or the 10% to 20% from biological decomposition (Lehmann *et al*., 2006). Consequently, numerous studies have shown that the use of biochar for soil remediation not only reduces the gases' emissions that cause global warming but also improves the quality of the soil (Yanai *et al*., 2007; Spokas *et al*., 2009; Thomazini *et al*., 2015).

(B) Applications of Biochar in Water Remediation

In recent years, the application of biochar has achieved some practical results on soil improvement, water pollution control, and other fields. At present, the biochar adsorption of dyed wastewater has become an important research in water pollution control technology. This is because biochar has a strong adsorption capacity as compared to other adsorbents and the sources of material are economical, and the production process is also simple and easy to recycle (Mohan *et al*., 2014).

(i) Colour/Dye Removal

The dyed wastewater can cause serious environmental pollution since it contains dissolved solids, bases or acids, toxic compounds and other pollutants. Additionally, most of the fabric dyes are stable against light, oxidizing agents, and resist aerobic digestion, hence, these dyes are hard to be removed by conventional treatment techniques (Joshi *et al*., 2004; Wang *et al*., 2011). Figure 2.5 schematically illustrates the mechanism between methylene blue and biochar, involving ion exchange, physical function, surface complexation, electrostatic interaction, and others (Fan *et al*., 2016).

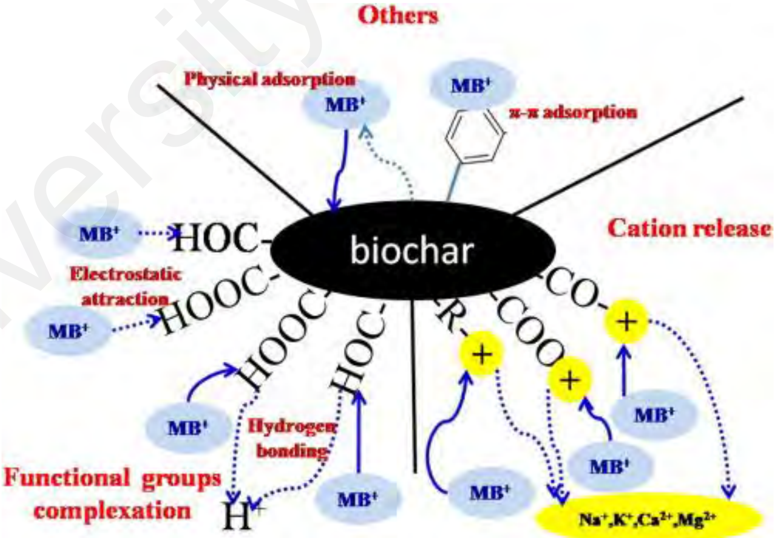

Figure 2.5: Schematic illustration of MB adsorption on biochar (Fan *et al*., 2016)

There are many different types of biochar, which can be prepared for the treatment of dyed wastewater. For example, biochar prepared from straw (Qiu *et al*., 2009; Xu *et al*., 2011) and bamboo (Mui *et al*., 2010; Yang *et al*., 2014) were used to remove dyes from textile wastewater. The soybean straw, peanut straw, rice hulls, and canola straw were slowly pyrolyzed for 4 hours in the muffle furnace at 350°C to prepare their respective biochar to remove methyl violet from wastewater (Xu *et al.*, 2011). The waste of bamboo scaffolding by slow pyrolysis under N_2 for 1 hour to 4 hours at 400°C to 900°C and different groups of biochar to adsorb acid yellow 117 (AY117), methylene blue and acid blue 25 (AB25) (Mui *et al.*, 2010). Table 2.14 briefly summarizes example adsorptions of dyes on various biochars (Tan *et al.*, 2015).

Table 2.14: Adsorption capacities for various biochars used to remove dyes from wastewater (Tan *et al.*, 2015)

Biomass Feedstocks	Dye	Adsorption Capacity (mg/g)	References
Rattan sawdust	Malachite green	62.71	(Hameed & El-Khaiary, 2008c)
Kenaf fiber	Methylene blue	18.18	(Mahmoud *et al.*, 2012)
Sludge-based	Methylene blue	90.91	(Shi *et al.*, 2014)
Eucalyptus	Methylene blue	2.06	(Sun *et al.*, 2013)
Rice hull	Methyl violet	123.5	(Xu *et al.*, 2011)
Palm bark	Methylene blue	2.66	(Sun *et al.*, 2013)
peanut straw	Methyl violet	256.4	(Xu *et al.*, 2011)
Soybean straw biochar	Methyl violet	178.6	(Xu *et al.*, 2011)
Pine sawdust	Methylene blue	16.75	(Cheng *et al.*, 2013)
Sawdust	Methylene blue	4.58	(Banerjee *et al.*, 2014)
Rice husk	Methylene blue	8.07	(Shih, 2012)

(ii) Metal Ion Removal

Nowadays, heavy metal contamination is a very serious environmental problem because heavy metals can cause serious threats to the environment and humans even at very low concentrations. Some heavy metals can accumulate poisons and can be assimilated, stored, and concentrated by organisms exposed for long periods (Mohan *et al.*, 2014). The accumulation of heavy metal in tissues can eventually cause some deleterious physiological effects since heavy metals are considered as the main pollutants of this century (Mohan *et al.*, 2014). Discharge of heavy metals poses a serious threat to human health and natural waters. Therefore, the studies of biochar adsorption mainly focused on the adsorption of Cr, Cu, Pb, Cd, Hg, Fe, Zn, and As metal ions. In the past studies, activated carbon has long been used to remove metal ions, but usually, only a few milligrams of metal ions are adsorbed per gram of activated carbon while problems related to regeneration and high investment exist (Mohan *et al*., 2014). Therefore, these factors make activated carbon use unfavourable for wastewater treatment when it contains a lot of heavy metals. Also, the use of activated carbon in developing countries will be subjected to the expensive cost. Alternatively, biochar is generally utilized as a part of industrial wastewater treatment and ground/surface waters, which can reduce the removal costs of the metal ion (Mohan *et al*., 2014). The summaries of various biochars produced from different feedstocks and technologies for the treatment of contaminated water are shown in Table 2.15 (Tan *et al*., 2015).

Table 2.15: The utilization of biochar produced from various raw materials in aqueous solutions (Tan *et al*., 2015)

Biomass Feedstocks	**Contaminants**	**References**
Brazilian pepper wood	Sulfamethoxazole	(Yao *et al*., 2012)
Bamboo	Sulfamethoxazole	(Yao *et al*., 2012)
Hardwood	Zinc and copper	(Chen *et al*., 2011)
Corn straw	Zine and copper	(Chen *et al*., 2011)
Dairy manure	Cd, Zn, Cu, and Pb	(Xu *et al*., 2013)
Dairy manure	Atrazine and lead	(Cao *et al*., 2009)
Cattle manure	Aluminium	(Qian & Chen, 2013)
Coconut coir	Chromium	(Shen *et al*., 2012)
Pinewood	Lead	(Liu & Zhang, 2009)
Rice husk	Lead	(Liu & Zhang, 2009)
Peanut shells	Trichloroethylene	(Ahmad *et al*., 2012)
Wood	Fluorinated herbicides	(Sun *et al*., 2011)
Sugarcane bagasse	Sulfamethoxazole	(Yao *et al*., 2012)
Swine manure	Herbicide Paraquat	(Tsai & Chen, 2013)
Orange peel	Fluoride	(Oh *et al*., 2012)
Rice straw	Aluminium	(Qian & Chen, 2013)
Pine needle	Hydrophobic organic compounds (HOCs)	(Chen *et al*., 2012a)

The focus of this review is on the recent development of the use of biochar to remove dyes and heavy metals from water. The surveys of biochar production literature reveal that the types of biomass materials can be used to prepare biochar are very numerous, biochar prepared by different processes can be effective to solve the water pollution. Literatures show that the result in previous studies on the application of biochar in wastewater have novelty values and viable adsorbent, contribute by its excellent adsorption capacity, beneficial for the environment and economical aspect.

CHAPTER 3: MATERIALS AND METHODS

3.1 Adsorbents Preparation Process

3.1.1 Pretreatment of Raw Material

The banana stem waste was obtained from a Kampung Bukit Cherakah plantation, Kuala Selangor, Malaysia. The collected banana stems were washed repeatedly using distilled water to remove soluble impurities and dirt attached to the banana stems and manually chopped into small pieces to dry under the sun for 2 days. Then, the banana stems were dried again in an oven at 100℃ for 48 hours to accelerate its drying and to further remove residual moisture contents. The dried products were ground and crushed using the cutter miller and passed through the standard metal sieves to achieve a uniform particle size of less than 1 mm. The banana stem powder was stored in a sealed container for the purpose of adsorption and characterization studies. The Methodology flowchart describing the overall research procedures was provided in the Figure 3.1.

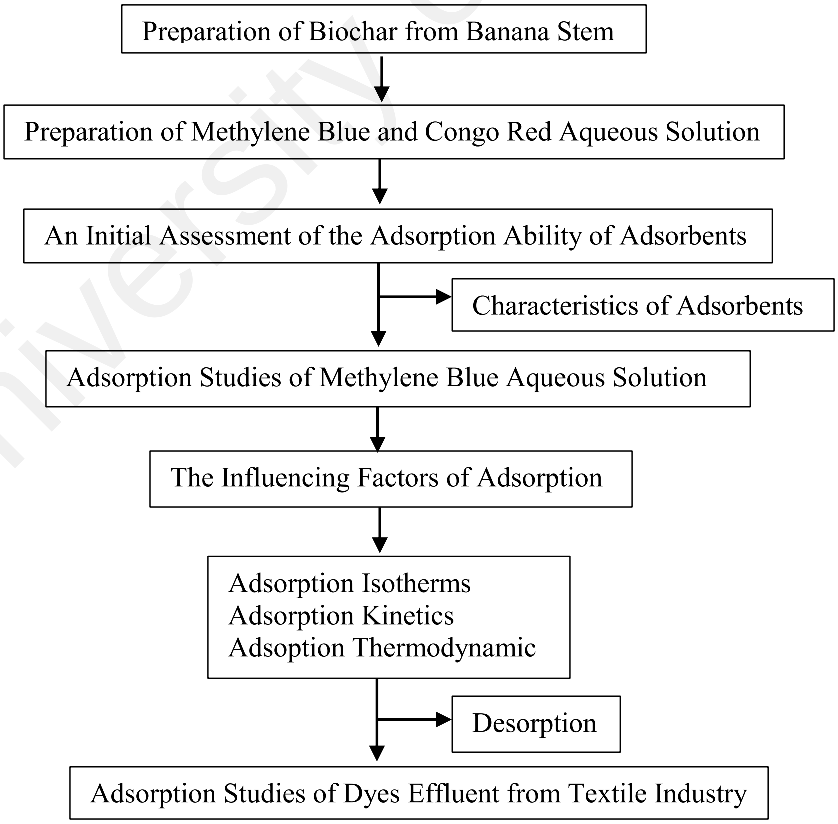

Figure 3.1: The flowchart of the entire research

3.1.2 Banana Stem Waste to Biochars Conversion Progress

The biochar production method was used as described by Karim *et al*. (2015) and Yang *et al*. (2016). Pyrolysis was carried out in a low-oxygen muffle furnace. The schematic diagram for experimental setup is provided in Figure 3.2 (Dooley, 2015).

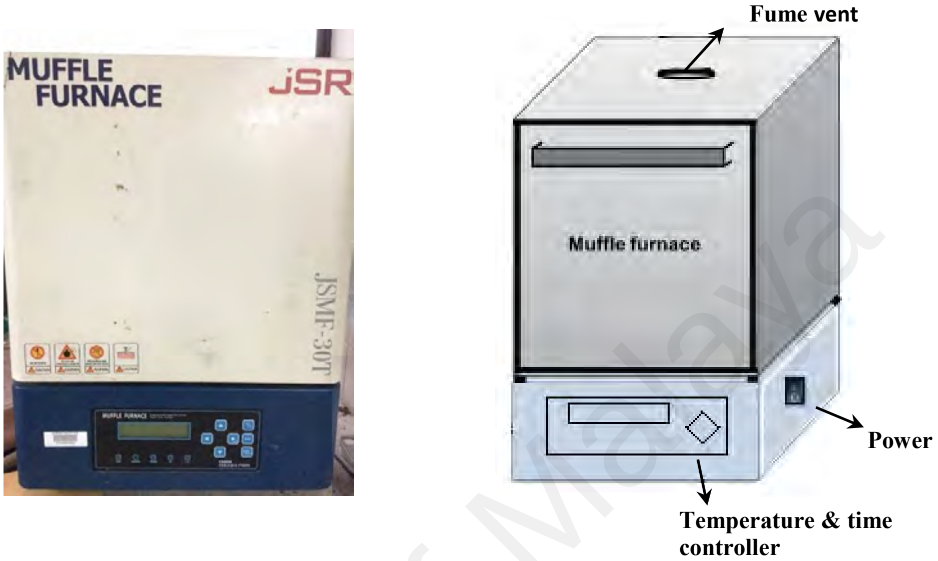

Figure 3.2: Photo and diagram of a muffle furnace pyrolysis apparatus (Dooley, 2015)

The muffle furnace was heated from 300℃ to 900℃ and banana stem waste was pyrolyzed for 1 hour at these temperatures, as described by Lee *et al.* (2013) that holding time maintained for at least 1 hour to allow sufficient time for complete pyrolysis, biochars prepared above or below 1 hour showed poorer adsorption efficiency (Lee *et al*., 2013). In this study, biochar developed with 1 hour was selected to carry out all the adsorption studies. The steps of preparing biochar were:

(a) 10 g of banana stem powder was put into a stamped porcelain crucible and inserted into a muffle furnace for carbonization under oxygen-limited conditions.

(b) Carbonization was conducted at various temperatures including 300, 400, 500, 600, 700, 800 and 900℃ at the holding time of 1 hour to allow sufficient time for complete pyrolysis, respectively.

(c) After putting the sample inside the furnace, the timer for holding time was started after the temperature reached the pre-determined temperature.

(d) The carbonized material was taken out after cooling to room temperature in the furnace, a small amount of the upper layer of ash was removed and sieved again to obtain a uniform size of 0.2-0.3 mm to avoid the particle size interference for adsorption experiments.

(e) The categories of biochar used in the current study were named BC300, BC400, BC500, BC600, BC700, BC800, and BC900, respectively.

3.2 Methylene Blue and Congo Red Aqueous Solution Preparation Process

The adsorbates were selected from the main contaminants in the textile industry. This is due to the fact that the MB and CR are the main organic pollutants in the textile industry and are considered to be visible pollution because they can cause serious harm to the environment and have a certain toxicity to humans and animals. Thus, the adsorption experiments of wastewater containing these two dyes were extensively used to evaluate the adsorption capacity of adsorbents. The molecular weight of the MB dye (cationic dye, chemical formula = $C_{16}H_{18}ClN3S$) is 373.9 g/mol and the structure of this dye is shown in Figure 3.3 (Doğan *et al.*, 2004). Besides, the adsorbate CR dye (anionic dye, chemical formula = $C_{32}H_{22}N_6Na_2O_6S_2$) has a molecular weight of 696.66 g/mol and its structure is illustrated in Figure 3.4 (Fu & Viraraghavan, 2002). In this study, the accurately weighed dyes were dissolved in distilled water to prepare 100 mg/L of MB and CR aqueous solutions as standard and stock solutions that could be diluted to obtain the required various concentrations for the following adsorption studies.

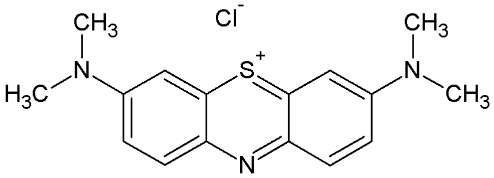

Figure 3.3: The molecular structure of MB (Doğan *et al.*, 2004)

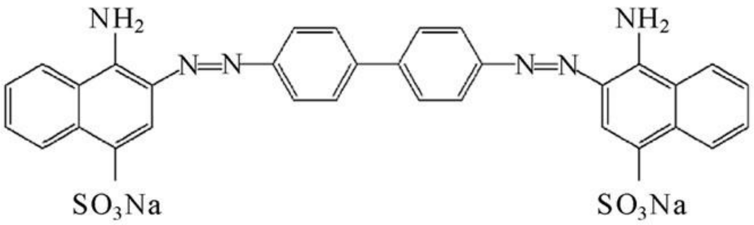

Figure 3.4: The molecular structure of CR (Fu & Viraraghavan, 2002)

3.3 Determine Maximum Wavelength and Calibration Curve

In the present study, the volumes of 1 mL, 2 mL, 3 mL, 4 mL, 5 mL, 6 mL, 7 mL of MB and CR were taken out from the stock solution and diluted in a 100mL volumetric flask with distilled water. The concentrations of MB and CR aqueous solutions were diluted to 1 mg/L, 2 mg/L, 3 mg/L, 4 mg/L, 5 mg/L, 6 mg/L, and 7 mg/L, accordingly. Their absorbance were measured by using the UV-Vis spectrophotometer to get the maximum absorption wavelength and the calibration curve. The maximum absorption wavelengths of MB and CR were found at 663 nm and 499 nm, respectively. Then, the 1 mg/L, 2 mg/L, 3 mg/L, 4 mg/L, 5 mg/L, 6 mg/L, and 7 mg/L absorbance of MB and CR also were measured and the calibration curves were plotted.

3.4 An Initially Assessment of the Adsorption Ability of Adsorbents

The MB and CR aqueous solutions were used to initially assess and investigate the adsorption ability of the adsorbents. 0.05 g of raw banana stems and the prepared biochar from the banana stem that was carbonized at various temperatures from 300℃ to 900℃ were accurately weighted. They were poured into 100 mL of 10 mg/L MB and CR aqueous solution. Then the mixed solution was placed on a shaker for 1 hour, at 150 rpm, and at room temperature (30°C ± 1°C). Then, the mixed solution was filtered using 0.45 μm membranes. Then the absorbance of the filtered MB and CR aqueous solutions were measured using the UV-Vis spectrophotometer at 663 nm and 499 nm, respectively. The adsorption capacity was calculated at equilibrium (q_e) based on the following Equation 3.1.

$$q_e = \frac{(C_0 - C_e)V}{W} \quad \text{(Equation 3.1)}$$

Where:

q_e (mg/g) = Adsorption capacity

V (L) = Volume of the dye solution

W (g) = Mass of the adsorbent

C_o (mg/L) = The initial concentration of dye

C_e (mg/L) = The equilibrium concentration of dye

Equation 3.2 was used to determine the decolouration efficiency of each experiment in percentage by calculating the difference in concentration of the dye before and after the treatment:

$$\% \text{ Dye Removal} = \frac{(Ab_1 - Ab_2) \text{ X } 100}{Ab_1} \quad \text{(Equation 3.2)}$$

Where:

Ab_1 = Initial dye concentration

Ab_2 = Dye concentration after treatment

After the preliminary adsorption study of the adsorbents was completed, it was found that the removal efficiency of all the adsorbents in the CR aqueous solution were very low, so the CR aqueous solution was not used for further adsorption studies. However, these adsorbents had good removal efficiency for the dye of MB. Also, the adsorbents of BC700, BC300, and raw banana stem all have good adsorption capacity compared with other adsorbents. Therefore, these three adsorbents were selected for further adsorption studies of MB aqueous solution.

3.5 Characteristics of Adsorbents Prepared

The sample is characterized through six different analyses as follows:

3.5.1 Biochar Yield

Before and after burning of biochar production, the samples were weighed to calculate the biochar yield as shown in Equation 3.3.

$$\text{Biochar yield (\%)} = \frac{W_2}{W_1} \times 100 \qquad \text{(Equation 3.3)}$$

Where:

W_1 = mass of dried raw material

W_2 = mass of biochar

3.5.2 Biochar pH Value

The steps of measuring the pH values of the adsorbents in distilled water are as follows: 0.5 g adsorbents were weighed accurately and placed in a beaker, 100 mL distilled water was added, then stirred for 15 minutes and settled for 1 hour. An appropriate amount of the supernatant of the clear aqueous solution was taken from the container into the beaker to measure the pH value by using the Hanna GLP pH meter HI 111.

3.5.3 The Surface Area and Pore Structure Analysis – BET

Generally, the BET method is important for measuring the surface area of biochar. In this study, the surface areas and characteristics of porous textures of the adsorbents were carried out using the BET equation that was calculated from the N_2 adsorption isotherms. The measuring instrument used in this study was the accelerated surface area and porosity determination system (ASAP 2020, Micromeritics, USA) by using nitrogen adsorption/desorption isotherms at 77K. The samples were degassed at 573K for 4 hours at a heating rate of 10°C/min prior to the adsorption measurement analysis.

3.5.4 The Surface Functional Groups Analysis – FTIR

In this research, the surface functional groups of the prepared adsorbents were determined through the FTIR spectroscopy (Perkin Elmer Frontier FTIR/FIR Spectrometers). It belongs to the absorption spectrum recorded by accumulating eight scans at a spectral resolution of 1cm^{-1} from 4000 cm^{-1} to 650 cm^{-1}.

3.5.5 The Surface Morphology Analysis – SEM

The surface physical morphology structural changes of three adsorbents have been observed directly by a field emission SEM in this research. High-resolution images of adsorbents were obtained using the SEM. SEM was required in order to observe the surface morphology and pore size of the adsorbents produced as well as to study and verify the presence and nature of porosities.

3.5.6 Proximate Analysis

Thermal behavior of the adsorbents was evaluated and characterized through a computerized Perkin-Elmer 7 Thermogravimetric analyzer with nitrogen and oxygen. In this research, the moisture, volatile matter (VM), fix carbon (FC) and ash content in the samples were measured using the proximate analysis with the aid of TGA (ASTM E1131 method) by continuously increasing the weight of the sample at increasing heat to 1000℃ . In the TG analysis, 10-30 mg of the sample was loaded into the instrument and the temperature range used was from room temperature up to 1000℃ at a heating rate of 10℃ min^{-1} with nitrogen gas at 30 mL/min volumetric flow during pyrolysis test. The system automatically records changes in mass of the samples in the combustion process to obtain a sample combustion curve. The results were offered in graphical form in which the temperature was plotted on the X-Axis and the weight percentage was plotted on the Y-Axis. The substance that burns off in nitrogen between ambient and 150°C is the highly volatile matter. The material that burns off in nitrogen between 150℃ and 700°C is the medium volatile matter. The combustible matter is a substance that burns off in the air rather than in nitrogen at 700℃ . The material left in the air at 900℃ is the ash content. The combustion characteristics of the samples were analysed by using the combustion characteristic curve (TG-DTS-DSC curve).

3.6 Adsorption Studies of Methylene Blue Aqueous Solution

3.6.1 Effects of Operating Conditions on Adsorption

Effects of operational conditions on adsorption were carried out using the raw banana stem, BC300, and BC700.

3.6.1.1 Effect of Adsorbent Dosage

The ability and effectiveness of the adsorbent to adsorb the dyes at the minimum dose was demonstrated by studying the effects of the adsorbent dose from economic point of view. The adsorption of MB on adsorbents (BC700, BC300, and raw banana stem) with the particle size of 0.2~0.3 mm was studied at different adsorbent dosages (0.05 g, 0.075 g, 0.1 g, 0.125 g and 0.15 g/100 mL) and placed into a 250 mL conical flask. The MB aqueous solution with an initial dye concentration of 20 mg/L was poured into these conical flasks and shaken for 1 hour, at 150 rpm, and at room temperature (30°C ± 1℃). The mixtures were filtered using a 0.45 µm membrane filter. The absorbance of filtered MB aqueous solution was measured at 663 nm by using UV-Vis spectrophotometer.

3.6.1.2 Effect of Initial Concentration

Adsorption studies were carried out to determine the effect of changes in dye solution concentration on adsorbent adsorption dyes. The adsorption capacity of adsorbents is significantly affected by the changes in solution concentration where 0.05 g of adsorbents with the particle size of 0.2~0.3 mm were weighed and placed into 250 mL conical flasks. Then, 100 mL of different concentration of MB aqueous solution (10 mg/L, 20 mg/L, 30 mg/L, 40 mg/L, 50 mg/L and 60 mg/L, respectively) were taken in these conical flasks and shaken for 1 hour, at 150 rpm, and at room temperature (30°C ± 1℃). The mixtures were filtered using a 0.45 μm membrane filter. The absorbance of filtered MB aqueous solution was analysed at 663 nm using UV-Vis spectrophotometer.

3.6.1.3 Effect of Contact Time

The effect of contact time on dye adsorption was determined by keeping the solution with a fixed adsorbent dose and the initial concentration of dye at different time intervals until equilibrium is reached (Bharathi & Ramesh, 2013). The dosage of the adsorbents were fixed at 0.05 g with the particle size of 0.2~0.3 mm and placed into 250 mL conical flasks. Then, 100 mL of MB solution with dye concentration 20 mg/L were poured into these conical flasks and kept on the shaker for different durations (30 min, 60 min, 90 min, 120 min, 150 min, 180 min, 210 min, 240 min, 270 min and 300 min, respectively), at 150 rpm, and at room temperature (30°C ± 1℃). The mixtures were filtered using a 0.45 μm membrane filter. The absorbance of filtered MB aqueous solution was analysed at 663 nm by using UV-Vis spectrophotometer.

3.6.1.4 Effect of Temperature

Solution temperature is also one of the most important factors affecting adsorption. It is also an indicator of the nature of adsorption and used to confirm whether it is an exothermic or endothermic process (Demirbaş & Alkan, 2015). The effect of temperature on the adsorption process was studied at various temperature (30℃ , 40℃ , 50℃ , 60℃ , 70℃) by using the incubator orbital shaker with temperature control. On the other hand, the other operating parameters such as adsorbent dosage (0.05 g), agitation time (1 hour), rotation speed (150 rpm), initial concentration and volume of solution (20 mg/L; 100 mL) were kept constant. Then, the mixtures were filtered using a 0.45 µm membrane filter. The absorbance of filtered MB aqueous solution was analysed at 663 nm by using UV-Vis spectrophotometer.

3.6.1.5 Effect of Agitation Speed

In the adsorption systems, agitation speed is an essential factor in affecting the distribution of the solute in the external boundary film and the bulk solution (Crini *et al.*, 2007). The effect of agitation on dye adsorption can be achieved by varying the agitation speed of the solution at different intervals while other parameters are kept constant. 0.05 g of adsorbents with the particle size of 0.2~0.3 mm were weighed and placed into 250 mL conical flasks. Then, 100 mL of 20 mg/L of MB aqueous solution were taken into these conical flasks and shaken for 1 hour, at different agitation speed (50 rpm, 100 rpm, 150 rpm, 200 rpm, 250 rpm, 300 rpm, 350 rpm, 400 rpm), and at the room temperature (30°C ± 1℃). The mixtures were filtered using a 0.45 µm membrane filter. The absorbance of filtered MB aqueous solution was analysed at 663 nm by using UV-Vis spectrophotometer.

3.6.1.6 Effect of pH

pH value is one of the most essential factors in affecting the adsorption capacity of adsorbents. The dye uptake was also observed under different pH values of MB aqueous solution with fixed other conditions remain unchanged. In order to study the effect of pH on the adsorption of MB dye, varied pH (pH 3, pH 4, pH 5, pH 6, pH 7, pH 8, pH 9, pH 10) were adjusted in different 250 mL conical flasks. The pH of the solutions were adjusted by using 0.1 mol/L HCl and NaOH standard solution and measured by using pH meter. Other operating parameters such as the amount of adsorbent were fixed at 0.05 g, with rotation speed (150 rpm), agitation time (1 hour), initial concentration (20 mg/L; 100 mL) and room temperature (30°C ± 1℃). The mixtures were filtered using a 0.45 µm membrane filter. The absorbance of filtered MB aqueous solution was analysed at 663 nm by using UV-Vis spectrophotometer.

3.7 Adsorption Isotherms

The adsorption isotherm is critical to how the adsorbate interacts with the adsorbent and the maximum adsorption capacity of the adsorbent can be predicted when the adsorption process is in the equilibrium state. The molecules motion between the liquid phase and solid phase are related to different isotherm studies, which can identify whether the distributions processed are homogeneous or heterogeneous (Goh *et al*., 2008). Different isotherm models and data adaptability analysis is a very crucial step in proper model determination. In order to simulate the adsorption isotherm, the following two different models were used to identify the adsorption mechanism of the biochar, they are the Freundlich (1906) and Langmuir (1917) models. They are the two most commonly used isotherm models selected to explicate dye-adsorbents interaction and to fit the equilibrium data observed in this study.

3.7.1 Langmuir Isotherm

The Langmuir isotherm is the most commonly used isotherm model and it is used to describe and correspond to the homogeneous monolayer adsorption process where the occupancy occurs at the homogeneous surface with no further adsorption taking place once the active sites are covered with dye molecules (Fytianos *et al*., 2000). It is used to determine the relationship between the amount of adsorbate that is adsorbed on an adsorbent and the partial pressure or the concentration at a specific temperature (isotherm) (Weber & Chakkravorti, 1974). In this research, the Langmuir equation described the distribution of MB dye between the solid-solution interface equilibrium. Equation 3.4 was used to represent the linear form of Langmuir isotherm.

$$\frac{C_e}{q_e} = \frac{1}{bQ_m} + \frac{C_e}{Q_m} \qquad \text{(Equation 3.4)}$$

Where:

C_e (mg/L) = The equilibrium concentration of MB aqueous solution

q_e (mg/g) = The amount of adsorbate adsorbed per unit mass of adsorbents at equilibrium

Q_m (mg/g) = Maximum amount of adsorption

b (L mg^{-1}) = The adsorption equilibrium constant

The values of Q_m and b were calculated from the slope and intercept of the linear plots C_e/q_e against C_e. The applicability of the Langmuir isotherm was shown linearly through the curve. The R_L is the dimensionless constant separation factor which represents the isotherm basic characteristics. It is known as equilibrium parameter, as described by Equation 3.5 (Weber & Chakkravorti, 1974).

$$R_L = \frac{1}{1+bC_0} \qquad \text{(Equation 3.5)}$$

Where:

b (L mg^{-1}) = The adsorption equilibrium constant

C_o (mg/L) = The highest initial MB aqueous solution concentration

The range of values of the parameter R_L can be used to indicate the shape of isotherm, as shown in Table 3.1.

Table 3.1: The range of values of the parameter R_L

Value of R_L	**Type of Isotherm**
$R_L > 1$	Unfavourable
$0 < R_L < 1$	Favourable
$R_L = 0$	Irreversible
$R_L = 1$	Linear

3.7.2 Freundlich Isotherm

The Langmuir isotherm model corresponds to the homogeneous monolayer adsorption and the monolayer coverage of the adsorbate at the outer surface of the adsorbent while the Freundlich model assumes that adsorption occurs on a heterogeneous surface containing unequally available sites with different energies of adsorption, which is characterized by the heterogeneity factor 1/n. The Freundlich isotherm model was defined by the following renowned logarithmic form as shown in Equation 3.6 (Freundlich, 1906).

$$\log q_e = \log K_F + \frac{1}{n} \log C_e \qquad \text{(Equation 3.6)}$$

Where:

q_e (mg/g) = The amount of adsorbate adsorbed per unit mass of adsorbent at equilibrium

K_F ((mg/L)(L/mg)$^{1/n}$) = Freundlich constant related to adsorption capacity of adsorbents

n = Freundlich exponent related to adsorption intensity

C_e (mg/L) = Equilibrium concentration of MB aqueous solution

The suitability of the Freundlich isotherm to adsorb MB on the adsorbent can be described by the linear curve of log q_e against log C_e. The intercept and slopes of the curve can be used to calculate the values of K_F and n. The value of n between 1 and 10 indicated that the adsorption of MB by the adsorbents was a beneficial adsorption.

3.8 Adsorption Kinetics

In order to explore the adsorption mechanism, adsorption kinetics is necessary because it can predict the removal rate of contaminants from aqueous solutions and provides valuable data to understand the mechanism of adsorption reactions (Li *et al.*, 2010). In the adsorption kinetics, the pseudo-first-order and the pseudo-second-order models are considered to identify the adsorption isotherm and are typically used to examine and fit the experimental data for adsorbing MB by adsorbents (Tan *et al.*, 2008). Generally, many studies have shown that the pseudo-second-order equation has been more successfully applied to the adsorption of dyes, herbicides, metal ions and other organic matters from aqueous solutions than the pseudo-first-order model (Park *et al.*, 2010).

3.8.1 Pseudo-First-Order

The pseudo-First-Order model can be represented by Equation 3.7.

$$\ln(q_e - q_t) = \ln q_e - k_1 t \qquad \text{(Equation 3.7)}$$

Where:

q_e and q_t (mg/g) = Amounts of MB adsorbed at adsorbents at equilibrium and at time t (min), respectively

k_1 (min^{-1}) = Rate constant of pseudo-first-order-adsorption

t (min) = The contact time

The plot of log (q_e-q_t) versus t can be used to calculate the value of the adsorption rate with the constant K_1.

3.8.2 Pseudo-Second-Order

When these values from the pseudo-first-order did not conform to the experimental results, this proved that the adsorption process did not follow the pseudo-first-order model. Therefore, in order to verify the applicability of the experimental data with the adsorption kinetics, the pseudo-second-order model also needs to be carried out. Then, the adsorption data was analysed according to the pseudo-second-order mechanism, and the formula of pseudo-second-order was expressed as Equation 3.8 based on equilibrium adsorption.

$$\frac{t}{q_t} = \frac{1}{k_2 q_e^2} + (\frac{1}{q_e})t \quad \text{(Equation 3.8)}$$

Where:

q_e and q_t (mg/g) = Amounts of MB adsorbed at adsorbents at equilibrium and at time t (min), respectively

k_2 (g/(mg min)) = Rate constant of pseudo-second-order-adsorption

t (min) = The contact time

The plot between t/q_t versus t can be calculated for the values of the constants k_2 (g/mg min) and q_e (mg/g).

3.9 Adsorption Thermodynamic

In order to develop the mechanism involved in the adsorption, thermodynamic parameters of entropy change (ΔS, kJ/mol), enthalpy change (ΔH, kJ/mol) and Gibb's free energy (ΔG, kJ/mol) were used to describe the thermodynamic behaviour of the adsorption of MB towards adsorbents (Shi *et al.*, 2014). The thermodynamic parameters such as entropy change (ΔS, kJ/mol), enthalpy change (ΔH, kJ/mol) and Gibb's free energy (ΔG, kJ/mol) of adsorbent adsorption dyes were calculated using the Equation 3.9 and Equation 3.10.

$$\Delta G = - RT\text{In}K_d \quad \text{(Equation 3.9)}$$

$$\text{In}K_d = \frac{\Delta S}{R} - \frac{\Delta H}{RT} \quad \text{(Equation 3.10)}$$

Where:

R (J K^{-1} mol^{-1}) = Gas constant (8.3145 J K^{-1} mol^{-1})

T (K) = Temperature in K

K_d (m^3/mol) = Equilibrium constant

q_e (mg/g) = The amount of MB adsorbed per unit mass of adsorbents

C_e (mg/L) = The equilibrium concentration

3.10 Desorption

Desorption studies were carried out at various pH levels to assess the possibility of regeneration of the adsorbent for further adsorption as well as to make the adsorption process of the adsorbent more economical. After adsorption experiments, the dye loaded adsorbents were separated from the solution and then dried at 100℃ in an oven overnight. Desorption studies were conducted using dried biochar samples. Various pH levels (3-10) of 100 mL distilled water were conducted using 0.05 g of the dye-loaded adsorbents. As Li *et al*. (2011) stated that the conditions of the desorption experiment should be consistent with the condition of the above adsorption experiments, thus, the suspension was agitated for 1 hour at 150 rpm for the parameters of the adsorption process. After desorption, the concentrations of dye desorbed C_{de} (mg/L) was similarly measured using the UV-vis spectrophotometer. The desorbed dye was estimated using Equation 3.11.

$$\text{Desorption (\%)} = \frac{C_{de}}{C_{ab}} \; X \; 100 \qquad \text{(Equation 3.11)}$$

Where:

C_{ab} (mg/L) = The difference between the initial and equilibrium concentration of dye

C_{de} (mg/L) = The concentration of dye desorbed

Desorption studies help to understand the adsorption mechanism. If the adsorbed dyes can be desorbed in neutral pH water, then the bonds to which the dye is attached to the adsorbent are weak. If the dye is desorbed in alkaline water, the surface adsorption is carried out by ion-exchange. If the dye is desorbed in the organic acid, then adsorption is by chemisorption (Salleh *et al*., 2011; Bharathi & Ramesh, 2013).

3.11 Adsorption Studies of Dyes Effluent from Textile Industry

3.11.1 General Characteristics of Dyes Effluent Samples

For the purpose of this study, textile wastewater sample was collected from a selected textile industry called craft complex centre in Kuala Lumpur, Malaysia. The latest Malaysian textiles such as batik, weaving and hand-woven songket which can be found at the craft complex centre. Textile wastewater was collected during wash out process for excess methylene blue dye on fabric. According to the laboratory protocol, these samples were sampled and stored at room temperature. This wastewater was the complex mixture because it contains a variety of toxic dyes, pigments, and many other used chemicals. The characteristics of dye effluent were analysed according to the standard methods. The analysis of characteristics included: chemical oxygen demand (COD), biochemical oxygen demand (BOD), pH, turbidity, total dissolved solid (TDS) and total suspended solid (TSS).

3.11.2 Adsorption of Dyes Effluent

Different amount of adsorbents were weighed (0.05 g, 0.1 g, 0.15 g, 0.2 g, 0.25 g and 0.3 g) and placed into 250 mL conical flask. 100 mL of the dye effluent were poured into these conical flasks and shaken for 1 hours at 150 rpm, natural pH, and room temperature. Then, the mixtures were centrifuged. The dye solution after adsorption treatment was also analysed for chemical oxygen demand (COD), biochemical oxygen demand (BOD), pH, turbidity, total dissolved solids (TDS) and total suspended solid (TSS). Data obtained were statistically analysed to determine the correlation of various factors. Besides, the MB removal percentage was also analysed using Equation 3.12.

$$\text{Pollutants removal efficiency (\%)} = \frac{\text{initial values} - \text{final values}}{\text{initial values}} X 100 \quad \text{(Equation 3.12)}$$

3.11.3 Analytical Procedure

3.11.3.1 Preparation of BOD Dilution Water

(a) Phosphate buffer solution: 8.5 g KH_2PO_4, 21.75 g K_2HPO_4, 33.4 g $Na_2HPO_4 \cdot 7H_2O$ and 1.7 g NH_4Cl were dissolved in 500 mL of distilled water and diluted to 1 L. The pH of this buffer was adjusted to 7.2.

(b) Magnesium sulphate solution: 22.5 g $MgSO_4 \cdot 7H_2O$ was dissolved in distilled water and diluted to 1 L.

(c) Calcium chloride solution: 27.5 g anhydrous $CaCl_2$ was dissolved in distilled water and diluted to 1 L.

(d) Ferric chloride solution: 0.25 g $FeCl_3 \cdot 7H_2O$ was dissolved in distilled water and diluted to 1 L.

1 mL of prepared Phosphate Buffer, Magnesium Sulphate, Calcium Chloride and Ferric Chloride solutions were each added to 1 L of distilled water to dilute and was mixed evenly to prepare the BOD dilution water. The BOD dilution water needs to be aerated at room temperature for 24 hours before the BOD testing.

3.11.3.2 Sample Preparation

The dye effluent was diluted 100X with the prepared BOD dilution water and the pH was adjusted to 7 using HCl or NaOH. The BOD bottles were filled up with the sample and the initial reading of DO_0 was determined using DO meter (YSI Pro Plus multi-probe meter). BOD bottles were completely filled up to the rim to avoid trapping of air bubbles in the bottles. The BOD bottles were closed tightly with stoppers and kept in the BOD incubator at 20℃ for 5 days. The final reading of DO_5 was taken after 5 days using YSI meter. The Equation 3.13 was used to measure the BOD value.

$$BOD_5 = DO_0 - DO_5 \text{ X dilution factor} \quad \text{(Equation 3.13)}$$

3.11.3.3 Chemical Oxygen Demand (COD)

HI 839800 COD reactor and UV-Vis spectrophotometer were used to test the COD value. The reactor was preheated to 148°C. 3 mL of textile sample was added into the vial from the pipette down to the inside of the tilted reaction cell onto the reagent carefully. The screw cap was replaced tightly attached to the cell and mixed by inverting the vial. The vials were inserted into the reactor and heated at 148°C in the preheated reactor for 120 min. Then, the hot vials were removed from the reactor and allowed to cool to room temperature, the cooling time at least 30 min. The value of COD was measured by using UV-Vis spectrophotometer with a measuring range of 25-1500 mg/L COD.

3.11.3.4 pH

pH was measured by using Hanna GLP pH meter HI 111.

3.11.3.5 Total Dissolved Solids (TDS)

TDS was determined by using YSI Pro Plus multi-probe meter.

3.11.3.6 Total Suspended Solids (TSS)

TSS was determined by using Hach DR 5000 UV-Vis spectrophotometer.

3.11.3.7 Turbidity

Turbidity was determined by using Hach DR 5000 UV-Vis spectrophotometer.

CHAPTER 4: RESULTS AND DISCUSSIONS

4.1 Calibration Curve of Methylene Blue/Congo Red Aqueous Solution

Different optical densities were identified by calibrating the MB and CR dyes at various concentrations namely 1 mg/L, 2 mg/L, 3 mg/L, 4 mg/L, 5 mg/L, 6 mg/L, 7 mg/L and 8 mg/L. Figure 4.1 shows the calibration curve of MB aqueous solution with Y=0.2052X + 0.03896. The coefficient value of the calibration curve was 0.99915 and the maximum absorbance wavelength was found at 663 nm for MB dye. Figure 4.2 shows the calibration curve of CR aqueous solution with Y=0.0537X + 0.0614. The coefficient value of the calibration curve was 0.9998 and the maximum absorbance wavelength was found at 499 nm for CR dye. The calibrated results showed the equilibrium concentration of MB and CR dyes after adsorption with adsorbents.

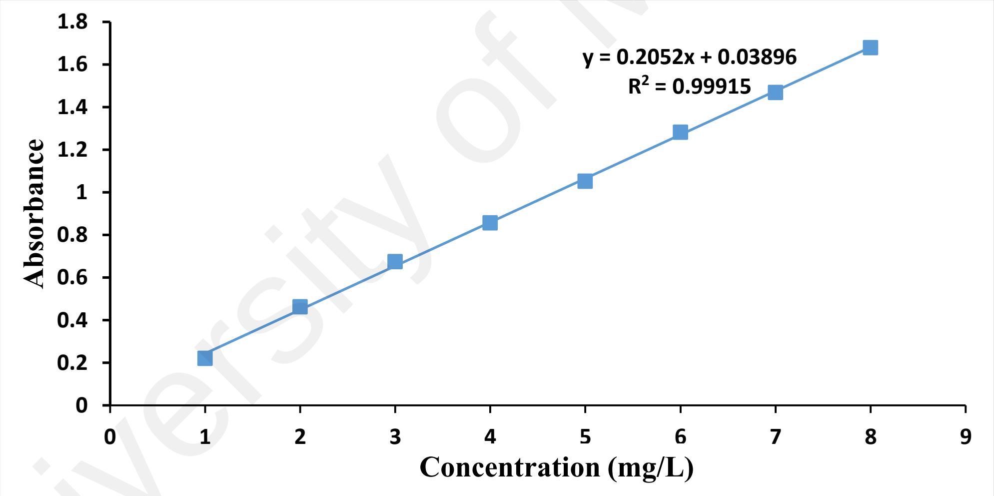

Figure 4.1: Calibration curve of MB aqueous solution

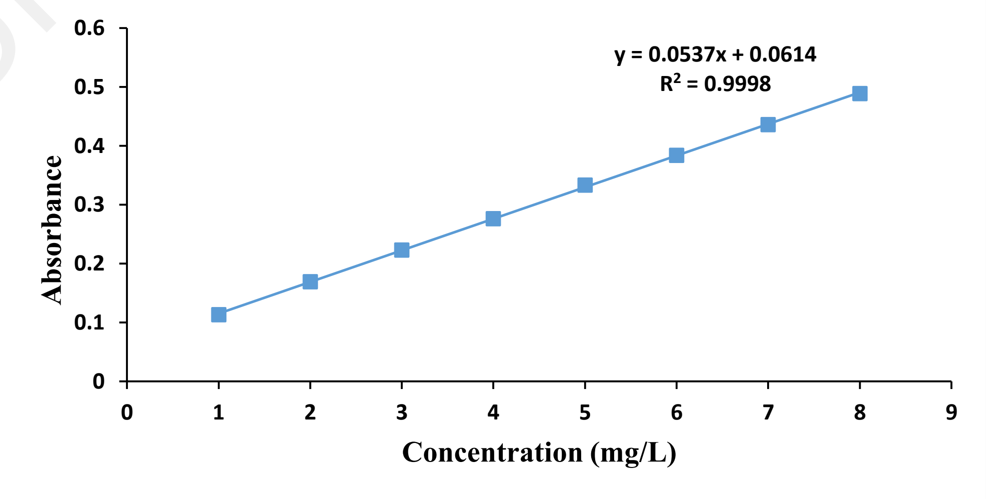

Figure 4.2: Calibration curve of CR aqueous solution

4.2 Adsorption Experiments

4.2.1 An Initial Assessment of the Adsorption Ability of Adsorbents

Table 4.1 and Table 4.2 show the results of the initial assessment of the adsorption ability of adsorbents to remove MB and CR from aqueous solutions (Plate 4.1 and Plate 4.2).

Table 4.1: The adsorption results of MB aqueous solution

NO.	Carbonization Temperature	Carbonization Time	Removal Efficiency (%)	Adsorption Capacity (mg/g)
1	300	1hr	90.60%±0.10%	18.12±0.02
2	400	1hr	62.10%±0.38%	12.42±0.08
3	500	1hr	39.90%±0.35%	7.98±0.07
4	600	1hr	40.30%±0.25%	8.06±0.05
5	700	1hr	98.50%±0.25%	19.70±0.05
6	800	1hr	96.10%±0.23%	19.22±0.05
7	900	1hr	93.90%±0.55%	18.78±0.11
8	Raw banana stem		91.20%±0.20%	18.24±0.04

Plate 4.1: Removal of MB onto the raw banana stem and biochars

Table 4.2: The adsorption results of CR aqueous solution

NO.	Carbonization Temperature	Carbonization Time	Removal Efficiency (%)	Adsorption Capacity (mg/g)
1	300	1hr	17.60%±0.26%	3.52±0.05
2	400	1hr	25.00%±0.26%	5.00±0.05
3	500	1hr	31.90%±0.23%	6.38±0.04
4	600	1hr	32.80%±0.35%	6.56±0.07
5	700	1hr	36.80%±0.31%	7.36±0.06
6	800	1hr	35.60%±0.38%	7.12±0.08
7	900	1hr	35.30%±0.23%	7.06±0.05
8	Raw banana stem		36.00%±0.18%	7.20±0.04

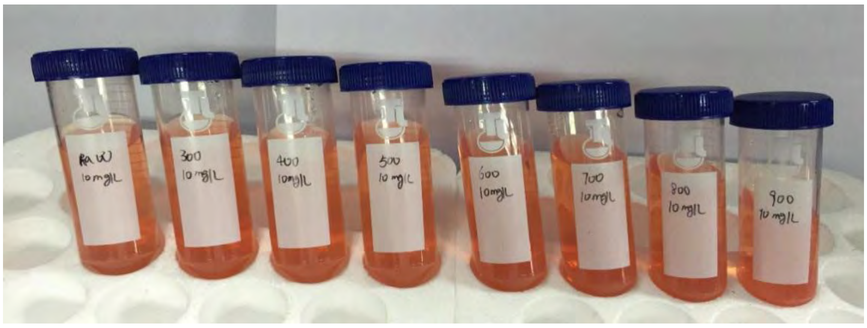

Plate 4.2: Removal of CR onto the raw banana stem and biochars

It can be observed from Table 4.1 that biochar at 700°C achieved 98.50% removal percentage in 10 mg/L of MB. However, all the adsorbents had little effect on the removal of CR with a removal efficiency ranging from 17.60% to 36.80%. Therefore, the MB was selected for the further adsorption studies. Besides, the biochars produced at 300°C and 700°C have shown better removal efficiency for MB in all biochars. Hence, the biochar BC300 and BC700 were chosen and used to examine the effects of the operational condition on adsorption of MB, the raw banana stem was also chosen for control test and compared with the biochar. Additionally, in order to obtain more reliable data and reduce error, each experimental analysis was repeated three times and the average of three experiments were used as the final result.

The results of the initial adsorption proved that adsorbents achieved favourable removal for the cationic dye MB than that of the anionic dye CR. A similar result was reported by Nasuha *et al.* (2011) who pointed out that papaya seeds was better in removing cationic dye (MB) from aqueous solution as compared to anionic dye (CR), mainly due to the fact that carboxyl groups were the main functional groups for cationic dyes adsorption. It indicated that negatively charged carboxyl groups inhibited the adsorption of anionic dyes (Nasuha *et al.*, 2011). The main factor that can positively affect the adsorption of MB is the cation exchange (Yang *et al.*, 2016). Salleh *et al.* (2011) also stated that the adsorption capacity of anionic dye is lower than cationic dye for the same adsorbent (Salleh *et al.*, 2011). The functional groups within the adsorbent have an important effect on the adsorption capacity according to the dye class. Since the carboxyl group is one of the major functional groups in agricultural wastes and the carboxyl group is negatively charged, therefore, it is beneficial to the adsorption of cationic dye. In contrast, the adsorption of anionic dyes will be inhibited (Gong *et al.*, 2005). Gong *et al.* (2005) demonstrated that the removal of negative charge from the carboxyl group by esterification can significantly increase the uptake of anionic dye CR.

As preliminarily analysed in Table 4.1 and Table 4.2, the cation exchange may be related to the MB adsorption and there are many carboxyl groups in the adsorbents. Herein, adsorbent was associated with the maximum adsorption capacity of MB compared to CR. The cation exchange and carboxyl groups may be the main mechanisms for the retention of MB using adsorbents derived from banana stem. The results would contribute to the design of wastewater treatment plants to remove various types of dyes, especially cationic dyes since the raw material namely banana stems, are abundant in nature and the treatment method is more economical.

4.3 Characteristics of the Adsorbents Prepared

4.3.1 The Yield of Biochar

The biochar percentage yield was calculated and presented in Figure 4.3. It is extensively recorded in the literature that the yield of biochar decreased with the increase in pyrolysis temperature (Sukiran *et al*., 2011; Capunitan & Capareda, 2012). This study also observed similar results, it can be found that the yield of biochar obtained from banana stem was significantly decreased as the pyrolysis temperature raised from 300°C to 900°C. The highest yield of biochar was obtained at the pyrolysis temperature of 300°C with 41.19%. When the temperature was raised to 900°C, the yield of biochar was the lowest, only at 12.90%. The maximum yield of biochar was obtained at lower temperature probably due to the structure of banana stem that was not completely decomposed, while the higher carbonization temperature could burn-off more carbon components of the raw materials which eventually reduced the yield of biochar prepared (Fu *et al*., 2011). With the increase in pyrolysis temperature, this downward trend in biochar yield was consistent with the observation by Shinogi and Kanri (2003) who stated that the yields of adsorbents significantly decreased between 200°C and 400°C probably due to the destruction of cellulose and hemicellulose.

Hossain *et al.* (2011) and Khanmohammadi *et al.* (2015) reported similar trends. Hossain *et al.* (2011) noted that the yield of biochar was decreased with the increase of pyrolysis temperature from 300°C to 700°C. Khanmohammadi *et al.* (2015) also illustrated that the yield of biochar was considerably decreased from 72.5% at 300°C to 52.9% at 700°C. From the above studies, it can be concluded that the yield of biochar decreased with the increase of pyrolysis temperature.

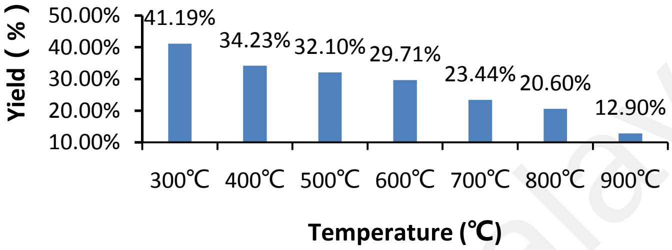

Figure 4.3: The yield of biochar

4.3.2 The pH Values of Adsorbents

The pH values of adsorbents are shown in Table 4.3. The pH value of raw banana stem was slightly acidic (pH 6.06). However, the pH of biochars was increased considerably as the pyrolysis temperature increased, indicating that as the pyrolysis temperature gradually increased, pH value of biochar also increased accordingly. As also listed in Table 4.3, the biochar tended to be highly alkaline (pH 10.04-10.56), except for BC300 (pH 7.58). Among the biochar samples, the biochar prepared at the lowest pyrolysis temperature (300°C) has the lowest pH value (7.58). However, when the pyrolysis temperature reached 400°C, pH of biochar increased rapidly and demonstrated to be an extremely strong alkaline and reached pH 10.40 and pH 10.50 for the biochar derived at 800°C and 900°C, respectively. After 400°C, the biochars was extremely strong alkaline.

Table 4.3: The pH values of adsorbents

Adsorbents	Raw	BC300	BC400	BC500	BC600	BC700	BC800	BC900
pH	6.06	7.58	10.04	10.20	10.27	10.38	10.40	10.56

The alkalinity of biochar is influenced by three factors, which are organic functional groups, carbonates, and inorganic alkalis (Yuan *et al*., 2011; Fidel, 2012). The contribution of organic functional groups such as carboxyl (-COOH) and phenolic (-OH) is known to be decreased, which would be minor on the alkalinity since these groups became depleted as the increase of pyrolysis temperature by the progress of thermal decomposition. The main reason for influencing the inherent alkaline pH of each biochar is probably the minerals. The increase trend in pH values was due to the fact that the number of alkaline groups retained by the biochar is higher at higher pyrolysis temperatures and the alkali salts (Ca, K, Mg, and Na) were separated from organic compounds (Yuan *et al*., 2011). Therefore, it can be easily identified that the main reason for the lowest pH values of BC300 and raw banana stem may be the lowest concentrations of alkali and alkali earth elements such as Na, Ca, Mg, and K. Tryon (1948) stated that the increased in the pH of the biochar was due to the increased in ash content in biochar, especially to hydrolyse Ca, K, and Mg salts in the presence of water. Mészáros *et al*. (2007) assumed that the formation of oxygen groups on the surface of biochar at low pyrolysis temperatures can be catalysed by K, Mg, Na, and P in the biomass. Oxygen groups like carboxyls, lactones, and phenols are important composition in the process by contributing to the formation of negative surface charges (Mukherjee *et al*., 2011). Similar trends were stated by Khanmohammadi *et al*. (2015) and Yuan *et al*. (2011) who found that the pH of biochar increased as the pyrolysis temperature increased. Hossain *et al*. (2011) also stated that the pH values of biochar were improved as the pyrolysis temperature raised from 300°C to 700°C. Ahmad *et al*. (2012) reported a similar result that biochar produced at higher temperatures displayed higher pH values. Furthermore, it was confirmed in a study by Shinogi and Kanri (2003) that due to the alkali release from the pyrolysis of feedstock which results in increasing pH value. The increasing trend of pH value was consistent with the ash content as the pyrolysis temperature increased. It is supported by the main component of ash, such as salts of alkali and alkaline elements (Ca, Na, Mg, K) and calcite (Singh *et al*., 2010). Mukherjee *et al*. (2011) illustrated that the most obvious explanation for the increase in biochar pH was due to the progressive loss of acidic surface functional groups, mainly aliphatic carboxylic acids as proposed by the Boehm titration data (Mukherjee *et al*., 2011). On the other hand, the high pH of biochar indicated their potential used as soil amendments for reducing soil acidity.

4.3.3 Surface Area and Pore Structure – BET

Generally, BET is an important method for measuring the surface area of adsorbents. The results of BET surface area, pore volume and average pore diameter of adsorbents are presented in Table 4.4.

Table 4.4: BET surface area characterization

Adsorbents	**Surface Area (m^2/g)**	**Pore Volume (cm^3/g)**	**Average Pore Diameter (Å)**
Raw banana stem	0.7030	0.002342	133.2340
BC300	0.9229	0.002655	115.0805
BC400	1.7437	0.003657	140.2188
BC500	1.8979	0.006112	77.0742
BC600	3.7818	0.008753	92.5838
BC700	26.7128	0.017413	26.0750
BC800	19.6022	0.012118	24.7274
BC900	13.6615	0.007591	22.2242

As can be observed from Table 4.4, the BET surface area and total pore volume were considerably increased as the pyrolysis temperature raised from 300°C to 700°C, which indicated when the degree of cracking of the raw material increased, the pore structure gradually developed. Previous studies have also reported similar surface area values (Park *et al*., 2014; Fu *et al*., 2011; Xiao *et al*., 2010). The volume of mesopores in the biochar was not large and maintains the specific surface area which is less than 100 m^2/g (Park *et al*., 2014). The total surface area was found to be less than 10 m^2/g at pyrolysis temperature from 300°C to 600°C and 26 m^2/g at 700°C. Generally, the surface area of biochar increases with increasing temperature at which deformation occurs (Brown *et al*., 2006). As shown in the SEM images, large diameter pores were observed on the surface of biochar BC300 due to the rapid evaporation of organic components, with the BC300 characterized by lower specific area and relatively large average pore size. It is also observed that, by the increment of the temperatures, the lamellar structure of biochar (BC700) became thinner and smoother, hence increases its surface area and made the pores smaller by the layered stack. The BET surface area of BC700 (26.7128 m^2/g) was extremely high compared to that of BC300 (0.9229 m^2/g) and raw banana stem (0.7030 m^2/g), indicating the better adsorption capacity of BC700.

However, at 800°C and 900°C, the trend was reversed. As the pyrolysis temperature raised to 700°C, the number of micropores significantly increased with the removal of volatile matters, resulting in an increase in the pore volume and surface area. When the temperature is higher than 700°C, the structural ordering, pore widening and the agglomeration of adjacent pores seemed to predominate, resulting in a decrease in the pore volume and surface area. In addition, pores in the biochar may be partially clogged due to softening, melting, fusing and carbonization (Fu *et al*., 2011). Park *et al*. (2014) reported similar trend that the decrease at 800°C and 900°C could be the results of carbon deposit formation on the surface of biochar from thermal and catalytic cracking of tar within the pyrolysis reactor (Park *et al*., 2014). The result of the present study is consistent with the findings of Angın (2013) who noted that as the pyrolysis temperature raised from 400°C to 500°C, the BET surface area and total pore volumes values increased significantly and reached the maximum. However, at 550°C and 600°C, the trend was reversed. This is agreeable to the Shaaban *et al*. (2013) reported that the pyrolysis temperature increased from 300°C to 500°C did not show a significant increase in BET surface area, but when the temperature increased to 700°C the surface area rose drastically to 5.493 m^2/g.

4.3.4 Surface Functional Groups – FTIR

The adsorption capacity of biochar is affected by the physical/porous structure of biochar, but also by the nature of its surface functional groups (Hassan *et al*., 2014). FTIR spectroscopy is an important tool for observing the shift change in chemical composition. The FTIR is used to determine the absorption of IR radiation on the materials by vibrating atoms on its bonds (Keleşoğlu, 2007). The band position in the FTIR spectra of the raw banana stem and biochar produced from different pyrolysis temperatures is presented in Figure 4.4. The FTIR analysis showed that the biochars obtained at different pyrolysis temperatures had similar functional groups, and that aromatic and aliphatic groups were predominant. Jindo *et al*. (2014) indicated that the presence of ethers groups, hydroxyl groups, and aromatic compounds are contributors to physical adsorption.

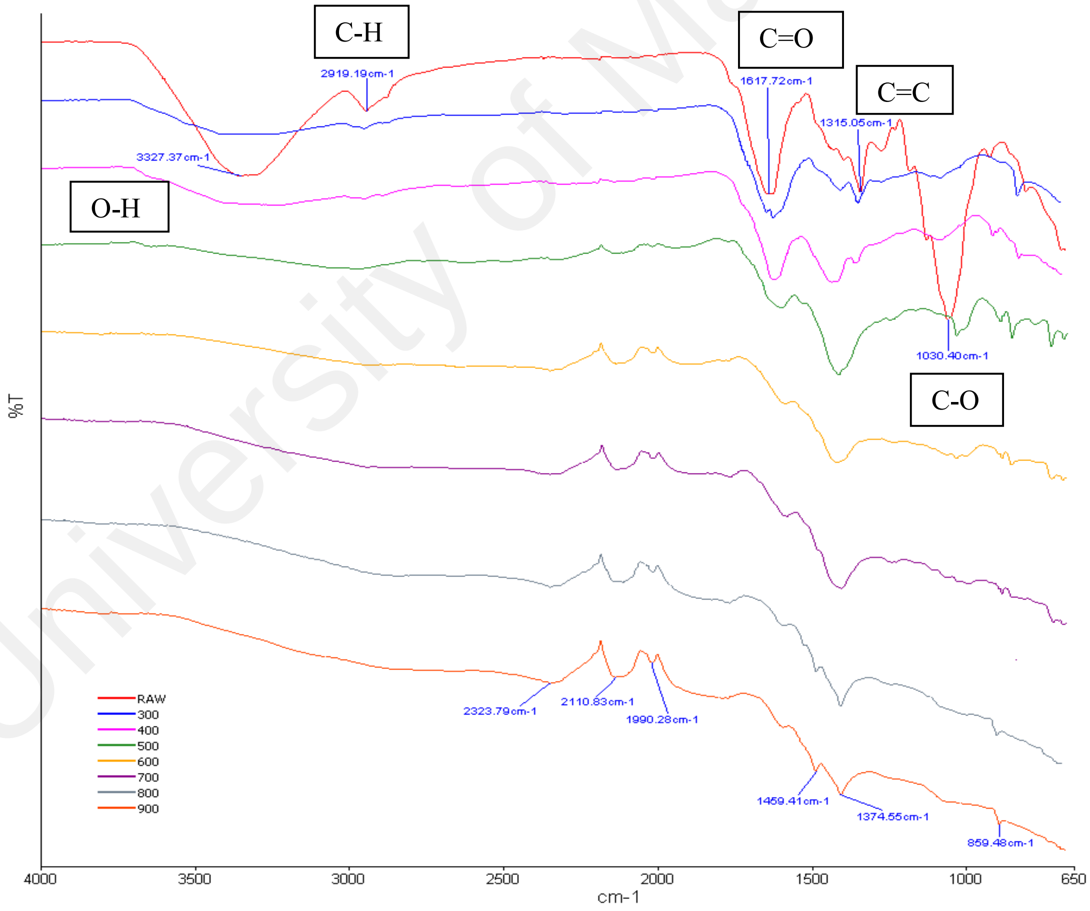

Figure 4.4: FTIR spectra of raw banana stem and biochars

As shown in Figure 4.4, it was found that the raw banana stem contained abundant peaks. However, some of the peaks disappeared or shifted and new peaks were also detected after pyrolysis as compared to biochar FTIR spectrum. Abundant functional groups are contained in the raw banana stem, the band at 3327.37 cm^{-1} was typically attributed to O-H (carboxylic, alcoholic, and phenolic groups) or N-H (amide and amino groups) stretching. Adsorption band at 2919.19 cm^{-1} was typically attributed to C-H groups (Peng *et al*., 2011). For the adsorption band at 1617.72 cm^{-1} is for aliphatic carboxyl and ketone groups which represent by the C=O stretching (Keiluweit *et al*., 2010). The presence of other functional groups/compounds, such as carbonyl (1315.05 cm^{-1}), cellulose/hemicellulose/lignin (1030.40 cm^{-1} indicates symmetric C-O stretching) and aromatic/heterocyclic compounds (800-500 cm^{-1} indicating C-H and C-N stretching) were also indicated (Ertugay & Malkoc, 2014; Malkoc & Nuhoglu, 2006).

At 300°C, the loss of aliphatic C-H stretching (2919.19 cm^{-1}) and C-O stretching (1030.40 cm^{-1}) of raw banana stem clearly showed that raw banana stem underwent gradual dehydration and depolymerisation. The main components of raw banana stem are hemicellulose and cellulose, their decomposition is much easier than lignin in the pyrolysis process (Yang *et al*., 2007). As the pyrolysis temperature increased, compared with raw banana stem, bands at 3327.37 cm^{-1} and 2919.19 cm^{-1} sharply decreased in biochar corresponding to the stretch vibration of the O-H groups and C-H groups. This is because of the higher pyrolysis temperature which results in the biomass component decomposition more fully and under the actions of dehydration and dehydroxylation, the O-H groups and C-H groups were lost and the peaks were obviously weakened on biochar (Fan *et al*., 2016). The disappearance of the peak representing aliphatic C-H stretching (2919.19 cm^{-1}) indicates that the loss of aliphatic compounds during the pyrolysis process is accompanied by the development of additional recalcitrant aromatic constituents (Wang *et al*., 2013). The loss of O-H and C-H groups indicate the formation of pores inside the biochar matrix with the simultaneous development of fused ring structures (Bagreev *et al*., 2001). Some new peaks were formed in the biochar produced at 400°C and above, these peaks between 1900 cm^{-1} and 2300 cm^{-1} indicate carboxyl and carbonly groups. The acidic group of C=O stretching for aliphatic carboxyl and ketone groups at around 1617.72 cm^{-1} in raw banana stem gradually decreased for biochar. However, The bands were more significant in biochars compared to in raw banana stem, which arises from aromatic C-H out of plane vibrations (700-900 cm^{-1}). This implies that the increased in aromatization and higher dehydration occurs within the range of this temperature (Angın, 2013). At the same time, cellulose-derived transformation products are reflected in more prominent peaks at 1459.41 cm^{-1} (aromatic C=C skeletal vibrations) and 1374.55 cm^{-1} (C-H deformation modes in alkenes) for biochar due to the decomposition and condensation of the cellulosic and lignin components (Angın, 2013). The peak at 1315.05 cm^{-1} decreased quantitatively with increased pyrolysis temperature and disappeared at 500°C and above. The peak at 1315.05 cm^{-1} occurred in the feedstock and the biochar produced at 300°C. This indicates that the biochar produced at the lower temperature retained some characteristics of its feedstock (Yuan *et al*., 2011). Biochar IR spectra exhibited that the loss of chemical diversity seen in the raw material formed a product that is essentially aromatic but has a low hydrogen content.

The FTIR data showed that the intermediates were formed and the aromatization was increased when the pyrolysis temperature of raw banana stem was heated from 400°C to 500°C. As the temperature gradually increased, biochar tended to be graphene-like structure, but still retained in the function of apparent O-contained (Wu *et al*., 2012). In general, the effect of pyrolysis temperature on the FTIR distribution of biochar is not very obvious. The increasing upward drift of the spectrum baseline from low to high wavenumbers at the high pyrolysis temperature may be due to an increase in the aromatics content (Hossain *et al*., 2011). The results of FTIR in this study was consistent with the findings of Wu *et al*. (2012) and Angın (2013). Fan *et al*. (2016) also showed a similar result that the number of bonds representing functional groups are present in tea waste and some peaks in biochar disappeared during the thermal degradation process. According to Islam *et al*. (2015), the presence of ethers groups, hydroxyl groups, and aromatic compounds verified to contribute to physical adsorption, and MB binding is mostly through the O-H and C-O groups. Kannan *et al*. (2009) and Jain and Jayaram (2010) also noted that the nitrogen atom of the amine group of dye and the hydroxyl groups and the oxygen groups of adsorbents were involved in adsorption. It is noticeable that the FTIR of BC700 is similar to BC800 and BC900. Therefore, it is a possibility that chemical bonding is not a core contributor to adsorption and it might be due to the mechanical absorption as shown in BET. The surface area of the raw banana stem, BC300 to BC600 were too low, only 0.70-3.78 m^2/g. Then, the raw banana stem with low surfaces area but good adsorption for MB, this is because its chemical bonding is strong in FTIR. As the pyrolysis temperature increased, the chemical bonding was decreased and destroyed. Therefore, the adsorption dropped from BC400 to BC600, but adsorption increased when pyrolysis temperature increased till 700°C because the surface area increases dramatically from 3.78 m^2/g to 26.71 m^2/g. The study of Yuan *et al*. (2011) has shown that there is a greater number of bonds representing functional groups in the biochar obtained at a lower temperature (300°C and 500°C) and these functional groups are absent in the biochar derived at 700°C (Yuan *et al*., 2011). This finding is similar to the observation by Jindo *et al*. (2014) that pointed out that the pyrolysis temperature of biochar was increased from 400°C to the 800°C, the intensity of the bands such as that of the hydroxyl groups and aromatic groups gradually weakens and there are many types of functional groups (such as C-H, C=C, C-C, C-O, etc) present on the biochar' surface derived from different agricultural residues. The main mechanism may involve surface complexation, including hydrogen bonding and electronic attraction. Oxygen-contained functional groups played a important role in the process of adsorption or binding (Sun *et al*., 2015).

4.3.5 Proximate Analysis

The moisture content, volatile matter (VM), fixed carbon (FC) and ash content (AC) of raw banana stem and biochar produced at 300°C to 900°C were analysed to evaluate the quality of adsorbents. The proximate analysis of the raw banana stem and the produced biochar was performed according to ASTM E1131 method, and the results are presented in Table 4.5.

Table 4.5: Proximate analysis of raw banana stem and biochars

Adsorbents	**Temperature Range/Decompost**			
	0-150°C	150-700°C	700-900°C	>900°C
	Moisture Content	Volatile Matter	Fixed Carbon	Ash Content
Raw banana stem	11.32%	58.46%	22.91%	7.31%
BC300	17.81%	30.74%	47.44%	4.01%
BC400	17.26%	21.54%	52.48%	8.72%
BC500	16.67%	17.88%	55.61%	9.84%
BC600	15.91%	16.85%	57.13%	10.11%
BC700	14.75%	14.98%	59.55%	10.72%
BC800	14.47%	14.35%	58.73%	12.45%
BC900	13.52%	12.68%	58.14%	15.66%

Table 4.5 presents the moisture content and volatile matter of biochar which decreased as the temperature increased, indicating that progressive loss of a more volatile component with the increase in the degree of carbonization, for the same biomass type, percentage of volatile matter and microporous surface area were considerably negatively correlated. Therefore, it seems clear that the micropores on the surface of biochar were filled with volatile components and were released from pores at higher pyrolysis temperatures, making them accessible to ions (Mukherjee *et al*., 2011). Ash content of biochar increased with increasing carbonization temperature, the loss of VM increased the relative proportion of the inert fraction (ash content). This trend might arise due to the decrease in the composition of elements such as carbon, nitrogen, hydrogen and nitrogen contents. These elements are more likely to lose their bonding than volatile inorganic salts, resulting in higher AC percentage at a higher pyrolysis temperature (Maiti *et al*., 2006). The ash content increased with the increase of pyrolysis temperature, which may be due to the complete combustion of C, indicating

that almost all of the biochar produced at above 800°C is ash (Cao & Harris, 2010). If there is a high AC content in the biochar, it indicates that the biochar is not preferred. The raw banana stem has the highest percentage of VM around 58.46%. AC of the raw banana stem was considerably low at around 7.31%. High VM and low AC are desirable for the thermal conversion process and were suitable to release more vapors emission while producing solid residue (biochar) that retain less ash, high fixed carbon and improving the calorific value of the product (Rahman *et al*., 2014). The VM of the biochar decreased from 30.74% to 12.68% with the increase of temperature from 300°C to 900°C. AC was found to be the highest for biochar at 900°C with 15.66% compared to another biochar at 300°C with 4.01%. FC of biochar ranged from 47.44% to 59.55% with the increase of temperature from 300°C to 900°C. With the gradual increase in pyrolysis temperature, biochar further released volatiles and became more carbonaceous. The fixed carbon content of biochar followed the similar trend as ash content, the fixed carbon content increased two times as compared to the feedstock. This means that the biochar became increasingly carbonaceous at high temperatures and released H and O. The fixed carbon content represents the proportion of solid carbon in the final product of carbonization. Therefore, a large amount of volatile matter and fixed carbon contents are essential for the production of highly-porous materials. When banana stem was subjected to carbonization temperature of 700°C, the biochar showed higher fixed carbon content, which is prominent properties to be used as a good potential adsorbent. It is well known that fixed carbon is the solid combustible residue remaining after carbonization of the particulate sample and volatile matters are expelled (Murage *et al*., 2007; Haefele *et al*., 2011). Therefore, it is used as an estimate of the number of carbonaceous material produced from a solid sample. The higher fixed carbon content refers to a large carbon surface to which the adsorbate is adsorbed (Ahmad *et al*., 2014b). However, the presence of ash may sinter and block the pores, which helps to decrease the surface area of pore (Huang *et al*., 2008). Similar result was reported by Park *et al*. (2014) who investigated the slow pyrolysis of rice straw at 300°C to 700°C.

4.3.6 Surface Morphology Characterization – SEM

In this study, the SEM images of adsorbents before and after adsorption of MB are presented in Figure 4.5.

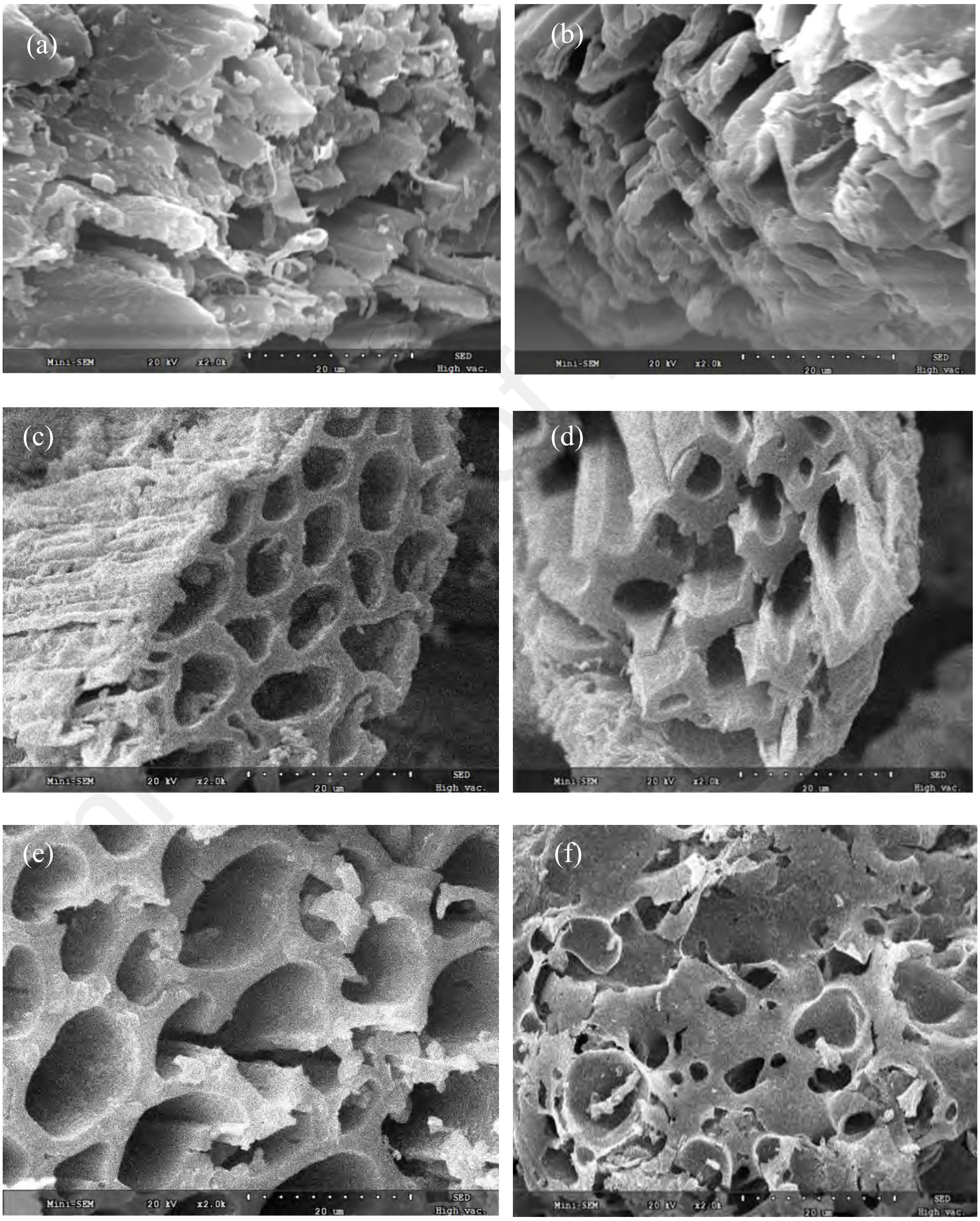

Figure 4.5: SEM images of (a) raw banana stem before adsorption, (b) raw banana stem with MB adsorbed, (c) BC300 before adsorption, (d) BC300 with MB adsorbed, (e) BC700 before adsorption, (f) BC700 with MB adsorbed

These images are used to compare the morphological changes in the pore structure of raw banana stem and biochar of BC300 and BC700 before and after MB was adsorbed. As can be observed from the Figure 4.5, the structure of raw banana stem was relatively compact and the pore structure was not obvious. Besides, the surface texture of raw banana stem waste presented was stalk-like, rough and irregular, which indicated that the main ingredients of banana stem waste were cellulose and hemicelluloses. Also, there were many impurities on it, hence the pores were covered by those impurities. Based on the research done by Baek *et al*. (2010), porous and rough surface offers better adsorption process. After the preparation of biochar, the primary surface structures changed during the carbonization process. Stem structures on the surface of the raw banana stem (Fig. 4.5a) were transformed into open pores and partially open channels in the biochar (Fig. 4.5c and e). More cleared pore structure and rough surface of biochar were formed, the pore structure of the porous biochar was uniform and the surface had many mesopores and micropores, such that the surface area was increased. As shown in Figure 4.5 (c) and (e), a fully developed pore structure identical to honeycomb voids was observed in the biochar obtained at a temperature of 300°C and 700°C, the pores were well pronounced and arranged in an array of honeycombed structures and the corner lines of the hole openings can be clearly seen. On the other hand, the pore structure of the biochars that were prepared composed of cylinder-like tubes. The pores were mainly developed along the axis parallel to the samples cylindrical structure. The structural properties of biochar determine its potential as an adsorbent. After the biomass is pyrolyzed, the volatile compounds are allowed to escape from inside the feedstock. Therefore, more void space and higher porosity can be detected on the surface of the biochar, which has higher surface areas than the raw biomass.

From these observations, it is clear that there was a significant difference in the appearance of the adsorbent surfaces. The availability of the pores and the internal surface of the adsorbents were clearly shown in the SEM images before adsorption and correspondingly shown is the coverage of the surface and the pores after adsorption of MB. It was suggested from the SEM images of the raw banana stem and biochar before the adsorption, the pores were highly heterogeneous within the adsorbent particles and exhibited honeycomb shape gaps with different sizes. Dye can be captured and adsorbed due to these heterogeneous pores. After the dye adsorption, it can be observed that the surface of adsorbents were covered with a thick layer of MB dye molecules (Mahmoud *et al*., 2012; Fan *et al*., 2016). For the BC300, very little changes were observed between the samples before and after adsorption of MB, the surface structure did not show any significant change indicating that no surface precipitation was involved in the removal of MB dye contaminant by BC300. The dye molecules may be bound to the active sites of the biosorbent through electrostatic attraction or hydrogen bonding (Albadarin *et al*., 2014). Hence, BC300 has a large diameter porous due to the rapid volatilization of organic components during the pyrolysis, which was consistent with the lower specific surface area. As the pyrolysis temperature was further increased, the lamellar structure of BC700 became thinner, smoother, and lead to an increase in the surface area, while the layered stack made the pores smaller. It can be noticed that the morphological structure of BC700 was uniform, more dense and lumpy as compared to raw banana stem and BC300, large pores of honeycomb shapes were found at the surface of BC700 and cell wall breakdown can be clearly observed for adsorbents after the MB was adsorbed. The obvious change in surface structure indicated that surface precipitation was involved in the removal of MB by BC700. Surface precipitation of dye was reported in other studies and accounted for nearly 70% of dye removal using lime treatment (Vimonses *et al*., 2010).

Overall, these images were evident that the surface morphology of the adsorbent was different before and after adsorption. Basically, after MB was adsorbed, the porous structure gets blurred because of adsorption. The white clumps on the adsorbent surface represent the adsorbate (Ghosh & Philip, 2005). The result of present study for SEM images is consistent with the findings of Fan *et al.* (2016) who stated that the surface texture of raw material was rough and irregular, but after pyrolysis, the pores within the adsorbent particles exhibit honeycomb shape gaps, the adsorbent surface was covered with a thick layer of MB dye molecules after the dye was adsorbed (Fan *et al.*, 2016).

4.4 Effects of Operating Conditions on Adsorption

4.4.1 Adsorption Studies of Methylene Blue Aqueous Solution

4.4.1.1 Effect of Adsorbent Dosage

Since the adsorption of MB is significantly affected by the dosage of the adsorbent due to its ability to predict the cost of adsorbent per unit contaminants to be treated (Kushwaha *et al.*, 2012). The effect of adsorbent dosage on the adsorption of MB by the raw banana stem, BC300 and BC700 were illustrated in Figure 4.6 by the plot of adsorption percentage of MB against the adsorbent dosage.

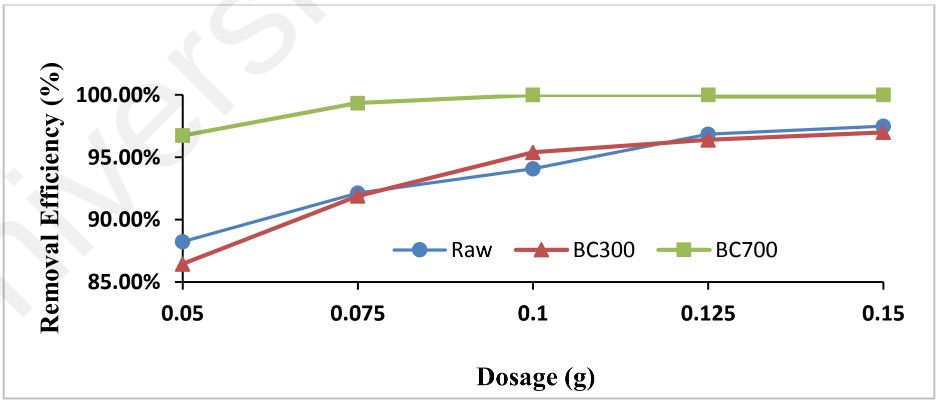

Figure 4.6: Percentage removal of MB onto the raw banana stem, BC300, and BC700 under different dosages (particle size=0.2~0.3 mm, initial dye concentration=20 mg/L, agitation time=1 hour, rotation speed=150 rpm, temperature=30°C)

It could be seen that the adsorption percentage of MB for each adsorbent adsorption increased with the increase in different adsorbent dosages from 0.05 g up to 0.15 g at a constant MB concentration (20 mg/l), and the adsorption capacity (q_e, mg/g) was decreased as the adsorbent dosage increased, it could be explained by an increase in the adsorbent surface area and pore volume at higher adsorbent doses. Hu *et al.* (2017) stated that higher dose of adsorbent contributed to the increase in surface area of adsorbent and availability of more potential binding sites, leading to higher adsorption of MB (Hu *et al*., 2017). This finding is agreeable to the observations of Garg *et al*. (2004) and Mahmoud *et al*. (2012) that the percentage of dye removal increased as the dose of the adsorbent was increased. In general, the removal percentage of dye increased as the dose of adsorbent increased. At the beginning, the percentage dye removal rate increased rapidly, but as the dose gradually increased, the removal rate of dye slowed down. The removal efficiency of BC300 and raw banana stem increased sharply when the dose of adsorbent was less than 0.125 g. However, only a slight increase in MB adsorption was observed for raw banana stem and BC300 as the adsorbent dose was further increased from 0.125 g to 0.15 g. Similar results were stated for the adsorption of MB (Hu *et al*., 2017) and CR (Tor & Cengeloglu, 2006) and remazol brilliant blue dye (Ratnamala *et al*., 2012) by red mud, the results showed that the removal percentage of dyes increased as the dose increased, however, when the dose of adsorbent exceeds the critical quantity, any additional adsorbent dose had little contribution to the adsorption process. The dye is easily accessible at lower adsorbent which has explained this phenomena. This resulted in higher removal rate per unit weight of the adsorbent (Bharathi & Ramesh, 2013). With the adsorbent dosage increased, the amount of adsorption is less commensurate increased due to the fact that many adsorption sites remain unsaturated during the adsorption (Jain *et al*., 2003). However, after a certain dose, the increase in adsorption efficiency is negligible in terms of adsorbent dose increase, because there is a very rapid superficial adsorption onto the surface of adsorbent under higher adsorbent concentration that produces a lower solute concentration in the solution than when adsorbent dose is lower. Therefore, as the adsorbent dose further increased, the amount of dye adsorbed per unit mass of adsorbent was reduced which resulted in values of q_e decreased (Han *et al.*, 2007).

Moreover, it is clear that the BC700 achieved the total (100%) of MB dye removal at 0.1 g, while the raw banana stem and BC300 were unable to achieve 100% of dye removal at 0.1 g even when the dose was up to 0.15 g. Even at the minimum adsorbent dose studied (0.05 g), the BC700 also reached 96.75% percentage removal of MB dye. Therefore, the BC700 biochar was found to be a better adsorbent for dye removal as compared to raw banana stem and BC300 biochar under the same adsorption conditions and dosage. Overall, the removal efficiency of MB was significantly affected by adsorbent dosage where high dosage can help to enhance adsorption of MB.

4.4.1.2 Effect of Initial Concentration

The effect of initial concentration on the adsorbents removal of MB was examined under different initial dye concentration and was presented in Figure 4.7.

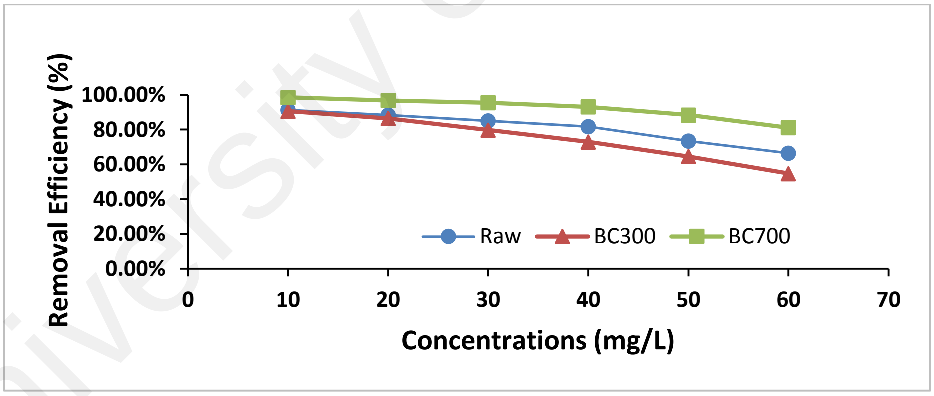

Figure 4.7: Adsorption percentage of MB onto the raw banana stem, BC300, and BC700 under different initial concentrations (adsorbent dose=0.05 g, particle size=0.2~0.3 mm, agitation time=1 hour, rotation speed=150 rpm, temperature=30°C)

The adsorption is greatly influenced by the solution concentration. As the initial concentration was raised from 10 mg/L to 60 mg/L, the removal efficiency of MB by each adsorbent was decreased because the capacity of the adsorbent materials was drastically deleted with the increased of dye initial concentration. This may be due to the adsorption sites of adsorbents were saturated at higher MB concentrations (Özer *et al.*, 2007). Similar results were described for the MB adsorption onto banana stalk waste

(Hameed & El-Khaiary, 2008a) and pomelo peel (Hameed & El-Khaiary, 2008b). Besides, Mahmoud *et al.* (2012) also showed similar result that the removal percentage of MB decreased as the concentration of initial MB increased. The MB removal percentage by BC700 was reduced from 98.50% to 81.12% with the concentration of initial MB was increased from 10 mg/l to 60 mg/l. It is clear that the removal efficiency of BC700 was better than BC300 and raw banana stem at the MB's initial concentration ranging from 10 mg/L to 60 mg/L, this is due to the different surface area and pore volume of the adsorbents. The higher surface area and larger pore volume of BC700 than that of BC300 and raw banana stem, the high surface area and large pore volume of the adsorbent that can provide more adsorption sites, thereby increasing the MB removal percentage. Besides, the removal efficiencies of BC300 and raw banana stem are decreased more obviously than that of BC700 sample from 10 mg/L to 60 mg/L, indicating that BC700 had better adsorption ability (Hu *et al*., 2017). The total available adsorption sites are limited to a fixed adsorbent dose, which was saturated at higher concentrations leading to decreased removal capacity (Dong *et al*., 2011). According to Khataee *et al*. (2013), the dye concentration provided an important driving force that could be used to overcome the mass transfer resistance between adsorbent and aqueous solution. The driving force increased with the initial MB concentration increase, which resulted in a higher q_e values and a lower removal percentage (Khataee *et al*., 2013). Based on Feng *et al*. (2011), at higher initial MB concentration, the MB molecules were rapidly attached to the outer surface of the adsorbent and then must penetrate the boundary layer of the adsorbent. But, at lower initial MB concentration, the adsorption of MB dyes primarily occurred rapidly on the outer surface of adsorbents. A similar trend was described for the adsorption of basic dye onto neem sawdust which concluded that the number of surface sites available will reduce over a period of time which will then repulse the solute molecules of bulk and solid phase (Khattri & Singh, 2009).

4.4.1.3 Effect of Contact Time

The contact time was also one of the most important factors affecting MB adsorption. From an economic point of view, useful information was obtained from the contact time on the feasibility and efficiency of a full-scale operation For the application of wastewater treatment, the efficiency of the adsorbents has to be able to absorb the dye quickly and attain equilibrium in a short period of time (Aghayan *et al.*, 2012; Chen *et al.*, 2012b). The results of the effect of contact time were presented in Figure 4.8.

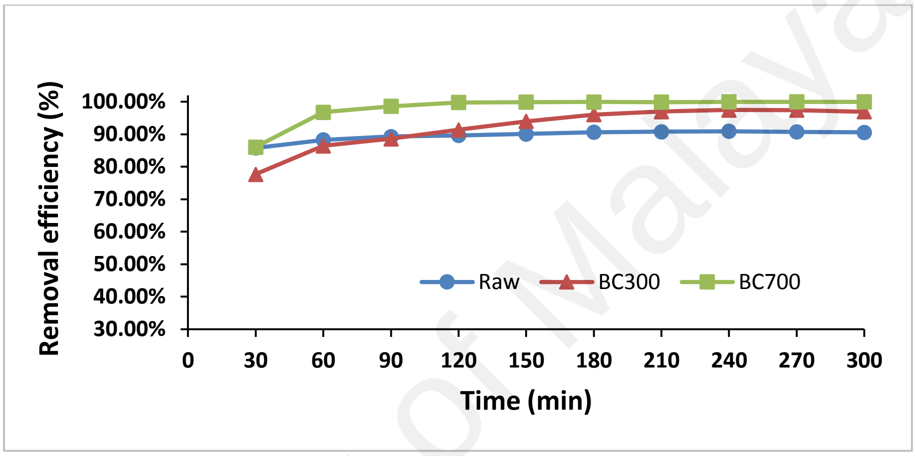

Figure 4.8: Adsorption percentage of MB onto the raw banana stem, BC300, and BC700 under different contact time (adsorbent dose=0.05 g, particle size=0.2~0.3 mm, initial dye concentration=20 mg/L, rotation speed=150 rpm, temperature=30°C)

Initially, it was clear that the dyes were quickly absorbed by each adsorbent in the first 30-60 min. Subsequently, the adsorption increased slowly over time and then gradually leading to equilibrium. Initially, the adsorption rate was very fast as the adsorbents adsorb dye ions on the exterior surface. At the point when the saturation of the exterior surface is achieved, the dye ions entered into the pores of the adsorbent particles and adsorbed by the solid particles' interior surface, this process takes a relatively long time and the adsorption rate was slowed down. In other words, this situation was essentially due to the fact that the saturation of active site did not allow further adsorption to occur. A similar trend was reported by Kumar and Ahmad (2011) that the adsorbents rapidly adsorbed the dye in the first 45-60 min, and then the rate of adsorption gradually slowed down and achieved equilibrium in about 150 min.

The adsorption equilibrium for BC700 was rapidly attained within 120 min where the adsorption efficiency eventually reached 100%. The adsorption equilibrium of BC300 and raw banana stem were achieved at 180 min. This result indicated that BC700 is a more efficient adsorbent than BC300 and raw banana stem due to the larger surface area of BC700 as according to BET surface area analysis. Large surface area enabled BC700 to perform rapid adsorption process which resulted in rapid equilibrium. The adsorption rate was very rapid at the initial stage due to the increase in the driving force provided by the MB concentration gradient in the aqueous solution and the availability of a huge number of active sites on the porous biochar surface (Olgun *et al*., 2013). Shi *et al*. (2014) stated that the shorter contact time required for the adsorbent to adsorb the dye is more favourable for its application in practical wastewater treatment. In addition, the change in the contact time of raw banana stem is smaller than BC300 and BC700 under the present conditions due to the larger surface area of BC300 and BC700 according to BET surface area analysis. Larger surface area enables BC300 and BC700 to perform rapid adsorption process which leads it achieving equilibrium rapidly. The result of the present study on the removal capacity of MB is consistent with those of Khattri and Singh (2009) who stated that an establishment of equilibrium in dye adsorption in a short time and a sharp uptake of dyes indicate the efficiency of the adsorbent. In general, the removal efficiency of dyes increases to some extent as the contact time increased. Crini and Badot (2008) stated that a further increment in contact time does not expand the deposition of dyes on the available adsorption sites of the adsorbent. At this point, the amount of desorbed dye from adsorbent is in a dynamic equilibrium state with the amount of dye adsorbed by the adsorbent. The time for reaching the equilibrium state is known as the equilibrium time, and the amount of dye adsorbed at equilibrium time reflects the maximum adsorption capacity of the adsorbent under those operating conditions (Crini & Badot, 2008).

4.4.1.4 Effect of Temperature

The adsorption process is additionally influenced by the solution temperature, the temperature change will cause the equilibrium capacity of the adsorbent to change (Qodah, 2000). The effect of solution temperature on the adsorption process was studied by changing the temperature of the dye solution at 30°C, 40°C, 50°C, 60°C, 70°C using the incubator orbital shaker with temperature control. Figure 4.9 illustrates the MB percentage removal on the adsorbents prepared versus the various solution temperature.

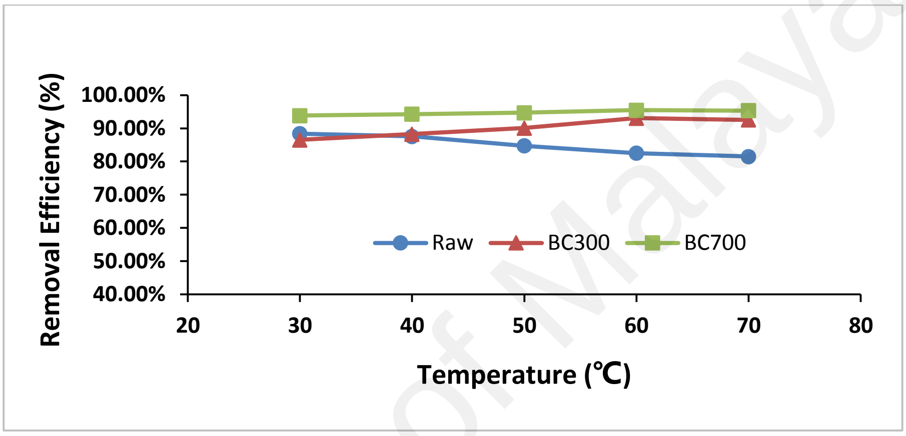

Figure 4.9: Adsorption percentage of MB onto the raw banana stem, BC300, and BC700 under different solution temperature (adsorbent dose=0.05 g, particle size=0.2~0.3 mm, initial dye concentration=20 mg/L, agitation time=1 hour, rotation speed=150 rpm)

The result indicated that BC300 and BC700 showed an optimum dye removal capability of 93.05% and 95.45%, respectively, at 60°C. For BC300 and BC700, the order of effective temperature for removing the MB dye were 60°C > 70°C > 50°C > 40°C > 30°C. 60°C showed the best adsorptive percentage compared to lower temperature and 70°C, this may be due to the fact that 70°C could have altered and destroyed the structure of BC300 and BC700 and caused a diminishment in adsorption percentage. The high temperature will destroy the covalent bond, thereby reducing the holding capacity of the adsorbents to capture dye molecules. The chemical reaction between the surface functional groups of the adsorbent and the adsorbate is a highly important factor for determining the adsorption capacity of adsorbent (Jayarajan *et al.*, 2011). When the solution temperature was raised from 30°C to 60°C for BC300 and

BC700, the adsorption capacity were increased due to the corresponding increase in the number of adsorption active sites, which indicated that the adsorption properties were endothermic (Senthilkumaar *et al*., 2006). Additionally, the relation in solution temperature increment and the increment of removal efficiency of MB may be contributed by the increment of large dye cations mobility, and may also be contributed by the elevated level of affinity sites for this dye and an increase of binding sites in the biomass (Aksu & Tezer, 2005). Another attribute to this phenomenon is the swelling effect of BC300 and BC700 internal structure which enables the large dye molecule to penetrate (Jayarajan *et al*., 2011; Dawood & Sen, 2012; Salleh *et al*., 2011). A similar observation was reported in the literature by Wang and Li (2007).

On the contrary, the optimum dye removal percentage of the raw banana stem was obtained at 30°C with 88.40%. It was found that the percentage of MB removal in raw banana stem tends to decrease when the solution temperature was raised from 30°C to 70°C. This indicated the exothermic nature of the adsorption reaction. Comparable perceptions were described for the adsorption of basic yellow 87 dye by two different mesoporous adsorbents (Wu *et al*., 2012) and the adsorption of MB by mesoporous silica (Huang *et al*., 2011), where the adsorption process of the aforementioned was an exothermic process. The increase in temperature may reduce the adsorptive forces between dyes and the active sites on the adsorbent surface, which result in lowering the adsorption capacity (Chowdhury & Saha, 2010; Salleh *et al*. 2011). The high temperature could destroy the covalent bond, thereby reducing the holding ability of the adsorbents to capture dye molecules. The adsorption capacity is to a great extent reliant on the chemical reaction between the functional groups of the adsorbent surface and adsorbate (Jayarajan *et al*., 2011). There are thermodynamic parameters such as changes in enthalpy (ΔH), Gibbs free energy (ΔG) and entropy (ΔS) to give information about the adsorption mechanism. The adsorption process was endothermic as shown by the positive ΔH values and this indicates a possibility of physical adsorption. Meanwhile, the negative ΔG values reveal that the adsorption is highly favourable. The positive values of ΔS indicated that the disorder and randomness increased at the interface of the solution and adsorbent (Demirbaş, 2009; Ge & Li, 2011).

4.4.1.5 Effect of Agitation Speed

Agitation speed has a significant effect on adsorption as it affects the distribution as can be shown by changing the agitation speed of the solution while maintaining other parameters constant and sampling at different intervals. In general, the adsorption percentage of dye increased as the agitation speed increased (Bharathi & Ramesh, 2013). If the appropriate speed of agitation is used, the mobility of ions in the solution is higher and mass transfer resistance is lower (Bulut & Karaer, 2015). The effect of agitation speed was studied by changing the agitation speed between 50 rpm and 400 rpm with a constant dye concentration (20 mg/L) and agitation time of 60 min. Figure 4.10 shows the adsorption percentage of adsorbents under various rotating speed.

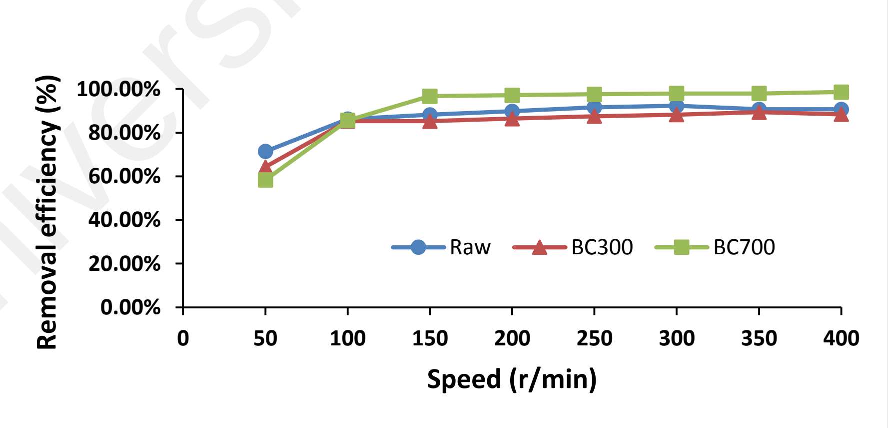

Figure 4.10: Adsorption percentage of MB onto the raw banana stem, BC300, and BC700 under different agitation speed (adsorbent dose=0.05 g, particle size=0.2~0.3 mm, initial dye concentration=20 mg/L, agitation time=1 hour, temperature=30°C)

The result demonstrated that a fast increment of dye percentage removal at the initial stage and afterward achieved the equilibrium. The adsorption equilibrium for BC700 was quickly achieved at 150 rpm, indicating a rapid adsorption process. But, for the BC300 and raw banana stem, they reached the equilibrium at 250 rpm which was slower than BC700. And after the equilibrium, the adsorption increases slowly over agitation speed and a stable percentage was attained. Overall, the change in agitation speed of all adsorbents under those present conditions were not the major factors that improve the removal efficiency of dye. Comparable outcomes were reported for the adsorption of MB from wastewater by pineapple leaf powder (Weng *et al*., 2009) and adsorption of crystal violet by tamarind seed powder (Patel & Vashi, 2010). These results can be contributed by the fact that the resistance through the boundary layer was very small and the mobility of the system was high under the experimental conditions. In other words, diffusion of MB ion from the solution onto the adsorbent surface to enter the pores occurred quickly and easily (Weng *et al*., 2009). Therefore, the uptake of MB was not significantly affected by the degree of agitation. The boundary layer becomes thinner with high agitation speeds. The rate of diffusion of solute through the boundary layer will be enhanced and external diffusion coefficient value is high (Mckay & Poots, 1980). In most cases, Weng *et al*. (2009) noted that the increment of agitation speed directly proportional to the adsorption rate increment, substantially in the early phase of the process. The increase in agitation speed will reduce the boundary layer resistance to the adsorbate molecules transfer to the adsorbent surface from the bulk solution. As a result, the adsorbate is forced towards the surface of adsorbent, of which the diffusion of adsorbate will be increased into the adsorbent surface (Demirbaş & Alkan, 2015; Malamis & Katsou, 2013).

Figure 4.10 shows the values of adsorption percentage firstly increased and then decreased as the agitation speed increased. Obviously, the removal efficiency of raw banana stem varied from 92.35% to 90.70% as the agitation speed raised from 300 rpm to 350 rpm, with removal efficiency of BC300 varied from 89.40% to 88.45% as the agitation speed raised from 350 rpm to 400 rpm. The change can be contributed by the increase in the desorption trend of dye molecules and the velocity of adsorbent particles and adsorbate ions, in which a more stable film around the adsorbent particles was formed similarly. Therefore, when the agitation speed was increased to 400 rpm, the stable film was deformed and film diffusion control disappeared due to the same speed of the movement of adsorbate ions and adsorbent particles (Gürses *et al.*, 2006).

4.4.1.6 Effect of pH

The pH of the aqueous solution was also a key factor affecting MB adsorption onto adsorbents. The change in pH will affect the changes in the adsorbate and adsorbent chemical nature. As a result, the adsorption percentage will change with the pH of an aqueous solution (Önal *et al.*, 2006). Figure 4.11 shows the MB dye removal rate by the effect of initial pH as analyzed by the change of pH from 3.0 to 10.0.

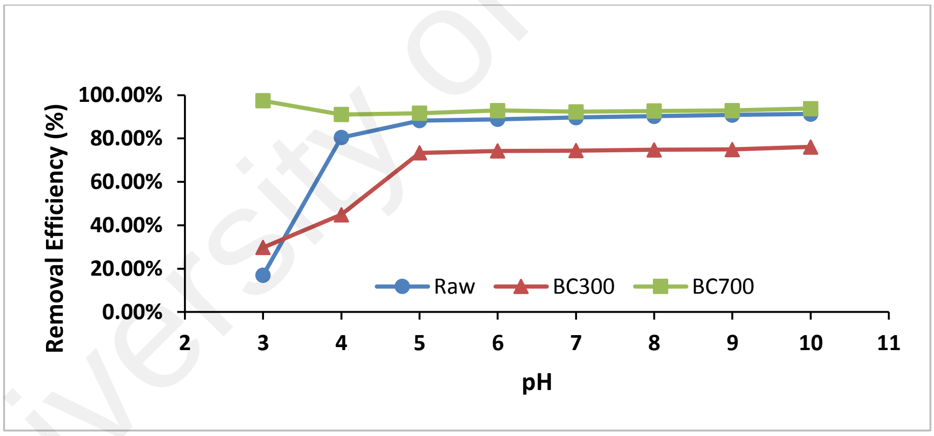

Figure 4.11: Adsorption efficiency of MB onto the raw banana stem, BC300, and BC700 under different initial solution pH (adsorbent dose=0.05 g, particle size=0.2~0.3 mm, initial dye concentration=20 mg/L, agitation time=1 hour, rotation speed=150 rpm, temperature=30°C)

For the raw banana stem and BC300, it was seen that the lowest adsorption percentage of MB was found at pH 3. As pH of the solution increased, the adsorption percentage also increased, and there was a rapid trend of adsorption percentage from pH 3.0 to pH 5.0. However, after pH 5.0, the removal efficiency changed insignificantly. It was obvious that the adsorption removal of MB by the raw banana stem and BC300 was better in neutral. In the lower pH range (acidic), the low adsorption of MB also exhibits the possibility of development of a neutral or weakened charge at the porous biochar surface, which decreases the electrostatic motivation for the adsorption of MB onto it. However, for the basic medium, the electric double layer formation changes its polarity and will result in the MB uptake increase (Hameed & EI-Khaiary, 2008b). In other words, this trend can be justified as the result of the change in the surface charge of BC300 and raw banana stem. At lower pH values (acidic), the H^+ ion concentration in the aqueous system is comparatively high. The surface of BC300 and raw banana stem achieved positive charge by absorbing H^+ ions. The positively-charged surface sites on BC300 and raw banana stem are not favourable for the adsorption of cationic dye due to the electrostatic repulsion. It will lead to the decreasing of the dye adsorption. As the pH of the aqueous solution increased, the quantity of negatively-charged sites increased by absorbing OH^- ions. As the surface of BC300 and raw banana stem are negatively-charged at high pH, an attraction of high electrostatic exist between the adsorbents and cationic dye molecules surface, resulting in maximum dye adsorption (Kumar & Ahmad, 2011). There is also a similar trend in early MB adsorption (Hu *et al*., 2017) that the adsorbents are favourable for the adsorption of MB at higher pH values. Definitely, the removal efficiency of MB increased dramatically when pH range from pH 3.0 to 5.0. When the initial value was higher than pH 5.0, only a slight increase in MB uptake was observed in both adsorbents.

By contrast, the BC700 showed the negative correlation in it. The maximum removal percentage was reached at pH 3.0 and then dropped in case of pH 3.0 to 5.0, as well as, remained almost constant from pH 5.0 to pH 10.0. Therefore, the adsorption removal of MB by BC700 could be more favourable in acidic conditions than the alkaline conditions. This could be explained by the formation of surface complex, surface hydroxylation, and acid-base dissociation. In addition, the BC700 presented the stronger alkalinity as the biochar was produced at a higher temperature, which caused the higher alkalinity in MB solution. Therefore, the BC700 adsorption to MB was impaired at the higher pH values. A similar result was reported by Hameed *et al*. (2008) who found that the adsorption capacity of banana stalk to adsorb cationic dye MB was at its minimum at pH 2.0 and was maximum at pH 4.0. Yang and Feng (2010) also showed a similar trend noting that the increased pH led to a decrease in adsorption capacity, presumably attributed to the deprotonation of the surface groups and protonation of the acidic functional groups of azo dye, leading to an electrostatic repulsion between adsorbent and adsorbate (Yang & Feng, 2010).

It was clear that there was an optimum pH for adsorption and it tended to decrease rapidly under strong acidic or strong alkaline conditions. Apart from affecting the surface charge of the adsorbent, the pH solution also affects the ionization and conformation degree of an adsorbate (MB) (Pavan *et al*., 2008). The pH of the dye solution has a significant impact on the adsorption capacity by making the ionization state of the binding groups to change, and by decreasing or increasing the competition between the adsorbate molecules and protonated materials for the active sites (Vieira *et al*., 2012). This adsorption mechanism can be explained by the interaction of the electrostatic between the surface of adsorbent that is negatively-charged and MB dye that is positively-charged (Hameed *et al*., 2007). Pavan *et al*. (2008) reported a similar result for the adsorption of MB onto yellow passion fruit peel (Pavan *et al*., 2008).

4.5 Adsorption Isotherms

The adsorption isotherm can illustrate the adsorption capacity at different aqueous equilibrium concentrations (Shi *et al*., 2014). It is an important procedure for the adaptive analysis between the data and different isotherm model for determining the appropriate model. Two commonly models are applied to reasonably observe the dye and adsorbent interaction in this study, namely, Langmuir and Freundlich models.

4.5.1 Langmuir Isotherm

The Langmuir adsorption isotherms of the raw banana stem, BC300, and BC700, were shown in Figure 4.12. The constant value of b and Q_{max} are obtained from the intercept and the slope of the linear plot of experimental data of (C_e/q_e) versus C_e.

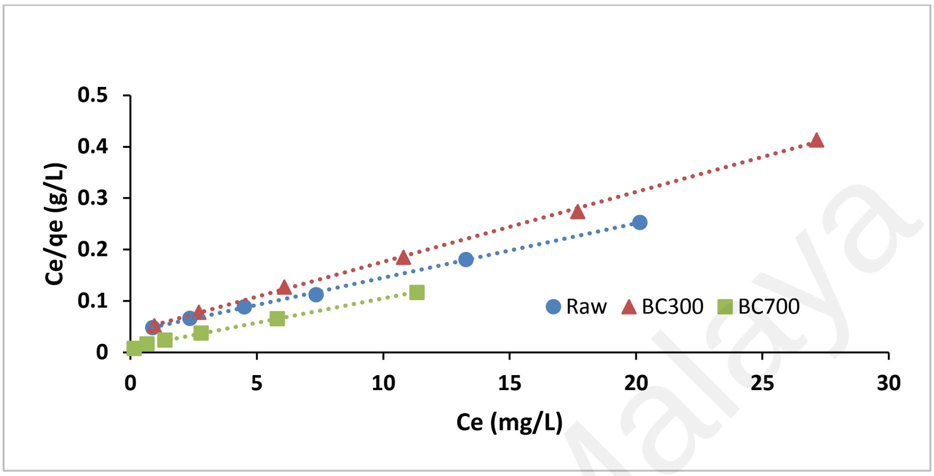

Figure 4.12: Langmuir adsorption isotherm of MB onto adsorbents

4.5.2 Freundlich Isotherm

The Freundlich isotherm results of the raw banana stem, BC300, and BC700, were shown in Figure 4.13. The constants K_F and n can be evaluated from the intercept and the slope of the linear plot of experimental data of log q_e versus log C_e.

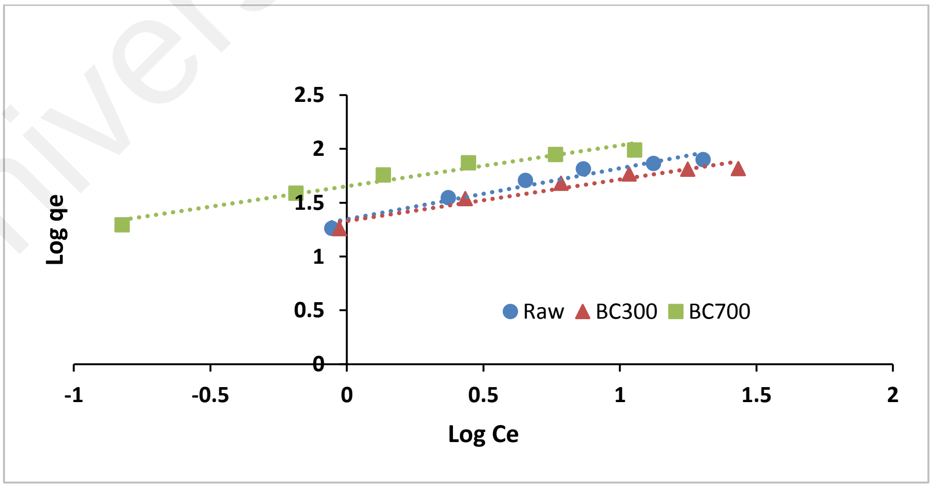

Figure 4.13: Freundlich adsorption isotherm of MB onto adsorbents

The constant values and correlation coefficients of Langmuir and Freundlich isotherms for adsorption of MB onto the raw banana stem, BC300, BC700 are listed in Table 4.6.

Table 4.6: Parameters and correlation coefficients of Langmuir and Freundlich isotherms for adsorption of MB onto the raw banana stem, BC300, BC700

Adsorbents	**Langmuir Isotherm Constants**				**Freundlich Isotherm Constants**		
	Q_{max} (mg/g)	R^2	b (L/mg)	R_L	n	K_F (mg/g)	R^2
Raw banana stem	94.34	0.9990	0.268	0.059	2.11	22.20	0.9517
BC300	73.53	0.9990	0.338	0.047	2.59	21.32	0.9426
BC700	105.26	0.9979	0.990	0.017	2.64	45.02	0.9658

According to the Langmuir isotherm, the maximum monolayer adsorption capacities of MB onto the raw banana stem, BC300 and BC700 were 94.34, 73.53 and 105.26 mg/g, respectively. Moreover, the Langmuir model showed a higher correlation coefficient (R^2) values (0.9979-0.9990) at all adsorbents compared to the Freundlich model, indicating a monolayer adsorption of MB onto the homogeneous surface of adsorbents. Besides, it also confirmed that Langmuir model was much better to describe the adsorption of MB onto adsorbents. A comparable result was noticed for the adsorption of MB onto kenaf fiber char with the highest values of correlation coefficient (R^2) of Langmuir isotherm compared to the Freundlich and Temkin models (Mahmoud *et al.*, 2012). Furthermore, the calculated parameter (R_L) for MB adsorption on the raw banana stem, BC300 and BC700 were found to be between 0 and 1 for dye concentrations of 20 mg/l. It indicated that the adsorption equilibrium was favourable on the operation condition. Mahmoud *et al.* (2012) showed similar results with R_L values and affirmed that there was the favourable adsorption of MB dye. In the Freundlich isotherm, the lower R^2 further supported the homogenous monolayer adsorption mechanism. Aljeboree *et al.* (2014) stated that if the n value is lower, this demonstrates that the adsorption process is chemical and if the value is above one, this suggests a favourable physical process. Therefore, in this study, the values of n of all the adsorbents were over 1, thereby indicating that good adsorption occurred. Mahmoud *et al.* (2012) proved a similar result that by showing the Freundlich model for the value of n was greater than 1 that represents favourable adsorption condition. Additionally, K_F is used to represent the relative size of adsorption capacity, as illustrated in Figure 4.7. The result indicated that the order of adsorption capacity for MB dye removal was BC700 > raw banana stem > BC300, and the high value of K_F for MB implied ready uptake of the dye from the solution with high adsorptive capacities of BC700.

4.6 Adsorption Kinetics

The adsorption kinetics has been also investigated. In order to further study the adsorption mechanisms, two widely utilized kinetic models were connected to fit the experimental data in this research, namely pseudo-first-order and pseudo-second-order. The adsorption rate constants for MB dye onto adsorbents were calculated based on the pseudo-first-order and pseudo-second-order models.

4.6.1 Pseudo-First-Order

The linear plot of ln (q_e - q_t) versus t was shown in Figure 4.14.

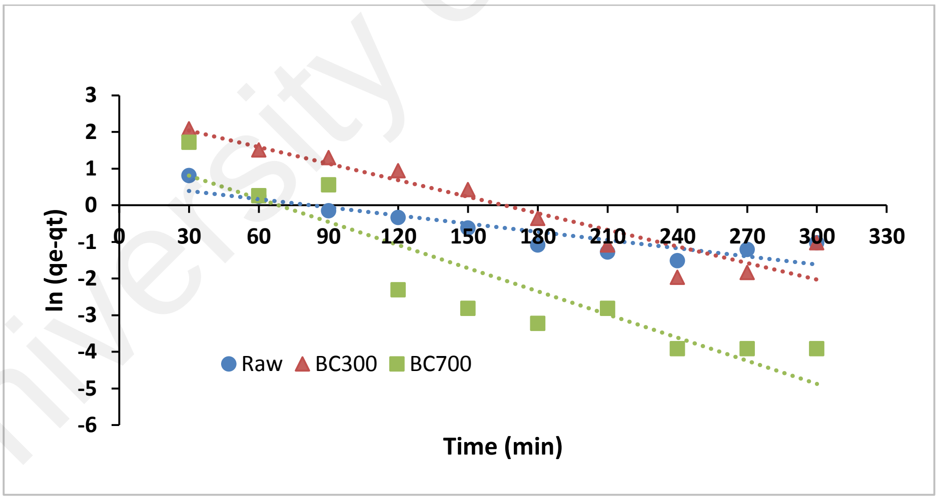

Figure 4.14: Pseudo-first-order kinetic for adsorption of MB onto adsorbents

4.6.2 Pseudo-Second-Order

The linear plot of t/q_t against t was shown in Figure 4.15.

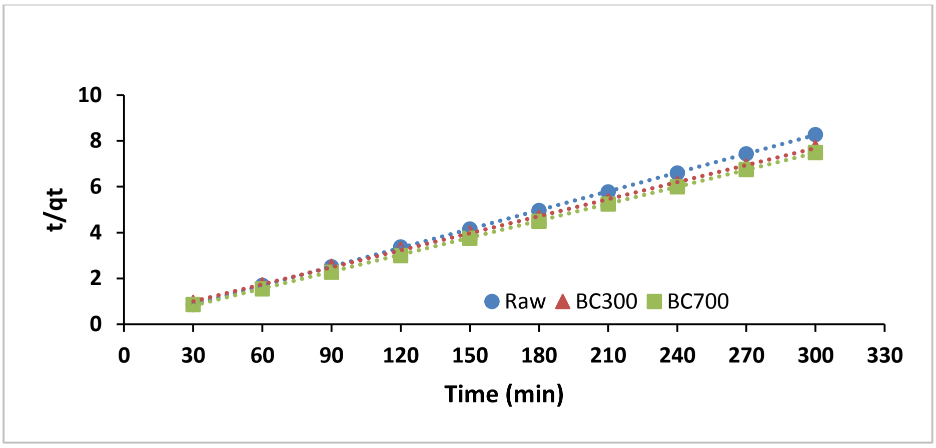

Figure 4.15: Pseudo-second-order kinetic for adsorption of MB onto the raw banana stem, BC300, and BC700

All parameters of pseudo-first-order and pseudo-second-order were calculated in each adsorbent. Both models have been fitted with experimental data and the results are shown in Table 4.7.

Table 4.7: Pseudo-first-order and Pseudo-second-order constants and correlation coefficients used to adsorb MB onto adsorbents

Adsorbents	**$q_{e,exp}$ (mg/g)**	**Pseudo-first-order**			**Pseudo-second-order**		
		k_1 (min)	$q_{e,cal}$ (mg/g)	R^2	k_2 (g/(mg/min))	$q_{e,cal}$ (mg/g)	R^2
Raw banana stem	36.58	0.0074	1.85	0.8119	0.0124	36.63	1
BC300	39.12	0.0151	12.06	0.8885	0.0023	40.49	0.9997
BC700	40.00	0.0211	4.22	0.8359	0.0081	40.49	0.9999

Table 4.7 shows that the calculated $q_{e,cal}$ values were lower than the pseudo-first-order experimental values ($q_{e,exp}$), indicating that the pseudo-first-order model was not fit to describe the adsorption process, this is supported by the low value of the correlation coefficients. However, for the pseudo-second-order model, it is clear that the $q_{e,cal}$ values determined using the pseudo-second-order showed a good agreement between the experimental and the calculated $q_{e,cal}$ values, as opposed to the values of $q_{e,cal}$ calculated using the pseudo-first-order. Besides, the values of the correlation coefficient for the second-order kinetic model were nearing one and all the values of correlation coefficients were greater than 0.9990 for all adsorbents. Therefore, when comparing the obtained R^2 values and q_e values between the first-order and second-order kinetics, it can be easily deduced that the pseudo-second-order model was more

suitable to describe the adsorption kinetics behaviours than the pseudo-first-order model. In view of these, it was concluded that the pseudo-second-order kinetic model is more suitable for interpreting the kinetic data and reasonably described the mechanism of the MB adsorption process (Salleh *et al.*, 2011). This observation supports the assumption that the adsorption is predominantly due to chemisorption (Malash & El-Khaiary, 2010). The good fit between the experimental data and the data calculated from the pseudo-second-order kinetic model indicates that the rate controlling mechanism for adsorption was a chemical adsorption between the adsorbate and adsorbent, as reported in some of the previous studies (Feng *et al.*, 2011; Mahmoud *et al.*, 2012). A similar result was observed for the adsorption of MB onto corncob hulls activated carbon (Wu *et al.*, 2011). In addition, Mahmoud *et al.* (2012) reported similar findings of the adsorption kinetic, where it was found that adsorption kinetic was better represented by the pseudo-second-order model due to higher correlation coefficients (R^2) and the calculated q_e values showed a good agreement with experimental q_e values.

4.7 Adsorption Thermodynamic

Figure 4.16 shows the Van's Hoff plots in Ink$_d$ versus 1/T.

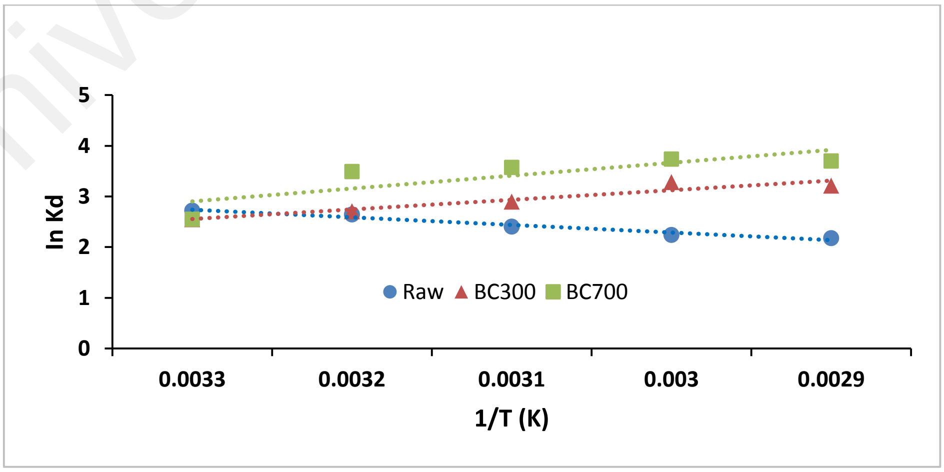

Figure 4.16: Van's Hoff plot for the estimation of thermodynamic parameters

The Gibb's free energy (ΔG), entropy (ΔS), and enthalpy (ΔH) used to determine the thermodynamics parameters are significant as they contribute features on the final state of the system. The values of ∆H and ∆S were calculated from the slope and intercept of the plot between Ink$_d$ versus 1/T, respectively. These parameters enable the justification on whether the process is favourable from the thermodynamic point of view, the spontaneity of the system and if the adsorption process occurs with absorption or release of energy (Vieira *et al.*, 2012). The calculated thermodynamic parameters at various temperature were listed in Table 4.8.

Table 4.8: Thermodynamic parameters for the raw banana stem, BC300, and BC700

Adsorbents	**Temperature (K)**	**∆G (kJ/mol)**	**∆H (J/mol)**	**∆S (J/K mol)**
Raw banana stem	303	-6900	1.2	24
	313	-6900		
	323	-6500		
	333	-6200		
	343	-6200		
BC300	303	-6400	-1.6	20
	313	-7100		
	323	-7800		
	333	-9100		
	343	-9200		
BC700	303	-6400	-2.1	22
	313	-9100		
	323	-9600		
	333	-10000		
	343	-11000		

As listed in Table 4.8, the raw banana stem showed positive values of ∆H which indicated that the adsorption process under the current conditions was endothermic in nature. This result is in agreement with the kinetic experiments discussed previously. A similar result was noticed for the adsorption of MB onto sludge-based biochar (Shi *et al.*, 2014). The adsorption reaction for the endothermic processes could be contributed by the temperature increment. It expanded the diffusion rate of the adsorbate molecules across the external boundary layer and in the internal pores of the solution (Ahmad *et al.*, 2014c). Besides, Senthilkumaar *et al.* (2006) illustrated that the decreased in the percentage of adsorption as the solution temperature increased was probably due to an increase in the mobility of the adsorbate molecules. However, BC300 and BC700 were shown to have the contrary trend with negative values of ∆H, which indicated that the adsorption of MB by BC300 and BC700 were an exothermic process. Moreover, the calculated △G for MB adsorptions were both negative for all adsorbents, indicating that the adsorption process followed a spontaneous and feasible trend (Wei *et al*., 2012). Furthermore, the positive values of △S obtained by all adsorbents indicated that the randomness at the solid/solution interface increased with the internal structure of the adsorbent adsorbed MB, and there are some structural changes in the adsorbates and adsorbents (Mahmoud *et al*., 2012). The boundary between physical adsorption and chemical adsorption is not very sharp. Usually, if the values of △H are lower than 40 KJ/mol, and the values of △G are within the ranges of -20 and 0 KJ/mol, physical adsorption was the main mechanism (Feng *et al*., 2011; Mahmoodi *et al*., 2010). According to Table 4.8, the △G values cannot meet the above criteria, which proved that the adsorption of adsorbents to MB was dominated by chemical adsorption. Similar results have been described in the literature for the adsorption of amido black 10B dye (Nethaji & Sivasamy, 2011) and malachite green dye (Nethaji *et al*., 2010) onto activated carbon derived from the waste of palm flower.

4.8 Desorption

In order to further study the adsorption mechanism and stability of MB dye adsorbed on the adsorbent, the adsorbent after saturated adsorption dye was added to deionized water with different pH value to study the desorption of dye. The contaminant-loaded adsorbents may cause secondary pollution effects if they are not handled carefully. Desorption is the most common treatment technique to deplete adsorbents, but it usually leads to serious side effects to the environment and is not economical (Feng *et al*., 2013). Therefore, it is necessary to recycle the used adsorbent to make this process more economical and increase its usability (Porselvi & Krishnamoorthy, 2014). The result of desorption study is shown in Figure 4.17.

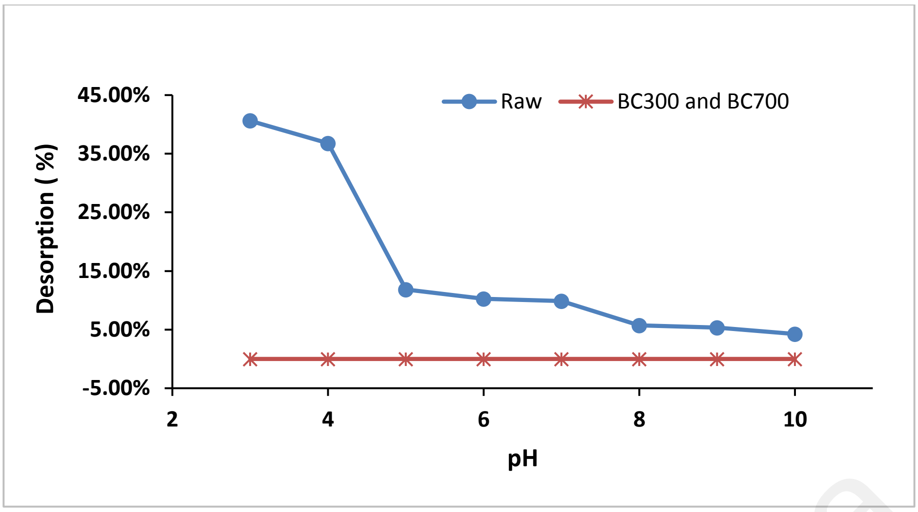

Figure 4.17: Desorption study of the raw banana stem, BC300, and BC700 under different solution pH (dye-loaded adsorbent dose=0.05 g, agitation time=1 hour, rotation speed=150 rpm, temperature=30°C)

As can be seen from Figure 4.17, as the desorbing pH was increased, the percentage desorption decreased from 40.62% at pH 3.0 to 4.25% at pH 10.0 for the raw banana stem. Desorption tests of raw banana stem showed that maximum dye releasing (40.62%) was achieved in aqueous solution at pH 3.0. This is just opposite to the pH effect in adsorption process which indicated the ion exchange is probably the major mode for the raw banana stem. The result of the present desorption study is in agreement with the findings of Kumar and Ahmad (2011) who found that the desorption of crystal violet dye from ginger waste did not show any impact using NaOH and H_2O, while the dye can be desorbed about 35% to 50% using acetic acid. Therefore, the dye-loaded raw banana stem can be more easily desorbed under the acid condition, it will cause secondary pollution if released to the environment. By contrast, the desorption of BC300 and BC700 is impossible, their desorption rates are 0.00%, suggesting that chemisorption might be the major mode of dye removal by the biochar. Li *et al*. (2011) also showed a similar result. The low desorption rates indicated that the dye was firmly adsorbed onto the biochar, that it will not cause secondary pollution to the environment and also can be reused through the regeneration technology. Therefore, biochar is more environment-friendly adsorbent to remove the dye from textile wastewater. The biochar prepared from dye-loaded adsorbents is propitious to avoid secondary pollution effects caused by the MB-loaded adsorbent, reducing the depleted adsorbents and purifying the dyed wastewater. This may be a suitable disposal methodology for the contaminant-loaded adsorbents. But, a systematic investigation and evaluation should be progressed when this technology is to be put into practice.

4.9 Adsorption Studies of Dye Wastewater from Textile Industry

4.9.1 Characteristics of Textile Effluent before the Treatment

In order to explore the effectiveness of the adsorbent for the actual textile wastewater, the initial characteristics of the actual textile effluent were determined. The characteristics of raw textile effluent are given in Table 4.9.

Table 4.9: Characteristics of raw textile effluent

Analysts	Textile Effluent	Standard A	Standard B
COD (mg/L)	14600	80	250
BOD_5 (mg/L)	456	20	50
pH	10.77	6.0-9.0	5.5-9.0
TDS (ppm)	5752	-	-
Turbidity (FAU)	1038	-	-
Total Suspended Solid (mg/L)	3.07	50	100

As shown in Table 4.9, the values of COD and BOD_5 of untreated effluent was 14,600 mg/L and 456 mg/L, respectively. The concentrations of COD and BOD_5 were extremely high as compared to the allowed limits for Standard A and Standard B. It was clear that this wastewater was contaminated by the organic load in addition to the dissolved and suspended matters. Organic load was expressed in terms of COD and BOD_5. The pH of raw wastewater is pH 10.77, this result clearly indicates that wastewater is alkaline in nature. This might be due to the presence of sodium hydroxide, silica and MB dye during the dyeing process. According to Saha *et al*. (2002), alkaline pH can cause severe physiological disturbance to most fish, inhibiting the rate of ammonia excretion, leading to its accumulation and toxicity (Saha *et al*., 2002). The precipitation of calcite from alkaline leachates smother benthic and littoral aquatic habitats, and reduces light penetration to primary benthic producers (Mayes & Younger, 2006). If this untreated effluent is discharged into natural streams and seeps into ground water, it will cause serious pollution. The amount of total dissolved solids in wastewater effluent was 5752 ppm. Dissolved solids contained in the industry wastewaters are also a critical parameter. Conventional treatment systems are difficult to treat TDS. Disposal of bearing effluents with high TDS can end up in the increase in TDS of ground and surface water. Vegetation and aquatic life are vulnerable to the dissolved solids in wastewater. Therefore, it was restricted for agricultural purpose.

The presence of high level of total dissolved solids is due to inorganic matter present in the effluent. A high content of TDS reduces the utility of water for drinking, irrigation, and industrial purposes. Total dissolved solids display the pollution strength of the wastewater. Higher concentration of total dissolved solids will convey the taste or odour of wastewater effluent. Total suspended solid of the effluent was 3.07 mg/L. The turbidity of the untreated effluent was 1038 FAU. Turbidity is a good parameter to measure the status of polluted water because the higher grouping of dyes, ions and other contaminating agents will cause the wastewater to become polluted and turbid. The low value in total suspended solids indicates that the amount of suspended particles in the wastewater effluent is lower than the standard permitted.

4.9.2 Removal Efficiency of the Dye from the Textile Effluent

The initial concentration of dye effluent was calculated using the MB calibration curves, and the result of the dye effluent initial concentration was 25.15 mg/L. Based on Table 4.10, after treatment of wastewater through adsorption, it was observed that the highest dye percentage removal by each adsorbent was attained at the dosages of 2.5 g and were more than 90%. Percentage of dye removal was 92.25%, 90.93% and 98.73% for the raw banana stem, BC300, and BC700, respectively. The sequence of dye removal ability was BC700 > raw banana stem > BC300. It is easily implied that the initial increase in the removal efficiency of MB dye as adsorbent dosages increased could be attributed to the increased in the surface areas of adsorbent, enlarging the number of available adsorption sites due to the increase in adsorbent dose. At adsorbent dosages higher than 2.5 g, the decrease in the removal percentage of MB may be attributed to the concentration gradient between adsorbate and adsorbent. Increasing biomass concentration may cause a decrease in the amount of metallic ion adsorbed per gram of biomass (Lin *et al*., 2011). The decrease in adsorption percentage with increasing adsorbent dose is mainly due to unsaturation of adsorption sites during the adsorption process (Shukla *et al*., 2002; Yu *et al*., 2003). It was also caused by the interaction of inter-particle due to the high adsorbent dose, such as aggregation. The result of this aggregation would decrease the adsorbent total surface area and the length of the diffusional path will be increased (Shukla *et al*., 2002).

Table 4.10: Adsorption of MB dye from the textile effluent

Amount of Adsorbents	**Raw Banana Stem**		**BC300**		**BC700**	
	Removal Efficiency (%)	Adsorption Capacity (mg/g)	Removal Efficiency (%)	Adsorption Capacity (mg/g)	Removal Efficiency (%)	Adsorption Capacity (mg/g)
0.5 g	85.21	4.29	80.68	4.06	90.85	4.57
1 g	87.91	2.21	83.54	2.10	92.68	2.33
1.5 g	90.58	1.52	86.12	1.44	94.83	1.59
2 g	91.89	1.16	88.87	1.11	97.14	1.22
2.5 g	92.25	0.93	90.93	0.92	98.73	0.99
3 g	91.57	0.77	89.26	0.75	98.13	0.82

4.9.3 General Characteristics of Dye Effluent after the Treatment

In order to reduce the concentrations of pollutants, the prepared adsorbents were utilized to treat the actual dye effluent at different doses. The treated effluent is characterized and the values of various parameters are compared with the raw effluent through different dosage of adsorbents as shown in Table 4.11, Table 4.12 and Table 4.13, respectively.

Table 4.11: Characteristics of effluent before and after treatment with raw banana stem

Analyst	**Raw Textile Effluent**	**Raw Banana Stem**						
		After Treatment						Maximum Reduction (%)
		0.5 g	1 g	1.5 g	2 g	2.5 g	3 g	
COD (mg/L)	14600	9700	9200	8700	6600	5500	5900	62.33
BOD_5 (mg/L)	456	312	288	269	256	237	245	48.03
pH	10.77	10.33	10.28	10.26	10.22	10.15	10.19	5.76
TDS (ppm)	5752	4459	4433	3971	3659	3172	3497	44.85
Turbidity (FAU)	1038	163	141	102	87	82	89	92.10
Total Suspended Solid (mg/L)	3.07	0.17	0.15	0.11	0.09	0.08	0.09	97.39

Table 4.12: Characteristics of textile effluent before and after treatment with BC300

Analysts	**Raw Textile Effluent**	**BC300**						
		After Treatment						Maximum Reduction (%)
		0.5 g	1 g	1.5 g	2 g	2.5 g	3 g	
COD (mg/L)	14600	11300	10100	9800	7900	6900	7100	52.74
BOD_5 (mg/L)	456	369	342	311	290	264	276	42.11
pH	10.77	10.44	10.41	10.49	10.37	10.31	10.33	4.27
TDS (ppm)	5752	5245	4764	4563	3828	3620	3796	37.07
Turbidity (FAU)	1038	189	175	153	127	96	113	90.75
Total Suspended Solid (mg/L)	3.07	0.38	0.32	0.27	0.22	0.14	0.20	95.44

Table 4.13: Characteristics of textile effluent before and after treatment with BC700

Analysts	**Raw Textile Effluent**	**BC700**						
		After Treatment						Maximum Reduction (%)
		0.5 g	1 g	1.5 g	2 g	2.5 g	3 g	
COD (mg/L)	14600	7600	6200	5200	4300	2600	3200	82.19
BOD_5 (mg/L)	456	267	245	207	171	157	165	65.57
pH	10.77	10.52	10.50	10.49	10.47	10.43	10.45	3.16
TDS (ppm)	5752	4158	3997	3875	3194	2964	3078	48.47
Turbidity (FAU)	1038	94	75	56	31	15	20	98.55
Total Suspended Solid (mg/L)	3.07	0.1	0.1	0.1	0.1	0.06	0.08	98.05

The water quality had improved after applying low-cost adsorbents. After the treatment of wastewater with the prepared low-cost adsorbent, the percentage of reduction in each specific contaminant was determined by varying the dose of the adsorbent. As can be seen from the Table 4.11 to Table 4.13, the adsorbent dosage has a great influence on the removal of contaminants in the textile wastewater. It was observed that the dose of the adsorbent gradually increased so that the removal efficiency of each contaminant was also improved accordingly. However, when the adsorbent dosages were more than 2.5 g, these indicators were stable and even decreased, which indicates that 2.5 g is the optimum dosages for adsorbents and the adsorption has reached saturation. In view of the outcomes, the effluent quality was improved after the treatment process. On increasing adsorbent dosage to 3.0 g, lower adsorption capacity for each pollutant was found. This indicated that the use of 3.0 g or higher dosage of adsorbent could not improve the removal efficiency of dye, which may be due to the availability of more adsorbent surfaces for wastewater contaminants to be adsorbed (Kamboh *et al.*, 2011). The adsorption was a surface phenomenon, where the percentage and degree of adsorption were influenced by the physicochemical properties of this specific adsorbent, such as pore size, surface area, and composition (Kamboh *et al.*, 2009). From the observation and laboratory work, when applied at 2.5 g adsorbent dosage, it was observed that raw banana stem as an adsorbent helped remove COD (62.33%), BOD_5 (48.03%), pH (5.76%), TDS (44.85%), Turbidity (92.10%), Total suspended solid (97.39%). For the case of BC300, it helped remove COD (62.33%), BOD_5 (48.03%), pH (5.76%), TDS (44.85%), Turbidity (90.75%), and Total suspended solid (95.44%). On the other hand, for the case of BC700, it showed the best removal percentage for each of pollutants than raw banana stem and BC300. The adsorbent of BC700 helped remove the COD (82.19%), BOD_5 (65.57%), pH (3.16%), TDS (48.47%), Turbidity (98.55%), and Total suspended solid (98.05%). As a result, it was clear that BC300 caused the least reduction in each pollutant content, which was smaller than the other two adsorbents BC700 and raw banana stem, and BC700 resulted in the highest reduction in the concentration of the pollutants.

4.9.3.1 Reduction in COD and BOD_5

It can be seen from Table 4.11 to Table 4.13 that the COD and BOD_5 of the wastewater are significantly reduced using various dosages of adsorbents. The values of BOD_5 and COD in the original wastewater were very high and the values decreased significantly when the wastewater passed through the adsorption process. From the result, it had been proved that the effective removal of BOD_5 and COD was achieved by the dosage of adsorbent at 2.5 g. It can be interpreted that the reduction in COD and BOD_5 might be due to adsorption of pollutants by adsorbents. At the optimum dosage of 2.5 g, the textile effluent after treatment was significantly reduced with a lower COD value which was 5500 mg/L,6900 mg/L and 2600 mg/L for the raw banana stem, BC300, and BC700, respectively, as compared to the raw wastewater effluent which was 14600 mg/L. The value of COD after treatment was significantly reduced by the raw banana stem, BC300, and BC700 with 62.33%, 52.74% and 82.19%, respectively. For BOD_5, it is evident from the results that the reduction efficiency of BC700 showed the highest reduction percentage with 65.57%. The reductions caused by BC300 and raw banana stem after treatment were 42.11% and 48.03%, respectively. Compared with BC700, it was observed that BC300 showed the poorest reduction efficiency than BC700 and raw banana stem. Overall, the BC700 showed the best reduction efficiency of COD and BOD_5, while BC300 showed the lowest removal efficiency. From Table 4.10, the order of dye removal efficiency was BC700 > raw banana stem > BC300. This corresponds to the efficiency of the removal of BOD_5 and COD. The high porosity in adsorbent could effectively capture and absorb the organic pollutants in the effluent. SEM analysis confirmed that adsorbents has high porosity, thus, adsorbents were able to capture organic pollutants. Dye compounds were decomposed and captured by pores of adsorbents, as well as the elemental chemical behaviour of adsorbents. From the material analysis, it was found that BC700 has high porosity, highest surface area and highest fixed carbon content which will result in the best performance in effluent pollutants reduction. The raw banana stem has a rough, porous surface and abundant functional groups which make it capable to result in reduced value of BOD_5 and COD.

Based on the research done by Baek *et al.* (2010), porous and rough surface offers better adsorption process. Thus, raw banana stem also has favourable morphological conditions for adsorption of pollutants. Besides, BC300 has moderate porosity and fixed carbon. Rajwar and Pandey (2015) stated that adsorbents containing higher carbon content have given better performance in the COD reduction. According to Islam *et al.* (2015), the existence of ethers groups, hydroxyl groups, and aromatic compounds revealed to help in physical adsorption and MB binding is mostly through the O-H and C-O groups. Devi (2010) clarified that the difference between the percentage reductions of pollutants could be attributed to the difference in the number of carbonaceous adsorption sites in the different adsorbents. Srivastava *et al.* (2005) noted that the removal percentage of COD in the pulp mill wastewater was 50% when treated with 2g sugarcane bagasse fly ash adsorbent at pH 4. The interface between effluent pollutants and the prepared adsorbents were highly vital on the adsorption capacity, the adsorption capacity of organic matters onto adsorbent can be improved with the presence of inorganic salts. The charges carried by these salt ions of adsorbent is opposite to the charge of the adsorbed organic ions so that these salt ions can be attracted to the spaces between adjacently adsorbed organic ions and able to reduce the strength of the repulsion of the adjacently adsorbed organic ions (Zhang & Chuang, 2001).

4.9.3.2 Reduction in pH

Based on the pH results, treated wastewater has a pH range from pH 10.15 to 10.43 by the raw banana stem and BC700. It is evident that there is a slight improvement in pH after the adsorption treatment compared to the initial values. The pH of textile effluent reduced to pH 10.15, pH 10.31 and pH 10.43 for the raw banana stem, BC300, and BC700 at the dosage of 2.5 g, respectively. Moreover, the original pH of the raw banana stem, BC300 and BC700 was pH 6.06, pH 7.58 and pH 10.38, respectively. Also, the reduction of MB present in the effluent will reduce the pH value. But, as the adsorbents dose added into wastewater could lead to the pH increase again, thus, the pH showed no significant improvement after the adsorption treatment. From the results, the pH removal percentage of the raw banana stem was better than BC700 and BC300.

4.9.3.3 Reduction in Total Dissolved Solids

After the adsorption treatment, the amount of total dissolved solids was slight improved and less than 50%. There is no significant change as compared to the initial values. This likely due to the fact that after the dyeing process, most of the solids such as wax will be removed and filtered before the wastewater is released into water bodies. Therefore, the remaining total dissolved solids in the wastewater were minimum. Table 4.11 to Table 4.13 shows that the amount of TDS was reduced 44.85%, 37.07% and 48.47% by raw banana stem, BC300, and BC700, respectively. BC700 also was the most effective for the removal of TDS from wastewater while BC300 was least efficient in removing TDS. The order in which TDS was removed and the order in which the dye was removed is also corresponding. The presence of a high level of total dissolved solids is due to inorganic matter present in the effluent. The dissolved solids were not effectively removed after treatment, thus, if the value needs to be significantly reduced, additional methods must be carried out.

4.9.3.4 Reduction in Total Suspended Solids and Turbidity

Total suspended solids and turbidity were the most visible indicators in observing water clarity. They were major parameters used to evaluate the intensity of domestic wastewater and to measure the efficiency of the processing units. As can be seen from Table 4.11 to Table 4.13, the total suspended solids and turbidity showed significant improvement with the applied adsorption treatment. The present study clearly shows that percentage removal of these two parameters was effectively achieved more than

90% at the dosage of 2.5 g. The number of suspended solids was reduced from initial value of 3.07 mg/L to 0.08 mg/L, 0.14 mg/L and 0.06 mg/L by the raw banana stem, BC300, and BC700, respectively. This contributes to a decrease in the turbidity of wastewater effluent from 1038 FAU to 29 FAU, 51 FAU and 13 FAU in treatment with raw banana stem, BC300, and BC700, respectively. Overall, the percentage reductions of turbidity obtained were 92.10%, 90.75% and 98.55% by raw banana stem, BC300, and BC700, respectively, and the percentage of the total suspended solids were 97.39%, 95.44% and 98.05% by raw banana stem, BC300, and BC700, respectively. The dye removal after adsorption treatment resulted in a decrease in the total suspended solids and turbidity in the wastewater. Materials with high porosity, high surface area and functional groups are capable of adsorbing more suspended solids. According to the adsorption capacity of adsorbent in Table 4.10, the BC700 is the best for removing the MB dye from effluent, followed by the raw banana stem and BC300. Therefore, the order of removal efficiency of TSS and turbidity also corresponds to the removal efficiency of dye. BC700 achieved the maximum removal of total suspended solids and turbidity from wastewater due to its high porosity and high surface area. Mahmoued (2010) stated that there is a connection between turbidity and suspended solids. It was concluded that all the adsorbents used have good removal capacity for COD, BOD_5, pH, total dissolved solid, turbidity and TSS. BC700 has high porosity and high surface area, leading to higher adsorption of pollutants in the effluent compared to another two adsorbents. These results could be utilized to develop the design parameters of an adsorption-based industrial wastewater treatment system. The adsorption process provides an effective and alternative effect in the removal of pH, COD, BOD_5, Colour, TDS, TSS and other parameters in the treatment of wastewater using low-cost adsorbents which are readily available and inexpensive (Arumai, 2008). Jatto *et al.* (2010) studied the use of snail shell to treat wastewater from food industry, the result showed that snail shell is effective for removing pollutants from wastewater as the turbidity, COD and BOD_5 decreased (Jatto *et al.*, 2010). Venkateswarlu *et al.* (2007) also illustrated that neem leaf powder can be utilized as an effective low-cost adsorbent to remove organic matters from wastewater.

4.10 Economic Feasibility

One of the key factors that must be considered in preparing the adsorbent was the cost of the adsorbent. In this study, the cost for raw banana stem and biochar as adsorbent were calculated and the results of a simple framework were presented in Table 4.14.

Table 4.14: Cost of preparing raw banana stem and biochars

Process	Charge of Raw Banana Stem (RM)	Charge of Biochars (RM)
Banana stem waste (per kg)	FOC	FOC
Drying (1 hour x 3.0Kw x RM0.218)	0.65	0.65
Grinding Process (1 hour x 4.0Kw x RM0.218)	0.88	0.88
Pyrolysis process (1 hour x 1.8Kw x RM0.218)	0.00	0.39
Total (RM/kg)	1.53	1.92
Activated carbon: 2 USD/kg ≈ 8.7 RM/kg (Oleszczuk *et al.*, 2012).		

The cost of biochar in this study was mainly affected by the consumption of raw banana stem. The agricultural waste was cheap, abundant and environmental-friendly in order to prepare biochar in Malaysia. It is also worth mentioning that the price of biochar is significantly lower as compared to activated carbon. The result of biochar price is in agreement with the findings of Oleszczuk *et al.* (2012) who estimated that biochar is about 10 times cheaper than activated carbon (2 USD/kg), about 8.7 RM/kg. Although activated carbon was very effective in removing dyes from aqueous solution, but the price is too high and some commercial activated carbons are used for the special purpose for which the price will cost more in the domestic and international markets (Sarbani *et al.*, 2016). In terms of economic advantage, the cost of biochar may make it a highly competitive alternative for the purification of dye-contaminated wastewater.

CHAPTER 5: CONCLUSION

This investigation showed that banana stem as an agricultural waste can efficiently be used to remove methylene blue dye. The results showed that raw banana stem, BC300, and BC700 exhibited more than 90% adsorption efficiency at 10 mg/L of methylene blue dye aqueous solution and at 25.15 mg/L of actual dye effluent. Among all of the adsorbents, BC700 was the best in removing methylene blue as it can achieve maximum removal percentage of 98.50% and 98.73% for 10 mg/L of methylene blue dye aqueous solution and 25.15 mg/L of actual dye effluent, respectively. However, these adsorbents were not suitable to remove congo red dye from aqueous solution. The results showed that the properties of biochar are strongly affected by pyrolysis temperature: (i) the yield of the biochar decreased with increasing pyrolysis temperature; (ii) the pH of biochar was significantly increased with increasing pyrolysis temperature. Biochar obtained at a high pyrolysis temperature (700°C) has high surface area, high porosity, high fixed carbon content and high pH. The removal percentage was found to increase with increasing dosage, contact time and agitation speed, but decrease with the increasing initial concentration of methylene blue.

The equilibrium data fitted better with the Langmuir isotherm equation compared to the Freundlich model. The pseudo-second-order kinetic model fitted very well with the dynamical adsorption behaviour of methylene blue dye, thus, the adsorption process is chemisorption. The calculated values of different thermodynamics parameters indicated that the adsorption process is feasible, giving the spontaneous trend for all adsorbents. Furthermore, the adsorbent of the raw banana stem was endothermic in nature while the biochars of BC300 and BC700 was an exothermic process. The desorption study indicated that the dye was firmly adsorbed onto the biochar, it will not cause the secondary pollution to the environment and also it can be reused through the regeneration technology. Hence, biochar is more environment-friendly adsorbent to remove the dye from textile wastewater. The actual dye effluent quality had improved after applying adsorbents, and BC700 resulted in the highest reduction in the concentration of the pollutants. The cost of preparation of raw banana stem and biochars ranged between RM1.53 to RM1.92. As compared to activated carbon, these adsorbents are more viable and economical than activated carbon. Overall, the biochar of banana stem is economical, effective and environment-friendly adsorbent for the removal of textile dyes from wastewater.

REFERENCES

Abdullah, N., Sulaiman, F., & Taib, R. M. (2013). Characterization of banana (Musa spp.) plantation wastes as a potential renewable energy source. *In AIP Conference Proceedings, 1528*(1), 325-330.

Aghayan, H., Mahjoub, A. R., & Khanchi, A. R. (2012). Immobilization of Tin (IV) molybdophosphate onto mesoporous silica SBA-15 and its application on strontium removal from aqueous solution. *Applied Surface Science, 261*, 14-20.

Ahmad, A. L., Harris, W. A., & Ooi, B. S. (2002). Removal of dye from wastewater of textile industry using membrane technology. *Journal of Technology, 36*, 31-44.

Ahmad, M., Lee, S. S., Dou, X., Mohan, D., Sung, J. K., Yang, J. E., & Ok, Y. S. (2012). Effects of pyrolysis temperature on soybean stover and peanut shell derived biochar properties and TCE adsorption in water. *Bioresource Technology, 118*, 536-544.

Ahmad, M., Rajapaksha, A. U., Lim, J. E., Zhang, M., Bolan, N., Mohan, D., ... Ok, Y. S. (2014a). Biochar as a sorbent for contaminant management in soil and water: a review. *Chemosphere, 99*, 19-33.

Ahmad, M. A., Herawan, S. G., & Yusof, A. A. (2014b). Effect of activation time on the pinang frond based activated carbon for remazol brilliant blue removal. *Journal of Mechanical Engineering and Sciences, 7*, 1085-1093.

Ahmad, M. A., Puad, N. A. A., & Bello, O. S. (2014c). Kinetic, equilibrium and thermodynamic studies of synthetic dye removal using pomegranate peel activated carbon prepared by microwave induced KOH activation. *Water Resources and Industry, 6*, 18-35.

Ahn, S. Y., Eom, S. Y., Rhie, Y. H., Sung, Y. M., Moon, C. E., Choi, G. M., & Kim, D. J. (2013). Utilization of wood biomass char in a direct carbon fuel cell (DCFC) system. *Applied Energy, 105*, 207-216.

Aksu, Z., & Tezer, S. (2005). Biosorption of reactive dyes on the green alga chlorella vulgaris. *Process Biochemistry, 40*(3), 1347-1361.

Albadarin, A. B., Mo, J., Glocheux, Y., Allen, S., Walker, G., & Mangwandi, C. (2014). Preliminary investigation of mixed adsorbents for the removal of copper and methylene blue from aqueous solutions. *Chemical Engineering Journal, 255*, 525-534.

Ali, H. (2010). Biodegradation of synthetic dyes-a review. *Water, Air, & Soil Pollution, 213*(1-4), 251-273.

Aljeboree, A. M., Alshirifi, A. N., & Alkaim, A. F. (2014). Kinetics and equilibrium study for the adsorption of textile dyes on coconut shell activated carbon. *Arabian Journal of Chemistry, 10,* 3381-3393.

Alkan, M., & Doğan, M. (2003). Adsorption kinetics of victoria blue onto perlite. *Fresenius Environmental Bulletin, 12*(5), 418-425.

Alkan, M., Demirbaş, Ö., Celikcapa, S., & Doğan, M. (2004). Sorption of acid red 57 from aqueous solution onto sepiolite. *Journal of Hazardous Materials, 116*(1), 135-145.

Allègre, C., Moulin, P., Maisseu, M., & Charbit, F. (2006). Treatment and reuse of reactive dyeing effluents. *Journal of Membrane Science, 269*(1), 15-34.

Allen, S. J., Gan, Q., Matthews, R., & Johnson, P. A. (2003). Comparison of optimised isotherm models for basic dye adsorption by kudzu. *Bioresource Technology, 88*(2), 143-152.

Ameloot, N., Graber, E. R., Verheijen, F. G., & De Neve, S. (2013). Interactions between biochar stability and soil organisms: review and research needs. *European Journal of Soil Science, 64*(4), 379-390.

Angın, D. (2013). Effect of pyrolysis temperature and heating rate on biochar obtained from pyrolysis of safflower seed press cake. *Bioresource Technology, 128*, 593-597.

Annadurai, G., Juang, R. S., & Lee, D. J. (2002). Use of cellulose-based wastes for adsorption of dyes from aqueous solutions. *Journal of Hazardous Materials*, *92*(3), 263-274.

Antal, M. J., & Grønli, M. (2003). The art, science, and technology of charcoal production. *Industrial & Engineering Chemistry Research, 42*(8), 1619-1640.

Ardejani, F. D., Badii, K., Limaee, N. Y., Shafaei, S. Z., & Mirhabibi, A. R. (2008). Adsorption of Direct Red 80 dye from aqueous solution onto almond shells: effect of pH, initial concentration and shell type. *Journal of Hazardous Materials, 151*(2), 730-737.

Arivoli, S., Hema, M., & Prasath, P. M. D. (2009). Adsorption of malachite green onto carbon prepared from borassus bark. *The Arabian Journal for Science and Engineering, 34*(2a).

Arumai, J. P. D. (2008). *Removal of cod and colour from textile wastewater using limestone and activated carbon.* (Published Doctoral Dissertation). The University Sains Malaysia, Malaysia.

Ashfaq, A., & Khatoon, A. (2014). Waste management of textiles: a solution to the environmental pollution. *International Journal of Current Microbiology and Applied Science, 3*(7), 780-787.

Babel, S., & Kurniawan, T. A. (2003). Low-cost adsorbents for heavy metals uptake from contaminated water: a review. *Journal of Hazardous Materials, 97*(1), 219-243.

Babu, B. R., Parande, A. K., Raghu, S., & Kumar, T. P. (2007). Cotton textile processing: waste generation and effluent treatment. *The Journal of Cotton Science, 11*, 141-153.

Baek, M. H., Ijagbemi, C. O., Se-Jin, O., & Kim, D. S. (2010). Removal of malachite green from aqueous solution using degreased coffee bean. *Journal of Hazardous Materials, 176*(1), 820-828.

Bagreev, A., Bandosz, T. J., & Locke, D. C. (2001). Pore structure and surface chemistry of adsorbents obtained by pyrolysis of sewage sludge-derived fertilizer. *Carbon, 39*(13), 1971-1979.

Banat, F., Al-Asheh, S., & Al-Makhadmeh, L. (2003). Evaluation of the use of raw and activated date pits as potential adsorbents for dye containing waters. *Process Biochemistry, 39*(2), 193-202.

Banat, F., Al-Asheh, S., Al-Ahmad, R., & Bni-Khalid, F. (2007). Bench scale and packed bed sorption of methylene blue using treated olive pomace and charcoal. *Bioresource Technology, 98*(16), 3017-3025.

Banerjee, S., Chattopadhyaya, M. C., Srivastava, V., & Sharma, Y. C. (2014). Adsorption studies of methylene blue onto activated saw dust: kinetics, equilibrium, and thermodynamic studies. *Environmental Progress & Sustainable Energy, 33*(3), 790-799.

Bekchanov, M., Lamers, J. P., Karimov, A., & Müller, M. (2012). Estimation of spatial and temporal variability of crop water productivity with incomplete data. *In Cotton, Water, Salts and Soums*, 329-344.

Benaissa, H. (2008). Removal of acid dyes from aqueous solutions using orange peel as a sorbent material. *International Journal of Environment and Pollution, 34*(1-4), 71-82.

Bernd, M., Steffen, W., Karsten, A., & Lübken, M. (2013). EGU general assembly, potential dual use of biochar for wastewater treatment and soil amelioration. *In Geophysical Research Abstracts*, *15*.

Bharathi, K. S., & Ramesh, S. T. (2013). Removal of dyes using agricultural waste as low cost adsorbents: a review. *Applied Water Science, 3*(4), 773-790.

Bhattacharyya, K. G., & Sharma, A. (2004). Adsorption of Pb (II) from aqueous solution by Azadirachta indica (neem) leaf powder. *Journal of Hazardous Materials, 113*(1), 97-109.

Bhattacharyya, K. G., & Sharma, A. (2005). Kinetics and thermodynamics of methylene blue adsorption on neem (Azadirachta indica) leaf powder. *Dyes and Pigments, 65*(1), 51-59.

Boyd, G. E., Schubert, J., & Adamson, A. W. (1947). The exchange adsorption of ions from aqueous solutions by organic zeolites. *Journal of the American Chemical Society, 69*(11), 2818-2829.

Brewer, C. E. (2012). *Biochar characterization and engineering*. (Published Doctoral Dissertation). The Iowa State University, United States.

Brick, S., & Lyutse, S. (2010). Biochar: assessing the promise and risks to guide US policy. *Natural Resource Defence Council, USA.*

Brown, R. A., Kercher, A. K., Nguyen, T. H., Nagle, D. C., & Ball, W. P. (2006). Production and characterization of synthetic wood chars for use as surrogates for natural sorbents. *Organic Geochemistry, 37*(3), 321-333.

Brown, R. (2009). Biochar production technology. *Biochar for Environmental Management: Science and Technology,* 127-146.

Bulut, Y., & Karaer, H. (2015). Adsorption of methylene blue from aqueous solution by crosslinked chitosan/bentonite composite. *Journal of Dispersion Science and Technology, 36*(1), 61-67.

Cao, X., Ma, L., Gao, B., & Harris, W. (2009). Dairy manure derived biochar effectively sorbs lead and atrazine. *Environmental Science & Technology, 43*(9), 3285-3291.

Cao, X., & Harris, W. (2010). Properties of dairy-manure-derived biochar pertinent to its potential use in remediation. *Bioresource Technology, 101*(14), 5222-5228.

Capunitan, J. A., & Capareda, S. C. (2012). Assessing the potential for biofuel production of corn stover pyrolysis using a pressurized batch reactor. *Fuel, 95*, 563-572.

Chatterjee, S., Lee, D. S., Lee, M. W., & Woo, S. H. (2009). Enhanced adsorption of congo red from aqueous solutions by chitosan hydrogel beads impregnated with cetyl trimethyl ammonium bromide. *Bioresource Technology, 100*(11), 2803-2809.

Chandra, T. C., Mirna, M. M., Sudaryanto, Y., & Ismadji, S. (2007). Adsorption of basic dye onto activated carbon prepared from durian shell: Studies of adsorption equilibrium and kinetics. *Chemical Engineering Journal, 127*(1), 121-129.

Chen, J., Liu, M., Zhang, J., Xian, Y., & Jin, L. (2003). Electrochemical degradation of bromopyrogallol red in presence of cobalt ions. *Chemosphere, 53*(9), 1131-1136.

Chen, X., Chen, G., Chen, L., Chen, Y., Lehmann, J., McBride, M. B., & Hay, A. G. (2011). Adsorption of copper and zinc by biochars produced from pyrolysis of hardwood and corn straw in aqueous solution. *Bioresource Technology, 102*(19), 8877-8884.

Chen, Z., Chen, B., Zhou, D., & Chen, W. (2012a). Bisolute sorption and thermodynamic behavior of organic pollutants to biomass-derived biochars at two pyrolytic temperatures. *Environmental Science & Technology, 46*(22), 12476-12483.

Chen, Z., Zhou, L., Zhang, F., Yu, C., & Wei, Z. (2012b). Multicarboxylic hyperbranched polyglycerol modified SBA-15 for the adsorption of cationic dyes and copper ions from aqueous media. *Applied Surface Science, 258*(13), 5291-5298.

Cheng, G., Sun, L., Jiao, L., Peng, L. X., Lei, Z. H., Wang, Y. X., & Lin, J. (2013). Adsorption of methylene blue by residue biochar from copyrolysis of dewatered sewage sludge and pine sawdust. *Desalination and Water Treatment, 51*(37-39), 7081-7087.

Chowdhury, S., & Saha, P. (2010). Sea shell powder as a new adsorbent to remove basic green 4 (malachite green) from aqueous solutions: equilibrium, kinetic and thermodynamic studies. *Chemical Engineering Journal, 164*(1), 168-177.

Chun, H. (2010). *A novel functionalized ordered mesoporous carbon as an efficient adsorbent for dye removal from water.* (Published Doctoral Dissertation). The Hong Kong University of Science and Technology, Hong Kong.

Couto, S. R. (2009). Dye removal by immobilised fungi. *Biotechnology Advances, 27*(3), 227-235.

Cowie, A. L., Downie, A. E., George, B. H., Singh, B. P., Van Zwieten, L., & O'Connell, D. (2012). Is sustainability certification for biochar the answer to environmental risks?. *Pesquisa Agropecuária Brasileira, 47*(5), 637-648.

Crini, G. (2006). Non conventional low cost adsorbents for dye removal: a review. *Bioresource Technology, 97*(9), 1061-1085.

Crini, G., Peindy, H. N., Gimbert, F., & Robert, C. (2007). Removal of CI basic green 4 (malachite green) from aqueous solutions by adsorption using cyclodextrin based adsorbent: Kinetic and equilibrium studies. *Separation and Purification Technology, 53*(1), 97-110.

Crini, G., & Badot, P. M. (2008). Application of chitosan, a natural aminopolysaccharide, for dye removal from aqueous solutions by adsorption processes using batch studies: a review of recent literature. *Progress in Polymer Science, 33*(4), 399-447.

Dawood, S., & Sen, T. K. (2012). Removal of anionic dye congo red from aqueous solution by raw pine and acid-treated pine cone powder as adsorbent: equilibrium, thermodynamic, kinetics, mechanism and process design. *Water Research, 46*(6), 1933-1946.

Demirbaş, A., & Arin, G. (2002). An overview of biomass pyrolysis. *Energy Sources, 24*(5), 471-482.

Demirbaş, A. (2009). Agricultural based activated carbons for the removal of dyes from aqueous solutions: a review. *Journal of Hazardous Materials, 167*(1), 1-9.

Demirbaş, Ö., & Alkan, M. (2015). Adsorption kinetics of a cationic dye from wastewater. *Desalination and Water Treatment, 53*(13), 3623-3631.

Dehkhoda, A. M., West, A. H., & Ellis, N. (2010). Biochar based solid acid catalyst for biodiesel production. *Applied Catalysis A: General, 382*(2), 197-204.

Devi, R. (2010). Innovative technology of COD and BOD reduction from coffee processing wastewater using avocado seed carbon (ASC). *Water, Air, & Soil Pollution, 207*(1-4), 299-306.

Doğan, M., Alkan, M., Türkyilmaz, A., & Özdemir, Y. (2004). Kinetics and mechanism of removal of methylene blue by adsorption onto perlite. *Journal of Hazardous Materials, 109*(1), 141-148.

Dooley, K. L. (2015). *Slow pyrolysis biochar from forestry residue and municipal and farm wastes: characterization and their use in greenhouses as a soil amendment.* (Published Doctoral Dissertation). Memorial University of Newfoundland.

Dong, X., Ma, L. Q., & Li, Y. (2011). Characteristics and mechanisms of hexavalent chromium removal by biochar from sugar beet tailing. *Journal of Hazardous Materials, 190*(1), 909-915.

EPA. (2004). *Technical support document for the 2004 effluent guidelines program plan*. U.S Environment Protection Agency.

Ertugay, N., & Malkoc, E. (2014). Adsorption isotherm, kinetic, and thermodynamic studies for methylene blue from aqueous solution by needles of pinus sylvestris L. *Polish Journal of Environmental Studies, 23*(6), 1995-2006.

Fan, S., Tang, J., Wang, Y., Li, H., Zhang, H., Tang, J., ... Li, X. (2016). Biochar prepared from co-pyrolysis of municipal sewage sludge and tea waste for the adsorption of methylene blue from aqueous solutions: kinetics, isotherm, thermodynamic and mechanism. *Journal of Molecular Liquids, 220*, 432-441.

Feng, Y., Yang, F., Wang, Y., Ma, L., Wu, Y., Kerr, P. G., & Yang, L. (2011). Basic dye adsorption onto an agro-based waste material-Sesame hull (Sesamum indicum L.). *Bioresource Technology, 102*(22), 10280-10285.

Feng, Y., Dionysiou, D. D., Wu, Y., Zhou, H., Xue, L., He, S., & Yang, L. (2013). Adsorption of dyestuff from aqueous solutions through oxalic acid-modified swede rape straw: adsorption process and disposal methodology of depleted bioadsorbents. *Bioresource Technology, 138*, 191-197.

Fernandes, A. N., Almeida, C. A. P., Menezes, C. T. B., Debacher, N. A., & Sierra, M. M. D. (2007). Removal of methylene blue from aqueous solution by peat. *Journal of Hazardous Materials, 144*(1), 412-419.

Fersi, C., Gzara, L., & Dhahbi, M. (2005). Treatment of textile effluents by membrane technologies. *Desalination, 185*(1-3), 399-409.

Fidel, R. (2012). *Evaluation and implementation of methods for quantifying organic and inorganic components of biochar alkalinity.* (Published Master's Thesis). The Iowa State university, United States.

Foo, K. Y., & Hameed, B. H. (2010). An overview of dye removal via activated carbon adsorption process. *Desalination and Water Treatment, 19*(1-3), 255-274.

Freundlich, H. M. F. (1906). Over the adsorption in solution. *The Journal of Physical Chemistry, 57*, 385-470.

Fu, Y., & Viraraghavan, T. (2002). Removal of congo red from an aqueous solution by fungus aspergillus niger. *Advances in Environmental Research, 7*(1), 239-247.

Fu, P., Yi, W., Bai, X., Li, Z., Hu, S., & Xiang, J. (2011). Effect of temperature on gas composition and char structural features of pyrolyzed agricultural residues. *Bioresource Technology, 102*(17), 8211-8219.

Fytianos, K., Voudrias, E., & Kokkalis, E. (2000). Sorption-desorption behaviour of 2, 4-dichlorophenol by marine sediments. *Chemosphere, 40*(1), 3-6.

Gao, Q., Liu, H., Cheng, C., Li, K., Zhang, J., Zhang, C., & Li, Y. (2013). Preparation and characterization of activated carbon from wool waste and the comparison of muffle furnace and microwave heating methods. *Powder Technology, 249*, 234-240.

Garg, V. K., Amita, M., Kumar, R., & Gupta, R. (2004). Basic dye (methylene blue) removal from simulated wastewater by adsorption using Indian Rosewood sawdust: a timber industry waste. *Dyes and Pigments, 63*(3), 243-250.

Ge, P., & Li, F. (2011). Kinetics and thermodynamics of heavy metal Cu (II) adsorption on mesoporous silicates. *Polish Journal of Environment Studies, 20*, 339-344.

Ghezzehei, T. A., Sarkhot, D. V., & Berhe, A. A. (2014). Biochar can be used to capture essential nutrients from dairy wastewater and improve soil physico-chemical properties. *Solid Earth, 5*(2), 953-962.

Ghoreishi, S. M., & Haghighi, R. (2003). Chemical catalytic reaction and biological oxidation for treatment of non-biodegradable textile effluent. *Chemical Engineering Journal, 95*(1), 163-169.

Ghosh, P. K., & Philip, L. (2005). Performance evaluation of waste activated carbon on atrazine removal from contaminated water. *Journal of Environmental Science and Health, Part B, 40*(3), 425-441.

Gil, M. V., Martínez, M., García, S., Rubiera, F., Pis, J. J., & Pevida, C. (2013). Response surface methodology as an efficient tool for optimizing carbon adsorbents for CO_2 capture. *Fuel Processing Technology, 106*, 55-61.

Giwa, A. A., Bello, I. A., & Olajire, A. (2013). Removal of basic dye from aqueous solution by adsorption on melon husk in binary and ternary systems. *Chemical and Process Engineering Research, 13*(1), 51-68.

Goh, K. H., Lim, T. T., & Dong, Z. (2008). Application of layered double hydroxides for removal of oxyanions: a review. *Water Research, 42*(6), 1343-1368.

Gong, R., Sun, Y., Chen, J., Liu, H., & Yang, C. (2005). Effect of chemical modification on dye adsorption capacity of peanut hull. *Dyes and Pigments, 67*(3), 175-181.

González, P. G., Hernández-Quiroz, T., & García-González, L. (2014). The use of experimental design and response surface methodologies for the synthesis of chemically activated carbons produced from bamboo. *Fuel Processing Technology, 127*, 133-139.

Grande, G. A. (2015). *Treatment of wastewater from textile dyeing by ozonization.* (Published Doctoral Dissertation). The Polytechnic University of Turin, Italy.

Gul, S., Whalen, J. K., Thomas, B. W., Sachdeva, V., & Deng, H. (2015). Physico-chemical properties and microbial responses in biochar-amended soils: mechanisms and future directions. *Agriculture, Ecosystems & Environment, 206*, 46-59.

Gupta, V. K., Mittal, A., Krishnan, L., & Gajbe, V. (2004). Adsorption kinetics and column operations for the removal and recovery of malachite green from wastewater using bottom ash. *Separation and Purification Technology, 40*(1), 87-96.

Gupta, V. K. (2009). Application of low-cost adsorbents for dye removal-A review. *Journal of Environmental Management, 90*(8), 2313-2342.

Gürses, A., Doğar, Ç., Yalçın, M., Açıkyıldız, M., Bayrak, R., & Karaca, S. (2006). The adsorption kinetics of the cationic dye, methylene blue, onto clay. *Journal of Hazardous Materials, 131*(1), 217-228.

Haefele, S. M., Konboon, Y., Wongboon, W., Amarante, S., Maarifat, A. A., Pfeiffer, E. M., & Knoblauch, C. (2011). Effects and fate of biochar from rice residues in rice-based systems. *Field Crops Research, 121*(3), 430-440.

Hale, S. E., Lehmann, J., Rutherford, D., Zimmerman, A. R., Bachmann, R. T., Shitumbanuma, V., ... Cornelissen, G. (2012). Quantifying the total and bioavailable polycyclic aromatic hydrocarbons and dioxins in biochars. *Environmental Science & Technology, 46*(5), 2830-2838.

Hameed, B. H., Ahmad, A. L., & Latiff, K. N. A. (2007). Adsorption of basic dye (methylene blue) onto activated carbon prepared from rattan sawdust. *Dyes and Pigments, 75*(1), 143-149.

Hameed, B. H., & El-Khaiary, M. I. (2008a). Batch removal of malachite green from aqueous solutions by adsorption on oil palm trunk fibre: equilibrium isotherms and kinetic studies. *Journal of Hazardous Materials, 154*(1), 237-244.

Hameed, B. H., & EI-Khaiary, M. I. (2008b). Sorption kinetics and isotherm studies of a cationic dye using agricultural waste: broad bean peels. *Journal of Hazardous Materials, 154*(1), 639-648.

Hameed, B. H., & EI-Khaiary, M. I. (2008c). Malachite green adsorption by rattan sawdust: Isotherm, kinetic and mechanism modeling. *Journal of Hazardous Materials, 159*(2), 574-579.

Hameed, B. H., & Hakimi, H. (2008). Utilization of durian (durio zibethinus murray) peel as low cost sorbent for the removal of acid dye from aqueous solutions. *Biochemical Engineering Journal, 39*(2), 338-343.

Hameed, B. H., Mahmoud, D. K., & Ahmad, A. L. (2008). Sorption equilibrium and kinetics of basic dye from aqueous solution using banana stalk waste. *Journal of Hazardous Materials, 158*(2), 499-506.

Han, R., Zou, W., Yu, W., Cheng, S., Wang, Y., & Shi, J. (2007). Biosorption of methylene blue from aqueous solution by fallen phoenix tree's leaves. *Journal of Hazardous Materials, 141*(1), 156-162.

Hao, W., Björkman, E., Lilliestråle, M., & Hedin, N. (2013). Activated carbons prepared from hydrothermally carbonized waste biomass used as adsorbents for CO_2. *Applied Energy, 112*, 526-532.

Hassan, A. F., Abdel-Mohsen, A. M., & Fouda, M. M. (2014). Comparative study of calcium alginate, activated carbon, and their composite beads on methylene blue adsorption. *Carbohydrate Polymers, 102*, 192-198.

Hossain, M. K., Strezov, V., Chan, K. Y., Ziolkowski, A., & Nelson, P. F. (2011). Influence of pyrolysis temperature on production and nutrient properties of wastewater sludge biochar. *Journal of Environmental Management, 92*(1), 223-228.

Houben, D., Evrard, L., & Sonnet, P. (2013). Mobility, bioavailability and pH dependent leaching of cadmium, zinc and lead in a contaminated soil amended with biochar. *Chemosphere, 92*(11), 1450-1457.

Hu, Z. P., Gao, Z. M., Liu, X., & Yuan, Z. Y. (2017). High-surface-area activated red mud for efficient removal of methylene blue from wastewater. *Adsorption Science & Technology, 0*(0), 1-18.

Huang, Y., Baosheng, J. I. N., Zhong, Z., Zhong, W., & Rui, X. I. A. O. (2008). Characteristic and mercury adsorption of activated carbon produced by CO_2 of chicken waste. *Journal of Environmental Sciences, 20*(3), 291-296.

Huang, C. H., Chang, K. P., Ou, H. D., Chiang, Y. C., & Wang, C. F. (2011). Adsorption of cationic dyes onto mesoporous silica. *Microporous and Mesoporous Materials, 141*(1), 102-109.

Hunger, K. (Ed.). (2007). *Industrial dyes: chemistry, properties, applications.* John Wiley & Sons.

Ioannidou, O., & Zabaniotou, A. (2007). Agricultural residues as precursors for activated carbon production-a review. *Renewable and Sustainable Energy Reviews, 11*(9), 1966-2005.

Islam, M. A., Tan, I. A. W., Benhouria, A., Asif, M., & Hameed, B. H. (2015). Mesoporous and adsorptive properties of palm date seed activated carbon prepared via sequential hydrothermal carbonization and sodium hydroxide activation. *Chemical Engineering Journal, 270*, 187-195.

Jaafar, S. N. S. (2006). *Adsorption study-dye removal using clay.* (Published Doctoral Dissertation). The University College of Engineering & Technology Malaysia, Pahang.

Jain, S., & Jayaram, R. V. (2010). Removal of basic dyes from aqueous solution by low-cost adsorbent: Wood apple shell (Feronia acidissima). *Desalination, 250*(3), 921-927.

Jain, A. K., Gupta, V. K., Bhatnagar, A., & Jain, S. (2003). A comparative assessment of adsorbents prepared from industrial wastes for the removal of cationic dye. *Journal of the Indian Chemical Society, 80*(4), 267-270.

Jatto, E. O., Asia, I. O., Egbon, E. E., Otutu, J. O., Chukwuedo, M. E., & Ewansiha, C. J. (2010). Treatment of waste water from food industry using snail shell. *Academia Arena, 2*(1), 32-36.

Jayarajan, M., Arunachalam, R., & Annadurai, G. (2011). Use of low cost nano-porous materials of pomelo fruit peel wastes in removal of textile dye. *Research Journal of Environmental Sciences, 5*(5), 434-443.

Jin, X. C., Liu, G. Q., Xu, Z. H., & Tao, W. Y. (2007). Decolourization of a dye industry effluent by aspergillus fumigatus XC6. *Applied Microbiology and Biotechnology, 74*(1), 239-243.

Jindo, K., Mizumoto, H., Sawada, Y., & Sonoki, T. (2014). Physical and chemical characterization of biochars derived from different agricultural residues. *Biogeosciences, 11*(23), 6613-6621.

Joseph, S., & Lehmann, J. (2009). *Biochar for environmental management: science and technology*. London, GB: Earthscan.

Joshi, M., Bansal, R., & Purwar, R. (2004). Colour removal from textile effluents. *Indian Journal of Fibre & Textile Research, 29*(2), 239-259.

Kadirvelu, K., Kavipriya, M., Karthika, C., Radhika, M., Vennilamani, N., & Pattabhi, S. (2003). Utilization of various agricultural wastes for activated carbon preparation and application for the removal of dyes and metal ions from aqueous solutions. *Bioresource Technology, 87*(1), 129-132.

Kamboh, M. A., Solangi, I. B., Sherazi, S. T. H., & Memon, S. (2009). Synthesis and application of calix [4] arene based resin for the removal of azo dyes. *Journal of Hazardous Materials, 172*(1), 234-239.

Kamboh, M. A., Solangi, I. B., Sherazi, S. T. H., & Memon, S. (2011). Synthesis and application of p-tert-butylcalix [8] arene immobilized material for the removal of azo dyes. *Journal of Hazardous Materials, 186*(1), 651-658.

Kannan, N., & Sundaram, M. M. (2001). Kinetics and mechanism of removal of methylene blue by adsorption on various carbons-a comparative study. *Dyes and Pigments, 51*(1), 25-40.

Kannan, C., Buvaneswari, N., & Palvannan, T. (2009). Removal of plant poisoning dyes by adsorption on tomato plant root and green carbon from aqueous solution and its recovery. *Desalination, 249*(3), 1132-1138.

Kanawade, S. M., Gaikwad, R. W., & Misal, A. (2010). Low cost sugarcane bagasse ash as an adsorbent for dye removal from dye effluent. *International Journal of Chemical Engineering and Applications, 1*(4), 309-318.

Karim, A. A., Kumar, M., Mohapatra, S., Panda, C. R., & Singh, A. (2015). Banana Peduncle Biochar: Characteristics and Adsorption of Hexavalent Chromium from Aqueous Solution. *International Research Journal of Pure & Applied Chemistry, 7*(1), 1-10.

Kastner, J. R., Miller, J., Geller, D. P., Locklin, J., Keith, L. H., & Johnson, T. (2012). Catalytic esterification of fatty acids using solid acid catalysts generated from biochar and activated carbon. *Catalysis Today, 190*(1), 122-132.

Kaur, S., Walia, T. P. S., & Kaur, R. (2008). Removal of health hazards causing acidic dyes from aqueous solutions by the process of adsorption. *Online Journal of Health and Allied Sciences, 6*(3).

Kdasi, A. A., Idris, A., Saed, K., & Guan, C. T. (2004). Treatment of textile wastewater by advanced oxidation processes-a review. *Global Nest: The International Journal, 6*(3), 222-230.

Keiluweit, M., Nico, P. S., Johnson, M. G., & Kleber, M. (2010). Dynamic molecular structure of plant biomass-derived black carbon (biochar). *Environmental Science & Technology, 44*(4), 1247-1253.

Keleşoğlu, S. (2007). *Comparative adsorption studies of heavy metal ions on chitin and chitosan biopolymers.* (Published Master's Thesis). İzmir Institute of Technology, Turkey.

Khalil, H. S. A., Alwani, M. S., & Omar, A. K. M. (2007). Chemical composition, anatomy, lignin distribution, and cell wall structure of Malaysian plant waste fibers. *BioResources, 1*(2), 220-232.

Khanmohammadi, Z., Afyuni, M., & Mosaddeghi, M. R. (2015). Effect of pyrolysis temperature on chemical and physical properties of sewage sludge biochar. *Waste Management & Research, 33*(3), 275-283.

Khataee, A. R., Vafaei, F., & Jannatkhah, M. (2013). Biosorption of three textile dyes from contaminated water by filamentous green algal spirogyra sp.: kinetic, isotherm and thermodynamic studies. *International Biodeterioration & Biodegradation, 83*, 33-40.

Khattri, S. D., & Singh, M. K. (2009). Removal of malachite green from dye wastewater using neem sawdust by adsorption. *Journal of Hazardous Materials, 167*(1), 1089-1094.

Kim, T. H., Park, C., Yang, J., & Kim, S. (2004). Comparison of disperse and reactive dye removals by chemical coagulation and fenton oxidation. *Journal of Hazardous Materials, 112*(1), 95-103.

Kornaros, M., & Lyberatos, G. (2006). Biological treatment of wastewaters from a dye manufacturing company using a trickling filter. *Journal of Hazardous Materials*, *136*(1), 95-102.

Kulyk, N. (2012). *Cost-benefit analysis of the biochar application in the US cereal crop cultivation.* (Published Master's Thesis). University of Massachusetts, Amherst.

Kumar, K. V., & Sivanesan, S. (2006). Equilibrium data, isotherm parameters and process design for partial and complete isotherm of methylene blue onto activated carbon. *Journal of Hazardous Materials, 134*(1), 237-244.

Kumar, R., & Ahmad, R. (2011). Biosorption of hazardous crystal violet dye from aqueous solution onto treated ginger waste (TGW). *Desalination, 265*(1), 112-118.

Kumar, M. R., Koushik, C. V., & Saravanan, K. (2013). Textile wastewater treatment using reverse osmosis and SDI. *Elixir Chemical Engineering International Journal, 54A*, 12713-12717.

Kushwaha, S., Sreedhar, B., & Sudhakar, P. P. (2012). A spectroscopic study for understanding the speciation of Cr on palm shell based adsorbents and their application for the remediation of chrome plating effluents. *Bioresource Technology, 116*, 15-23.

Laird, D. A., Brown, R. C., Amonette, J. E., & Lehmann, J. (2009). Review of the pyrolysis platform for coproducing bio-oil and biochar. *Biofuels, Bioproducts and Biorefining, 3*(5), 547-562.

Lam, L. Y. F. (2005). *Development of MCM-41 based catalysts for the photo-fenton's degradation of dye pollutants.* (Published Doctoral Dissertation). University of Science and Technology, Hong Kong.

Langmuir, I. (1917). The constitution and fundamental properties of solids and liquids. *Journal of the Franklin Institute, 183*(1), 102-105.

Lee, J. W., Choi, S. P., Thiruvenkatachari, R., Shim, W. G., & Moon, H. (2006). Evaluation of the performance of adsorption and coagulation processes for the maximum removal of reactive dyes. *Dyes and Pigments, 69*(3), 196-203.

Lee, Y., Park, J., Ryu, C., Gang, K. S., Yang, W., Park, Y. K., Jung, J., & Hyun, S. (2013). Comparison of biochar properties from biomass residues produced by slow pyrolysis at 500 ºC. *Bioresource Technology, 148*, 196-201.

Lehmann, J., Gaunt, J., & Rondon, M. (2006). Biochar sequestration in terrestrial ecosystems-a review. *Mitigation and Adaptation Strategies for Global Change, 11*(2), 395-419.

Lehmann, J. (2009). Terra Preta Nova-where to from here. *In Amazonian dark earths: Wim Sombroek's vision* (pp. 473-486). Dordrecht: Springer Science.

Lehmann, J., Rillig, M. C., Thies, J., Masiello, C. A., Hockaday, W. C., & Crowley, D. (2011). Biochar effects on soil biota–a review. *Soil Biology and Biochemistry, 43*(9), 1812-1836.

Li, K., Zheng, Z., & Li, Y. (2010). Characterization and lead adsorption properties of activated carbons prepared from cotton stalk by one-step H_3PO_4 activation. *Journal of Hazardous Materials, 181*(1), 440-447.

Li, W. H., Yue, Q. Y., Gao, B. Y., Ma, Z. H., Li, Y. J., & Zhao, H. X. (2011). Preparation and utilization of sludge-based activated carbon for the adsorption of dyes from aqueous solutions. *Chemical Engineering Journal, 171*(1), 320-327.

Liang, B., Lehmann, J., Solomon, D., Kinyangi, J., Grossman, J., O'neill, B., & Neves,

E. G. (2006). Black carbon increases cation exchange capacity in soils. *Soil Science Society of America Journal, 70*(5), 1719-1730.

Libra, J. A., Ro, K. S., Kammann, C., Funke, A., Berge, N. D., Neubauer, Y., ... Emmerich, K. H. (2011). Hydrothermal carbonization of biomass residuals: a comparative review of the chemistry, processes and applications of wet and dry pyrolysis. *Biofuels, 2*(1), 71-106.

Lima, I. M., Boateng, A. A., & Klasson, K. T. (2010). Physicochemical and adsorptive properites of fast-pyrolysis biochars and their steam activated counterparts. *Journal of Chemical Technology and Biotechnology, 85*(11), 1515-1521.

Lin, Y., He, X., Han, G., Tian, Q., & Hu, W. (2011). Removal of crystal violet from aqueous solution using powdered mycelial biomass of ceriporia lacerata P2. *Journal of Environmental Sciences, 23*(12), 2055-2062.

Liu, Z., & Zhang, F. S. (2009). Removal of lead from water using biochars prepared from hydrothermal liquefaction of biomass. *Journal of Hazardous Materials, 167*(1), 933-939.

Mahmoodi, N. M., Hayati, B., Arami, M., & Lan, C. (2011). Adsorption of textile dyes on pine cone from coloured wastewater: kinetic, equilibrium and thermodynamic studies. *Desalination, 268*(1), 117-125.

Mahmoodi, N. M., Arami, M., Bahrami, H., & Khorramfar, S. (2010). Novel biosorbent (Canola hull): surface characterization and dye removal ability at different cationic dye concentrations. *Desalination, 264*(1), 134-142.

Mahmoud, D. K., Salleh, M. A. M., Karim, W. A. W. A., Idris, A., & Abidin, Z. Z. (2012). Batch adsorption of basic dye using acid treated kenaf fibre char: equilibrium, kinetic and thermodynamic studies. *Chemical Engineering Journal, 181*, 449-457.

Mahmoued, E. K. (2010). Cement kiln dust and coal filters treatment of textile industrial effluents. *Desalination, 255*(1), 175-178.

Maiti, S., Dey, S., Purakayastha, S., & Ghosh, B. (2006). Physical and thermochemical characterization of rice husk char as a potential biomass energy source. *Bioresource Technology, 97*(16), 2065-2070.

Malamis, S., & Katsou, E. (2013). A review on zinc and nickel adsorption on natural and modified zeolite, bentonite and vermiculite: examination of process parameters, kinetics and isotherms. *Journal of Hazardous Materials, 252*, 428-461.

Malash, G. F., & El-Khaiary, M. I. (2010). Methylene blue adsorption by the waste of Abu-Tartour phosphate rock. *Journal of Colloid and Interface Science, 348*(2), 537-545.

Malkoc, E., & Nuhoglu, Y. (2006). Removal of Ni (II) ions from aqueous solutions using waste of tea factory: Adsorption on a fixed-bed column. *Journal of Hazardous Materials, 135*(1), 328-336.

Mani, S., Kastner, J. R., & Juneja, A. (2013). Catalytic decomposition of toluene using a biomass derived catalyst. *Fuel Processing Technology, 114*, 118-125.

Manocha, S., Bhagat, J., Patel, M., Patel, N., & Manocha, L. (2000). Adsorption behavior of carbons from biomass. *In Adsorption Science and Technology,* 727-731.

Mansour, H. B., Houas, I., Montassar, F., Ghedira, K., Barillier, D., Mosrati, R., & Chekir-Ghedira, L. (2012). Alteration of in vitro and acute in vivo toxicity of textile dyeing wastewater after chemical and biological remediation. *Environmental Science and Pollution Research, 19*(7), 2634-2643.

Martin, M. J., Artola, A., Balaguer, M. D., & Rigola, M. (2003). Activated carbons developed from surplus sewage sludge for the removal of dyes from dilute aqueous solutions. *Chemical Engineering Journal*, *94*(3), 231-239.

Mayes, W. M., Younger, P. L., & Aumo, J. (2006). Buffering of alkaline steel slag leachate across a natural wetland. *Environmental Science & Technology, 40*(4), 1237-1243.

Mckay, G., & Poots, V. J. (1980). Kinetics and diffusion processes in colour removal from effluent using wood as an adsorbent. *Journal of Chemical Technology and Biotechnology, 30*(1), 279-292.

Mckay, G., Porter, J. F., & Prasad, G. R. (1999). The removal of dye colours from aqueous solutions by adsorption on low-cost materials. *Water, Air, & Soil Pollution, 114*(3), 423-438.

Meng, J., Feng, X., Dai, Z., Liu, X., Wu, J., & Xu, J. (2014). Adsorption characteristics of Cu (II) from aqueous solution onto biochar derived from swine manure. *Environmental Science and Pollution Research, 21*(11), 7035-7046.

Meriç, S., Selçuk, H., & Belgiorno, V. (2005). Acute toxicity removal in textile finishing wastewater by fenton's oxidation, ozone and coagulation–flocculation processes. *Water Research, 39*(6), 1147-1153.

Mészáros, E., Jakab, E., Várhegyi, G., Bourke, J., Manley-Harris, M., Nunoura, T., & Antal, M. J. (2007). Do all carbonized charcoals have the same chemical structure? Implications of thermogravimetry mass spectrometry measurements. *Industrial & Engineering Chemistry Research, 46*(18), 5943-5953.

Mianwu, L. Q. L. Q. M., Caiyan, Z. Y. J. X. K., & Siyu, H. (2011). Study on preparation of rice husk-based activated carbon and its adsorption of methylene blue. *Chinese Journal of Environmental Engineering, 11*, 009.

MIDA (Malaysian Investment Development Authority). (2015). *Industries in Malaysia: textilea and apparels industry.* Retrieved from: http://www.mida.gov.my/env3/index.php?page=textiles and apparel industry.

MITI (Ministry of International Trade and Industry, Malaysia. (2006). *Third industrial master plan (IMP3)*, Kuala Lumpur.

Mohammed, M. A. A., Salmiaton, A., Azlina, W. W., Amran, M. M., Fakhru'l-Razi, A., & Taufiq-Yap, Y. H. (2011). Hydrogen rich gas from oil palm biomass as a potential source of renewable energy in Malaysia. *Renewable and Sustainable Energy Reviews, 15*(2), 1258-1270.

Mohan, D., Pittman, C. U., & Steele, P. H. (2006). Pyrolysis of wood/biomass for bio-oil: a critical review. *Energy & Fuels, 20*(3), 848-889.

Mohan, D., Sarswat, A., Ok, Y. S., & Pittman, C. U. (2014). Organic and inorganic contaminants removal from water with biochar, a renewable, low cost and sustainable adsorbent–a critical review. *Bioresource Technology, 160*, 191-202.

Morali, E. K. (2010). *Ozonation of a denim producing textile industry wastewater-process optimization.* (Published Doctoral Dissertation). Middle East Technical University, Turkey.

Mui, E. L., Cheung, W. H., Valix, M., & McKay, G. (2010). Dye adsorption onto char from bamboo. *Journal of Hazardous Materials, 177*(1), 1001-1005.

Mukherjee, A., Zimmerman, A. R., & Harris, W. (2011). Surface chemistry variations among a series of laboratory-produced biochars. *Geoderma, 163*(3), 247-255.

Murage, E. W., Voroney, P., & Beyaert, R. P. (2007). Turnover of carbon in the free light fraction with and without charcoal as determined using the 13C natural abundance method. *Geoderma, 138*(1), 133-143.

Namasivayam, C., & Kavitha, D. (2002). Removal of congo red from water by adsorption onto activated carbon prepared from coir pith, an agricultural solid waste. *Dyes and Pigments, 54*(1), 47-58.

Namasivayam, C., & Sumithra, S. (2005). Removal of direct red 12B and methylene blue from water by adsorption onto Fe (III)/Cr (III) hydroxide, an industrial solid waste. *Journal of Environmental Management, 74*(3), 207-215.

Nartey, O. D., & Zhao, B. (2014). Biochar preparation, characterization, and adsorptive capacity and its effect on bioavailability of contaminants: an overview. *Advances in Materials Science and Engineering, 10*(1), 1-12.

Nasuha, N., Zurainan, H. Z., Maarof, H. I., Zubir, N. A., & Amri, N. (2011). Effect of cationic and anionic dye adsorption from aqueous solution by using chemically modified papaya seed. *In International Conference on Environment Science and Engineering, 8*, 50-54.

Nethaji, S., Sivasamy, A., Thennarasu, G., & Saravanan, S. (2010). Adsorption of malachite green dye onto activated carbon derived from borassus aethiopum flower biomass. *Journal of Hazardous Materials, 181*(1), 271-280.

Nethaji, S., & Sivasamy, A. (2011). Adsorptive removal of an acid dye by lignocellulosic waste biomass activated carbon: equilibrium and kinetic studies. *Chemosphere, 82*(10), 1367-1372.

Oh, T. K., Choi, B., Shinogi, Y., & Chikushi, J. (2012). Effect of pH conditions on actual and apparent fluoride adsorption by biochar in aqueous phase. W*ater, Air, & Soil Pollution, 223*(7), 3729-3738.

Oladoja, N. A., Aboluwoye, C. O., & Oladimeji, Y. B. (2009). Kinetics and isotherm studies on methylene blue adsorption onto ground palm kernel coat. *Turkish Journal of Engineering and Environmental Sciences, 32*(5), 303-312.

Oleszczuk, P., Hale, S. E., Lehmann, J., & Cornelissen, G. (2012). Activated carbon and biochar amendments decrease pore water concentrations of polycyclic aromatic hydrocarbons (PAHs) in sewage sludge. *Bioresource Technology, 111*, 84-91.

Olgun, A., Atar, N., & Wang, S. (2013). Batch and column studies of phosphate and nitrate adsorption on waste solids containing boron impurity. *Chemical Engineering Journal, 222*, 108-119.

Önal, Y., Akmil-Başar, C., Eren, D., Sarıcı-Özdemir, Ç., & Depci, T. (2006). Adsorption kinetics of malachite green onto activated carbon prepared from Tunçbilek lignite. *Journal of Hazardous Materials, 128*(2), 150-157.

Özer, D., Dursun, G., & Özer, A. (2007). Methylene blue adsorption from aqueous solution by dehydrated peanut hull. *Journal of Hazardous Materials, 144*(1), 171-179.

Park, D., Yun, Y. S., & Park, J. M. (2010). The past, present, and future trends of biosorption. *Biotechnology and Bioprocess Engineering, 15*(1), 86-102.

Park, J., Lee, Y., Ryu, C., & Park, Y. K. (2014). Slow pyrolysis of rice straw: analysis of products properties, carbon and energy yields. *Bioresource Technology, 155*, 63-70.

Patel, H., & Vashi, R. T. (2010). Adsorption of crystal violet dye onto tamarind seed powder. *Journal of Chemistry, 7*(3), 975-984.

Pavan, F. A., Mazzocato, A. C., & Gushikem, Y. (2008). Removal of methylene blue dye from aqueous solutions by adsorption using yellow passion fruit peel as adsorbent. *Bioresource Technology, 99*(8), 3162-3165.

Peng, X., Ye, L. L., Wang, C. H., Zhou, H., & Sun, B. (2011). Temperature and duration dependent rice straw derived biochar: characteristics and its effects on soil properties of an Ultisol in southern China. *Soil and Tillage Research, 112*(2), 159-166.

Ponnusami, V., Vikram, S., & Srivastava, S. N. (2008). Guava (Psidium guajava) leaf powder: novel adsorbent for removal of methylene blue from aqueous solutions. *Journal of Hazardous Materials, 152*(1), 276-286.

Porselvi, E., & Krishnamoorthy, P. (2014). Removal of acid yellow by agricultural waste*. Journal of Materials and Environmental Science, 5*(2), 408-415.

Qada, E. N. E. I., Allen, S. J., & Walker, G. M. (2008). Adsorption of basic dyes from aqueous solution onto activated carbons. *Chemical Engineering Journal, 135*(3), 174-184.

Qian, K., Kumar, A., Zhang, H., Bellmer, D., & Huhnke, R. (2015). Recent advances in utilization of biochar. *Renewable and Sustainable Energy Reviews, 42*, 1055-1064.

Qian, L., & Chen, B. (2013). Dual role of biochars as adsorbents for aluminum: the effects of oxygen-containing organic components and the scattering of silicate particles. *Environmental Science & Technology, 47*(15), 8759-8768.

Qingye, L., Hao, A., Mianwu, M., Yuelin, W., Mingdeng, L., & Ximin, D. (2012). Preparation of activated carbon from sugarcane leaves. *Environmental Protection of Chemical Industry, 6*, 026.

Qiu, Y., Zheng, Z., Zhou, Z., & Sheng, G. D. (2009). Effectiveness and mechanisms of dye adsorption on a straw-based biochar. *Bioresource Technology, 100*(21), 5348-5351.

Qodah, Z. A. (2000). Adsorption of dyes using shale oil ash. *Water Research, 34*(17), 4295-4303.

Radha, K. V., Sridevi, V., & Kalaivani, K. (2009). Electrochemical oxidation for the treatment of textile industry wastewater. *Bioresource Technology, 100*(2), 987-990.

Rafatullah, M., Sulaiman, O., Hashim, R., & Ahmad, A. (2010). Adsorption of methylene blue on low-cost adsorbents: a review. *Journal of Hazardous Materials, 177*(1), 70-80.

Rahman, A. A., Abdullah, N., & Sulaiman, F. (2014). Temperature effect on the characterization of pyrolysis products from oil palm fronds. *Advances in Energy Engineering, 2*, 14-21.

Rai, H. S., Bhattacharyya, M. S., Singh, J., Bansal, T. K., Vats, P., & Banerjee, U. C. (2005). Removal of dyes from the effluent of textile and dyestuff manufacturing industry: a review of emerging techniques with reference to biological treatment. *Critical Reviews in Environmental Science and Technology, 35*(3), 219-238.

Rajkumar, D., Song, B. J., & Kim, J. G. (2007). Electrochemical degradation of Reactive Blue 19 in chloride medium for the treatment of textile dyeing wastewater with identification of intermediate compounds. *Dyes and Pigments, 72*(1), 1-7.

Rajwar, B. S., & Pandey, I. K. (2015). Removal of COD & BOD from contaminanted water by using fly ash as an adsorbent: A review. *International Journal of Logistics & Supply Chain Management Perspective, 4*(1), 1537-1543.

Raposo, F., De La Rubia, M. A., & Borja, R. (2009). Methylene blue number as useful indicator to evaluate the adsorptive capacity of granular activated carbon in batch mode: influence of adsorbate/adsorbent mass ratio and particle size. *Journal of Hazardous Materials, 165*(1), 291-299.

Ratnamala, G. M., Shetty, K. V., & Srinikethan, G. (2012). Removal of remazol brilliant blue dye from dye-contaminated water by adsorption using red mud: equilibrium, kinetic, and thermodynamic studies. W*ater, Air, & Soil Pollution, 223*(9), 6187-6199.

Rauf, M. A., Shehadeh, I., Ahmed, A., & Al-Zamly, A. (2009). Removal of methylene blue from aqueous solution by using gypsum as a low cost adsorbent. *World Academy of Science, Engineering and Technology, 55*, 608-613.

Reichenberg, D. (1953). Properties of ion-exchange resins in relation to their structure. III. Kinetics of exchange. *Journal of the American Chemical Society, 75*(3), 589-597.

Robinson, T., McMullan, G., Marchant, R., & Nigam, P. (2001). Remediation of dyes in textile effluent: a critical review on current treatment technologies with a proposed alternative. *Bioresource Technology, 77*(3), 247-255.

Saha, N., Kharbuli, Z. Y., Bhattacharjee, A., Goswami, C., & Häussinger, D. (2002). Effect of alkalinity (pH 10) on ureogenesis in the air-breathing walking catfish, Clarias batrachus. *Comparative Biochemistry and Physiology Part A: Molecular & Integrative Physiology, 132*(2), 353-364.

Salleh, M. A. M., Mahmoud, D. K., Karim, W. A. W. A., & Idris, A. (2011). Cationic and anionic dye adsorption by agricultural solid wastes: a comprehensive review. *Desalination, 280*(1), 1-13.

Santos, A. B. D., Cervantes, F. J., Yaya-Beas, R. E., & Van Lier, J. B. (2003). Effect of redox mediator, AQDS, on the decolourisation of a reactive azo dye containing triazine group in a thermophilic anaerobic EGSB reactor. *Enzyme and Microbial Technology, 33*(7), 942-951.

Santos, A. B. D., Cervantes, F. J., & van Lier, J. B. (2007). Review paper on current technologies for decolourisation of textile wastewaters: perspectives for anaerobic biotechnology. *Bioresource Technology, 98*(12), 2369-2385.

Sarbani, N., Muhammad, W., Shariman, M., Syed Radzi, R., SA, C. G., & Anwaruddin, H. (2016). Technical and economic feasibility study of coconut shell charcoal production as precursor to activated carbon in east coast Malaysia. *ABRIC*, 1-11.

Saxena, S., & Raja, A. S. M. (2014). Natural dyes: sources, chemistry, application and sustainability issues. *In Roadmap to Sustainable Textiles and Clothing*, 37-80.

Sen, T. K., Afroze, S., & Ang, H. M. (2011). Equilibrium, kinetics and mechanism of removal of methylene blue from aqueous solution by adsorption onto pine cone biomass of Pinus radiata. *Water, Air, & Soil Pollution, 218*(1-4), 499-515.

Senthilkumaar, S., Kalaamani, P., & Subburaam, C. V. (2006). Liquid phase adsorption of crystal violet onto activated carbons derived from male flowers of coconut tree. *Journal of Hazardous Materials, 136*(3), 800-808.

Seong, L. W. (2007). Malaysia textile & apparel industry. *Penang Economic Monthly, 9*, 1-28.

Shaaban, A., Se, S. M., Mitan, N. M. M., & Dimin, M. F. (2013). Characterization of biochar derived from rubber wood sawdust through slow pyrolysis on surface porosities and functional groups. *Procedia Engineering, 68*, 365-371.

Shah, J., Kumar, S., Sharma, S., Sharma, R., & Sharma, R. (2016). Removal of Nickel from aqueous solution by using low cost adsorbents: a review. *International Journal of Scientific Engineering and Applled Science (USEAS), 2*(7), 2395-3470.

Shan, H. Y. (2004). Citation review of Lagergren kinetic rate equation on adsorption reactions. *Scientometrics, 59*(1), 171-177.

Shen, Y. S., Wang, S. L., Tzou, Y. M., Yan, Y. Y., & Kuan, W. H. (2012). Removal of hexavalent Cr by coconut coir and derived chars-The effect of surface functionality. *Bioresource Technology, 104*, 165-172.

Sheng, J., Xie, Y., & Zhou, Y. (2009). Adsorption of methylene blue from aqueous solution on pyrophyllite. *Applied Clay Science, 46*(4), 422-424.

Shi, B., Li, G., Wang, D., Feng, C., & Tang, H. (2007). Removal of direct dyes by coagulation: The performance of preformed polymeric aluminum species. *Journal of Hazardous Materials, 143*(1), 567-574.

Shi, L., Zhang, G., Wei, D., Yan, T., Xue, X., Shi, S., & Wei, Q. (2014). Preparation and utilization of anaerobic granular sludge-based biochar for the adsorption of methylene blue from aqueous solutions. *Journal of Molecular Liquids, 198*, 334-340.

Shih, M. C. (2012). Kinetics of the batch adsorption of methylene blue from aqueous solutions onto rice husk: effect of acid-modified process and dye concentration. *Desalination and Water Treatment, 37*(1-3), 200-214.

Shinogi, Y., & Kanri, Y. (2003). Pyrolysis of plant, animal and human waste: physical and chemical characterization of the pyrolytic products. *Bioresource Technology, 90*(3), 241-247.

Shkuri, N. S. M. (2015). *Production of ferulic acid from banana stem waste by using co-culture.* (Published Doctoral Dissertation). The University Malaysia Pahang, Malaysia.

Shukla, A., Zhang, Y. H., Dubey, P., Margrave, J. L., & Shukla, S. S. (2002). The role of sawdust in the removal of unwanted materials from water. *Journal of Hazardous Materials, 95*(1), 137-152.

Singh, K. P., Mohan, D., Sinha, S., Tondon, G. S., & Gosh, D. (2003). Colour removal from wastewater using low-cost activated carbon derived from agricultural waste material. *Industrial & Engineering Chemistry Research, 42*(9), 1965-1976.

Singh, B., Singh, B. P., & Cowie, A. L. (2010). Characterisation and evaluation of biochars for their application as a soil amendment. *Soil Research, 48*(7), 516-525.

Singh, Z., & Chadha, P. (2016). Textile industry and occupational cancer. *Journal of*

Occupational Medicine and Toxicology, 11(1), 39.

Sivakumar, P., & Palanisamy, N. (2010). Mechanistic study of dye adsorption on to a novel non-conventional low-cost adsorbent. *Advances in Applied Science Research, 1*(1), 58-65.

Sivaraj, R., Namasivayam, C., & Kadirvelu, K. (2001). Orange peel as an adsorbent in the removal of acid violet 17 (acid dye) from aqueous solutions. *Waste Management, 21*(1), 105-110.

Sohi, S. P., Krull, E., Lopez-Capel, E., & Bol, R. (2010). A review of biochar and its use and function in soil. *Advances in Agronomy, 105*, 47-82.

Soni, M., Sharma, A. K., Srivastava, J. K., & Yadav, S. J. (2012). Adsorptive removal of methylene blue dye from an aqueous solution using water hyacinth root powder as a low adsorbent. *International Journal of Chemical Sciences and Applications, 3*(3), 338-345.

Spokas, K. A., Koskinen, W. C., Baker, J. M., & Reicosky, D. C. (2009). Impacts of woodchip biochar additions on greenhouse gas production and sorption/degradation of two herbicides in a Minnesota soil. *Chemosphere, 77*(4), 574-581.

Srinivasan, P., Sarmah, A. K., Smernik, R., Das, O., Farid, M., & Gao, W. (2015). A feasibility study of agricultural and sewage biomass as biochar, bioenergy and biocomposite feedstock: production, characterization and potential applications. *Science of the Total Environment, 512*, 495-505.

Srivastava, V. C., Mall, I. D., & Mishra, I. M. (2005). Treatment of pulp and paper mill wastewaters with poly aluminium chloride and bagasse fly ash. *Colloids and Surfaces A: Physicochemical and Engineering Aspects, 260*(1), 17-28.

Srivastava, V. C., Swamy, M. M., Mall, I. D., Prasad, B., & Mishra, I. M. (2006). Adsorptive removal of phenol by bagasse fly ash and activated carbon: equilibrium, kinetics and thermodynamics. *Colloids and Surfaces A: Physicochemical and Engineering Aspects, 272*(1), 89-104.

Sukiran, M. A., Kheang, L. S., Bakar, N. A., & May, C. Y. (2011). Production and characterization of biochar from the pyrolysis of empty fruit bunches. *American Journal of Applied Sciences, 8*(10), 984.

Sun, K., Keiluweit, M., Kleber, M., Pan, Z., & Xing, B. (2011). Sorption of fluorinated herbicides to plant biomass-derived biochars as a function of molecular structure. *Bioresource Technology, 102*(21), 9897-9903.

Sun, H., Hockaday, W. C., Masiello, C. A., & Zygourakis, K. (2012). Multiple controls on the chemical and physical structure of biochars. *Industrial & Engineering Chemistry Research, 51*(9), 3587-3597.

Sun, L., Wan, S., & Luo, W. (2013). Biochars prepared from anaerobic digestion residue, palm bark, and eucalyptus for adsorption of cationic methylene blue dye: characterization, equilibrium, and kinetic studies. *Bioresource Technology, 140*, 406-413.

Sun, Y., Yang, S., Chen, Y., Ding, C., Cheng, W., & Wang, X. (2015). Adsorption and desorption of U (VI) on functionalized graphene oxides: a combined experimental and theoretical study. *Environmental Science & Technology, 49*(7), 4255-4262.

Suyamboo, B. K., & Perumal, R. S. (2012). Equilibrium, thermodynamic and kinetic studies on adsorption of a basic dye by Citrullus lanatus rind. *Iranica Journal of Energy & Environment, 3*(1), 23-34.

Syafalni, S., Abustan, I., Dahlan, I., Wah, C. K., & Umar, G. (2012). Treatment of dye wastewater using granular activated carbon and zeolite filter. *Modern Applied Science, 6*(2), 37.

Tan, I. A. W., Ahmad, A. L., & Hameed, B. H. (2008). Adsorption of basic dye on high-surface-area activated carbon prepared from coconut husk: Equilibrium, kinetic and thermodynamic studies. *Journal of Hazardous Materials, 154*(1), 337-346.

Tan, X., Liu, Y., Zeng, G., Wang, X., Hu, X., Gu, Y., & Yang, Z. (2015). Application of biochar for the removal of pollutants from aqueous solutions. *Chemosphere, 125*, 70-85.

Tanyildizi, M. Ş. (2011). Modeling of adsorption isotherms and kinetics of reactive dye from aqueous solution by peanut hull. *Chemical Engineering Journal, 168*(3), 1234-1240.

Thomazini, A., Spokas, K., Hall, K., Ippolito, J., Lentz, R., & Novak, J. (2015). GHG impacts of biochar: Predictability for the same biochar. *Agriculture, Ecosystems & Environment, 207*, 183-191.

Tongpoothorn, W., Sriuttha, M., Homchan, P., Chanthai, S., & Ruangviriyachai, C. (2011). Preparation of activated carbon derived from Jatropha curcas fruit shell by simple thermo-chemical activation and characterization of their physico-chemical properties. *Chemical Engineering Research and Design, 89*(3), 335-340.

Tor, A., & Cengeloglu, Y. (2006). Removal of congo red from aqueous solution by adsorption onto acid activated red mud. *Journal of Hazardous Materials, 138*(2), 409-415.

Tryon, E. H. (1948). Effect of charcoal on certain physical, chemical, and biological properties of forest soils. *Ecological Monographs, 18*(1), 81-115.

Tsai, W. T., & Chen, H. R. (2013). Adsorption kinetics of herbicide paraquat in aqueous solution onto a low cost adsorbent, swine manure derived biochar. International *Journal of Environmental Science and Technology, 10*(6), 1349-1356.

Vadivelan, V., & Kumar, K. V. (2005). Equilibrium, kinetics, mechanism, and process design for the sorption of methylene blue onto rice husk. *Journal of Colloid and Interface Science, 286*(1), 90-100.

Valix, M., Cheung, W. H., & McKay, G. (2004). Preparation of activated carbon using low temperature carbonisation and physical activation of high ash raw bagasse for acid dye adsorption. *Chemosphere, 56*(5), 493-501.

Venkateswarlu, P., Ratnam, M. V., Rao, D. S., & Rao, M. V. (2007). Removal of chromium from an aqueous solution using Azadirachta indica (neem) leaf powder as an adsorbent. *International Journal of Physical Sciences, 2*(8), 188-195.

Verma, A. K., Dash, R. R., & Bhunia, P. (2012). A review on chemical coagulation/flocculation technologies for removal of colour from textile wastewaters. *Journal of Environmental Management, 93*(1), 154-168.

Vieira, S. S., Magriotis, Z. M., Santos, N. A., das Graças Cardoso, M., & Saczk, A. A. (2012). Macauba palm (Acrocomia aculeata) cake from biodiesel processing: an efficient and low cost substrate for the adsorption of dyes. *Chemical Engineering Journal, 183*, 152-161.

Vimonses, V., Jin, B., & Chow, C. W. (2010). Insight into removal kinetic and mechanisms of anionic dye by calcined clay materials and lime. *Journal of Hazardous Materials, 177*(1), 420-427.

Wang, S., & Li, H. (2007). Kinetic modelling and mechanism of dye adsorption on unburned carbon. *Dyes and Pigments, 72*(3), 308-314.

Wang, Z., Xue, M., Huang, K., & Liu, Z. (2011). Textile dyeing wastewater treatment. *In Advances In Treating Textile Effluent.* InTech.

Wang, Z., Guo, H., Shen, F., Yang, G., Zhang, Y., Zeng, Y., ... Deng, S. (2015). Biochar produced from oak sawdust by Lanthanum (La)-involved pyrolysis for adsorption of ammonium (NH_4^+), nitrate (NO_3^-), and phosphate (PO_4^{3-}). *Chemosphere, 119*, 646-653.

Wang, Y., Hu, Y., Zhao, X., Wang, S., & Xing, G. (2013). Comparisons of biochar properties from wood material and crop residues at different temperatures and residence times. *Energy & Fuels, 27*(10), 5890-5899.

Weber, T.W., & Chakravorti, R. K. (1974). Pore and solid diffusion models for fixed-bed adsorbers. *AIChE Journal, 20*(2), 228-238.

Wei, Z. H., Lv, X. J., & Wang, Z. F. (2012). Preparation of iron-supported activated carbon and its adsorption properties of P(V). *Kunming Ligong Daxue Xuebao(Ligong Ban)/ Journal of Kunming University of Science and Technology (Science and Technology), 37*(2), 72-77.

Weng, C. H., Lin, Y. T., & Tzeng, T. W. (2009). Removal of methylene blue from aqueous solution by adsorption onto pineapple leaf powder. *Journal of Hazardous Materials, 170*(1), 417-424.

Wiedner, K., Rumpel, C., Steiner, C., Pozzi, A., Maas, R., & Glaser, B. (2013). Chemical evaluation of chars produced by thermochemical conversion (gasification, pyrolysis and hydrothermal carbonization) of agro-industrial biomass on a commercial scale. *Biomass and Bioenergy, 59*, 264-278.

Worch, E. (2012). *Adsorption technology in water treatment: Fundamentals, processes and modelling*. Berlin, Germany: Water de Gruyter.

Wu, F. C., Wu, P. H., Tseng, R. L., & Juang, R. S. (2011). Preparation of novel activated carbons from H_2SO_4-pretreated corncob hulls with KOH activation for quick adsorption of dye and 4-chlorophenol. *Journal of Environmental Management, 92*(3), 708-713.

Wu, X., Hui, K. N., Hui, K. S., Lee, S. K., Zhou, W., Chen, R., ... Son, Y. G. (2012). Adsorption of basic yellow 87 from aqueous solution onto two different mesoporous adsorbents. *Chemical Engineering Journal, 180*, 91-98.

Xiao, R., Chen, X., Wang, F., & Yu, G. (2010). Pyrolysis pretreatment of biomass for entrained-flow gasification. *Applied Energy, 87*(1), 149-155.

Xu, R. K., Xiao, S. C., Yuan, J. H., & Zhao, A. Z. (2011). Adsorption of methyl violet from aqueous solutions by the biochars derived from crop residues. *Bioresource Technology, 102*(22), 10293-10298.

Xu, X., Cao, X., & Zhao, L. (2013). Comparison of rice husk-and dairy manure-derived biochars for simultaneously removing heavy metals from aqueous solutions: role of mineral components in biochars. *Chemosphere, 92*(8), 955-961.

Yanai, Y., Toyota, K., & Okazaki, M. (2007). Effects of charcoal addition on N_2O emissions from soil resulting from rewetting air-dried soil in short-term laboratory experiments. *Soil Science and Plant Nutrition, 53*(2), 181-188.

Yang, G., Wu, L., Xian, Q., Shen, F., Wu, J., & Zhang, Y. (2016). Removal of congo red and methylene blue from aqueous solutions by vermicompost-derived Biochars. *PLOS ONE, 11*(5).

Yang, H., Yan, R., Chen, H., Lee, D. H., & Zheng, C. (2007). Characteristics of hemicellulose, cellulose and lignin pyrolysis. *Fuel, 86*(12), 1781-1788.

Yang, H., & Feng, Q. (2010). Characterization of pore-expanded amino-functionalized mesoporous silicas directly synthesized with dimethyldecylamine and its application for decolourization of sulphonated azo dyes. *Journal of Hazardous Materials, 180*(1), 106-114.

Yang, Y., Lin, X., Wei, B., Zhao, Y., & Wang, J. (2014). Evaluation of adsorption potential of bamboo biochar for metal-complex dye: equilibrium, kinetics and artificial neural network modeling. *International Journal of Environmental Science and Technology, 11*(4), 1093-1100.

Yao, Z., Wang, L., & Qi, J. (2009). Biosorption of methylene blue from aqueous solution using a bioenergy forest waste: xanthoceras sorbifolia seed coat. *CLEAN-Soil, Air, Water*, 37(8), 642-648.

Yao, Y., Gao, B., Chen, H., Jiang, L., Inyang, M., Zimmerman, A. R., ... Li, H. (2012). Adsorption of sulfamethoxazole on biochar and its impact on reclaimed water irrigation. *Journal of Hazardous Materials, 209*, 408-413.

Yasmin, C. A. (2004). *Adsorption studies of dyes using clay-based and activated carbon adsorbents.* (Published Master's Thesis). Universiti Sains Malaysia, Penang.

Yu, L. J., Shukla, S. S., Dorris, K. L., Shukla, A., & Margrave, J. L. (2003). Adsorption of chromium from aqueous solutions by maple sawdust. *Journal of Hazardous Materials, 100*(1), 53-63.

Yuan, H., Lu, T., Huang, H., Zhao, D., Kobayashi, N., & Chen, Y. (2015). Influence of pyrolysis temperature on physical and chemical properties of biochar made from sewage sludge. *Journal of Analytical and Applied Pyrolysis, 112*, 284-289.

Yuan, J. H., Xu, R. K., & Zhang, H. (2011). The forms of alkalis in the biochar produced from crop residues at different temperatures. *Bioresource Technology, 102*(3), 3488-3497.

Zahrim, A. Y., Tizaoui, C., & Hilal, N. (2011). Coagulation with polymers for nanofiltration pre-treatment of highly concentrated dyes: a review. *Desalination, 266*(1), 1-16.

Zhang, Q., & Chuang, K. T. (2001). Adsorption of organic pollutants from effluents of a Kraft pulp mill on activated carbon and polymer resin. *Advances in Environmental Research, 5*(3), 251-258.

Zhang, Z., Moghaddam, L., O'Hara, I. M., & Doherty, W. O. (2011). Congo Red adsorption by ball-milled sugarcane bagasse. *Chemical Engineering Journal, 178,* 122-128.

Zhang, A., Bian, R., Pan, G., Cui, L., Hussain, Q., Li, L., ... Yu, X. (2012). Effects of biochar amendment on soil quality, crop yield and greenhouse gas emission in a Chinese rice paddy: a field study of 2 consecutive rice growing cycles. *Field Crops Research, 127*, 153-160.

Zhang, P., Sun, H., Yu, L., & Sun, T. (2013). Adsorption and catalytic hydrolysis of carbaryl and atrazine on pig manure-derived biochars: impact of structural properties of biochars. *Journal of Hazardous Materials, 244*, 217-224.

Zhao, X. B., Xiao, B., Fletcher, A. J., & Thomas, K. M. (2005). Hydrogen adsorption on functionalized nanoporous activated carbons. *The Journal of Physical Chemistry B, 109*(18), 8880-8888.

Zhong, Z. Y., Yang, Q., Li, X. M., Luo, K., Liu, Y., & Zeng, G. M. (2012). Preparation of peanut hull-based activated carbon by microwave-induced phosphoric acid activation and its application in remazol brilliant blue R adsorption. *Industrial Crops and Products, 37*(1), 178-185.

Zhou, Y., Liang, Z., & Wang, Y. (2008). Decolourization and COD removal of secondary yeast wastewater effluents by coagulation using aluminum sulfate. *Desalination, 225*(1-3), 301-311.